AD NUMBER

AD888671

LIMITATION CHANGES

TO:

Approved for public release; distribution is unlimited.

FROM:

Distribution authorized to U.S. Gov't. agencies only; Test and Evaluation; OCT 1971. Other requests shall be referred to Air Force Armament Laboratory, Attn DLGD, Eglin AFB, FL 32542.

AUTHORITY

AFATL ltr, 16 Jun 1974

AEDC-TR-71-222
AFATL-TR-71-130

CAPTIVE-TRAJECTORY STORE-SEPARATION CHARACTERISTICS OF THE SUU-51/B WITH MODIFIED TAIL FINS FROM THE F-4C AIRCRAFT

J. M. Whoric

ARO, Inc.

October 1971

PROPULSION WIND TUNNEL FACILITY
ARNOLD ENGINEERING DEVELOPMENT CENTER
AIR FORCE SYSTEMS COMMAND
ARNOLD AIR FORCE STATION, TENNESSEE

NOTICES

When U. S. Government drawings specifications, or other data are used for any purpose other than a definitely related Government procurement operation, the Government thereby incurs no responsibility nor any obligation whatsoever, and the fact that the Government may have formulated, furnished, or in any way supplied the said drawings, specifications, or other data, is not to be regarded by implication or otherwise, or in any manner licensing the holder or any other person or corporation, or conveying any rights or permission to manufacture, use, or sell any patented invention that may in any way be related thereto.

Qualified users may obtain copies of this report from the Defense Documentation Center.

References to named commercial products in this report are not to be considered in any sense as an endorsement of the product by the United States Air Force or the Government.

CAPTIVE-TRAJECTORY STORE-SEPARATION CHARACTERISTICS OF THE SUU-51/B WITH MODIFIED TAIL FINS FROM THE F-4C AIRCRAFT

J. M. Whoric
ARO, Inc.

FOREWORD

The work reported herein was sponsored by the Air Force Armament Laboratory (DLGD/Capt. M. Runkle), Air Force Armament Development and Test Center, Air Force Systems Command (AFSC), under Program Element 64724F, Project 1120, Task 07.

The test results presented were obtained by ARO, Inc. (a subsidiary of Sverdrup & Parcel and Associates, Inc.), contract operator of the Arnold Engineering Development Center (AEDC), AFSC, Arnold Air Force Station, Tennessee, under Contract F40600-72-C-0003. The test was conducted from July 9 to 19, 1971, under ARO Project No. PC0158. The manuscript was submitted for publication on August 31, 1971.

This technical report has been reviewed and is approved.

George F. Garey
Lt Colonel, USAF
AF Representative, PWT
Directorate of Test

Joseph R. Henry
Colonel, USAF
Director of Test

ABSTRACT

A wind tunnel test was conducted using 0.05-scale models to study the separation characteristics of the SUU-51/B external store with modified tail fins from the F-4C aircraft. Captive-trajectory store-separation data were obtained for two store cg locations and for 10 store wing loading configurations. The separation trajectories were initiated from the right-wing inboard pylon station utilizing the Triple Ejection Rack and from the centerline pylon utilizing the Multiple Ejection Rack. The flight conditions simulated were Mach numbers from 0.66 to 0.90 at an altitude of 5000 ft. Parent aircraft dive angles of 0 and 45 deg were simulated.

CONTENTS

APPENDIXES

Figure Page

II. TABLES

NOMENCLATURE

BL Aircraft buttock line from plane of symmetry, in., model scale

b Store reference dimension, ft full scale

C_A Store axial-force coefficient, axial force/$q_\infty S$

C_m Store pitching-moment coefficient, referenced to the store center of gravity (cg), pitching moment/$q_\infty Sb$

C_{m_q} Store pitch-damping derivative, $dC_m/d(qb/2V_\infty)$

C_n Store yawing-moment coefficient, referenced to the store cg, yawing moment/$q_\infty Sb$

C_{n_r} Store yaw-damping derivative, $dC_n/d(rb/2V_\infty)$

FS Aircraft fuselage station, in., model scale

F_Z MER/TER ejector force, lb

H Pressure altitude, ft

I_{xx} Full-scale moment of inertia about the store X_B axis, slug-ft^2

I_{xz} Full-scale product of inertia, X_B-Z_B axis, slug-ft^2

I_{yy} Full-scale moment of inertia about the store Y_B axis, slug-ft^2

I_{zz} Full-scale moment of inertia about the store Z_B axis, slug-ft^2

M_∞ Free-stream Mach number

$\overline{m}$ Full-scale store mass, slugs

p_∞ Free-stream static pressure, psfa

q Store angular velocity about the Y_B axis, radians/sec

q_∞ Free-stream dynamic pressure, $0.7\ p_\infty M_\infty^2$, psf

r Store angular velocity about the Z_B axis, radians/sec

S Store reference area, ft^2, full scale.

t Real trajectory time from initiation of trajectory, sec

V_∞ Free-stream velocity, ft/sec

WL Aircraft waterline from reference horizontal plane, in., model scale

X Separation distance of the store cg parallel to the flight axis system X_F direction, ft, full scale measured from the prelaunch position

$\overline{X}$ Center-of-gravity location index (see Table I)

X_{cg} Full-scale cg location, ft from nose of store (see Table I)

X_L Ejector piston location relative to the store cg, positive forward of store cg, ft, full scale

Y Separation distance of the store cg parallel to the flight axis system Y_F direction, ft, full scale measured from the prelaunch position

Z Separation distance of the store cg parallel to the flight-axis system Z_F direction, ft, full scale measured from the prelaunch position

Z_E Ejector stroke length, ft, full scale

α Parent-aircraft or store model angle of attack relative to the free-stream velocity vector, deg

θ Angle between the store longitudinal axis and its projection in the X_F-Y_F plane, positive when store nose is raised as seen by pilot, deg

$\bar{\theta}$ Simulated parent-aircraft climb angle. Angle between the flight direction and the earth horizontal, deg, positive for increasing altitude

ψ Angle between the projection of the store longitudinal axis in the X_F-Y_F plane and the X_F axis, positive when the store nose is to the right as seen by the pilot, deg

FLIGHT-AXIS SYSTEM COORDINATES

Directions

X_F Parallel to the free-stream wind vector, positive direction is forward as seen by the pilot

Y_F Perpendicular to the X_F and Z_F directions, positive direction is to the right as seen by the pilot

Z_F In the aircraft plane of symmetry, perpendicular to the free-stream wind vector, positive direction is downward

The flight-axis system origin is coincident with the aircraft cg and remains fixed with respect to the parent aircraft during store separation. The X_F, Y_F, and Z_F coordinate axes do not rotate with respect to the initial flight direction and attitude.

STORE BODY-AXIS SYSTEM COORDINATES

Directions

X_B Parallel to the store longitudinal axis, positive direction is upstream in the prelaunch position

Y_B Perpendicular to the store longitudinal axis, and parallel to the flight-axis system X_F-Y_F plane when the store is at zero roll angle, positive direction is to the right looking upstream when the store is at zero yaw and roll angles

Z_B Perpendicular to both the X_B and Y_B axes, positive direction is downward as seen by the pilot when the store is at zero pitch and roll angles

The store body-axis system origin is coincident with the store cg and moves with the store during separation from the parent airplane. The X_B, Y_B, and Z_B coordinate axes rotate with the store in pitch, yaw, and roll so that mass moments of inertia about the three axes are not time-varying quantities.

SECTION I
INTRODUCTION

This investigation was conducted in the Aerodynamic Wind Tunnel (4T) of the Propulsion Wind Tunnel Facility (PWT) to obtain captive-trajectory store-separation data for the SUU-51/B store with modified tail fins when released from various F-4C inboard and centerline multiple carriage configurations. Separation trajectories with the folded-fin configuration were initiated from the launch positions with simulated ejector forces acting on the store. If a trajectory was of sufficient length to reach the position where the fins could be deployed, the open-fin configuration was used to obtain additional data initiated from the chosen store location along the original trajectory. The criterion for fin deployment was a clearance of at least 1.5 ft between the rack and the aft end of the store.

To simulate the separation trajectories, 0.05-scale models of the F-4C and the store were employed. The store models were attached to the Captive Trajectory System (CTS) in Tunnel 4T. Flight conditions simulated were Mach numbers from 0.66 to 0.90, an altitude of 5000 ft, and parent-aircraft angles of attack from 1.6 to 0.1 deg in level flight. At most test conditions, a parent-aircraft dive angle of 45 deg was also simulated.

SECTION II
APPARATUS

2.1 TEST FACILITY

Tunnel 4T is a closed-loop, continuous flow, variable density tunnel in which the Mach number can be varied from 0.2 to 1.3. At all Mach numbers, the stagnation pressure can be varied from 200 to 3400 psfa. The test section is 4 ft square and 12.5 ft long with perforated, variable porosity (0.5- to 10-percent-open) walls. It is completely enclosed in a plenum chamber from which the air can be evacuated, allowing part of the tunnel airflow to be removed through the perforated walls of the test section.

For store separation testing, two separate and independent support systems are used to support the models. The parent aircraft model is inverted in the test section and supported by an offset sting attached to the main pitch sector. The store model is supported by the CTS which extends down from the tunnel top wall and provides store movement (six degrees of freedom) independent of the parent-aircraft model. An isometric drawing of a typical store separation installation is shown in Fig. 1, Appendix I.

Also shown in Fig. 1 is a block diagram of the computer control loop used during captive trajectory testing. The analog system and the digital computer work as an integrated unit and, utilizing required input information, control the store movement during a trajectory. Store positioning is accomplished by use of six individual d-c electric motors. Maximum translational travel of the CTS is ±15 in. from the tunnel centerline in the lateral and vertical directions and 36 in. in the axial direction. Maximum angular displacements are ±45 deg in pitch and yaw and ±360 deg in roll. A more complete

description of the test facility can be found in the Test Facilities Handbook.[1] A schematic showing the test section details and the location of the models in the tunnel is shown in Fig. 2. Figure 3 is a photograph of the model installation in the wind tunnel.

2.2 TEST ARTICLES

The test articles were 0.05-scale models of the F-4C parent aircraft and the SUU-51/B store. A sketch showing the basic dimensions of the F-4C parent model is shown in Fig. 4. For this test, only the right wing and fuselage centerline of the F-4C were instrumented for store separation. Details and dimensions of the pylons are shown in Fig. 5 The surfaces of the fuselage centerline and wing inboard pylons are inclined at a 2.5- and 1.0-deg nosedown angle, respectively, with respect to the aircraft waterline.

The Triple Ejection Rack (TER) and Multiple Ejection Rack (MER) were mounted on the inboard and centerline pylons, respectively, and matched to the 30-in. suspension lugs of the pylons. Details and dimensions of the TER and MER are shown in Figs. 6 and 7, respectively. Indicated also in these figures is the line of application of the ejector force.

Details and dimensions of the SUU-51/B store model indicating the fin modification are shown in Fig. 8. Only two of the dummy stores were modified. Before each run these particular dummy stores were installed at the MER or TER station adjacent to the launch station so that the fin clearances would be properly simulated. A dimensional sketch of the 370-gal dummy fuel tank is shown in Fig. 9. A schematic of the TER and MER store stations and orientation is given in Fig. 10, and the weapons loading configurations for which trajectory data were obtained are shown in Fig. 11. The store fin orientation on the MER and TER racks was an "X" configuration with respect to the line of application of the ejector force. Figure 12 is a photograph of the dummy store arrangement of load configuration 1.

2.3 INSTRUMENTATION

A five-component, internal strain-gage balance was used to obtain the force and moment data on the SUU-51/B model. Translational and angular positions of the store model were obtained from the CTS analog outputs. An angular position indicator on the main pitch sector was used to determine the parent-model angle of attack. The MER and TER were instrumented with a touch wire at each station which aided in the positioning of the sting-mounted store model at the launch position on the rack. The system was also electrically connected to automatically stop the CTS movement if the store model or sting contacted the rack or the aircraft-model surface.

---

[1]Test Facilities Handbook (Ninth Edition). "Propulsion Wind Tunnel Facility, Vol. 4." Arnold Engineering Development Center, July 1971.

SECTION III
TEST DESCRIPTION

3.1 TEST CONDITIONS

Separation trajectory data were obtained at Mach numbers from 0.66 to 0.90. Tunnel dynamic pressure was 500 psf at all Mach numbers, and tunnel stagnation temperature was maintained near 100°F.

Tunnel conditions were held constant at the desired Mach number and stagnation pressure while data for each trajectory were obtained. The trajectories were terminated when the store or sting contacted the parent-aircraft model or when a CTS limit was reached.

3.2 TRAJECTORY DATA ACQUISITION

To obtain a trajectory, test conditions were established in the tunnel and the parent model was positioned at the desired angle of attack. The store model was then oriented to a position corresponding to the store carriage location. After the store was set at the desired initial position, operational control of the CTS was switched to the digital computer which controlled the store movement during the trajectory through commands to the CTS analog system (see block diagram, Fig. 1). Data from the wind tunnel, consisting of measured model forces and moments, wind tunnel operating conditions, and CTS rig positions, were input to the digital computer for use in the full-scale trajectory calculations.

The digital computer was programmed to solve the six-degree-of-freedom equations to calculate the angular and linear displacements of the store relative to the parent aircraft pylon. In general, the program involves using the last two successive measured values of each static aerodynamic coefficient to predict the magnitude of the coefficients over the next time interval of the trajectory. These predicted values are used to calculate the new position and attitude of the store at the end of the time interval. The CTS is then commanded to move the store model to this new position and the aerodynamic loads are measured. If these new measurements agree with the predicted values, the process is continued over another time interval of the same magnitude. If the measured and predicted values do not agree within the desired precision, the calculation is redone over a time interval one-half the previous value. This process is repeated until a complete trajectory has been obtained.

In applying the wind tunnel data to the calculations of the full-scale store trajectories, the measured forces and moments are reduced to coefficient form and then applied with proper full-scale store dimensions and flight dynamic pressure. Dynamic pressure was calculated using a flight velocity equal to the free-stream velocity component plus the components of store velocity relative to the aircraft, and a density corresponding to the simulated altitude.

The initial portion of each launch trajectory incorporated simulated ejector forces in addition to the measured aerodynamic forces acting on the store. The ejector force

function for the SUU-51/B store is presented in Fig. 13. The ejector force was considered to act perpendicular to the rack mounting surface. The locations of the applied ejector forces and other full-scale store parameters used in the trajectory calculations are listed in Table I, Appendix II.

3.3 CORRECTIONS

Balance, sting, and support deflections caused by the aerodynamic loads on the store models were accounted for in the data reduction program to calculate the true store-model angles. Corrections were also made for model weight tares to calculate the net aerodynamic forces on the store model.

3.4 PRECISION OF DATA

The trajectory data are subject to error from several sources including tunnel conditions, balance measurements, extrapolation tolerances allowed in the predicted coefficients, and CTS positioning control. Maximum error in the CTS position control was ±0.05 in. for the translational settings and ±0.15 deg for angular displacement settings in pitch and yaw. Extrapolation tolerances were ±0.10 for each of the aerodynamic coefficients. The maximum uncertainties in the full-scale position data caused by the balance precision limitations are given in Table II.

The estimated uncertainty in setting Mach number was no greater than ±0.003, and the uncertainty in parent-model angle of attack was estimated to be ±0.1 deg.

SECTION IV
RESULTS AND DISCUSSION

4.1 GENERAL

All trajectories obtained are for use in the determination of safe-separation envelopes of the modified-fin SUU-51/B store from the F-4C aircraft. No attempt is made in this report to establish these envelopes or to qualify the store as safe or unsafe for aircraft separation. The trajectory data are presented as obtained from the wind tunnel along with comments regarding the aerodynamics of the store in the aircraft flow field. Trajectory data for the unmodified SUU-51/B can be found in a recently published report.[2]

Data taken during this test consisted of ejector-separated trajectories simulating release from multiple carriage positions on the left and right wing inboard and centerline positions of the F-4C aircraft. Trajectories from the left wing were simulated by launching from the right wing with a reversed (1, 3, and 2) TER ejection sequence. Data showing the

[2]J. Kukainis. "Separation Characteristics of the SUU-51/B from the F-4C Aircraft." AEDC-TR-71-129, July 1971.

linear and angular displacements of the store relative to the mate position on the racks or pylons are presented as functions of full-scale trajectory time in Figs. 14 through 26. Positive X, Y, and Z displacements (as seen by the pilot) are forward, to the right (outboard), and down, respectively. Positive changes in pitch and yaw (as seen by the pilot) are nose up and nose right (outboard), respectively. Open fin data were obtained at Mach number 0.82 for load configuration 2 only and are presented in Figs. 14c, 17a, and 19c.

Ten wing loading configurations of the SUU-51/B were tested. Most of the trajectories obtained were terminated because of CTS rig limitations before the model fins could be deployed. Data are presented for only nine load configurations. No data are presented for load configuration 1 because at all test conditions the launch store either contacted the TER or the fin of an adjacent store after a very short time and terminated the trajectory. Data are compared on the basis of store cg location (Figs. 14 through 16), Mach numbers (Figs. 17 and 18), and aircraft dive angle (Figs. 19 through 26).

4.2 EFFECT OF STORE CENTER-OF-GRAVITY LOCATION

The data in Figs. 14 through 16 show, in general, that the effect of shifting the store cg from the nominal position, which is aft of the point of application of the ejector force, to a point forward of the point of application of the ejector force was to reduce the store pitch and yaw rates without affecting the store displacements.

4.3 EFFECT OF MACH NUMBER

The effect of Mach number, as shown by the data in Figs. 17 and 18, was that before fin deployment the "X" and "Z" store displacements, as well as the store pitch and yaw rates, increased as the Mach number increased. The store "Y" displacement was essentially independent of Mach number.

4.4 EFFECT OF AIRCRAFT DIVE ANGLE AND STORE FIN DEPLOYMENT

Aircraft dive angle (Figs. 19 through 26) produced only small changes in the trajectory for a particular load configuration at a particular test condition. Moreover, as shown by the data in Figs. 14c, 17a, and 19c, fin deployment at a Mach number of 0.82 resulted in both pitch and yaw recovery in the motion of the store.

APPENDIXES
I. ILLUSTRATIONS
II. TABLES

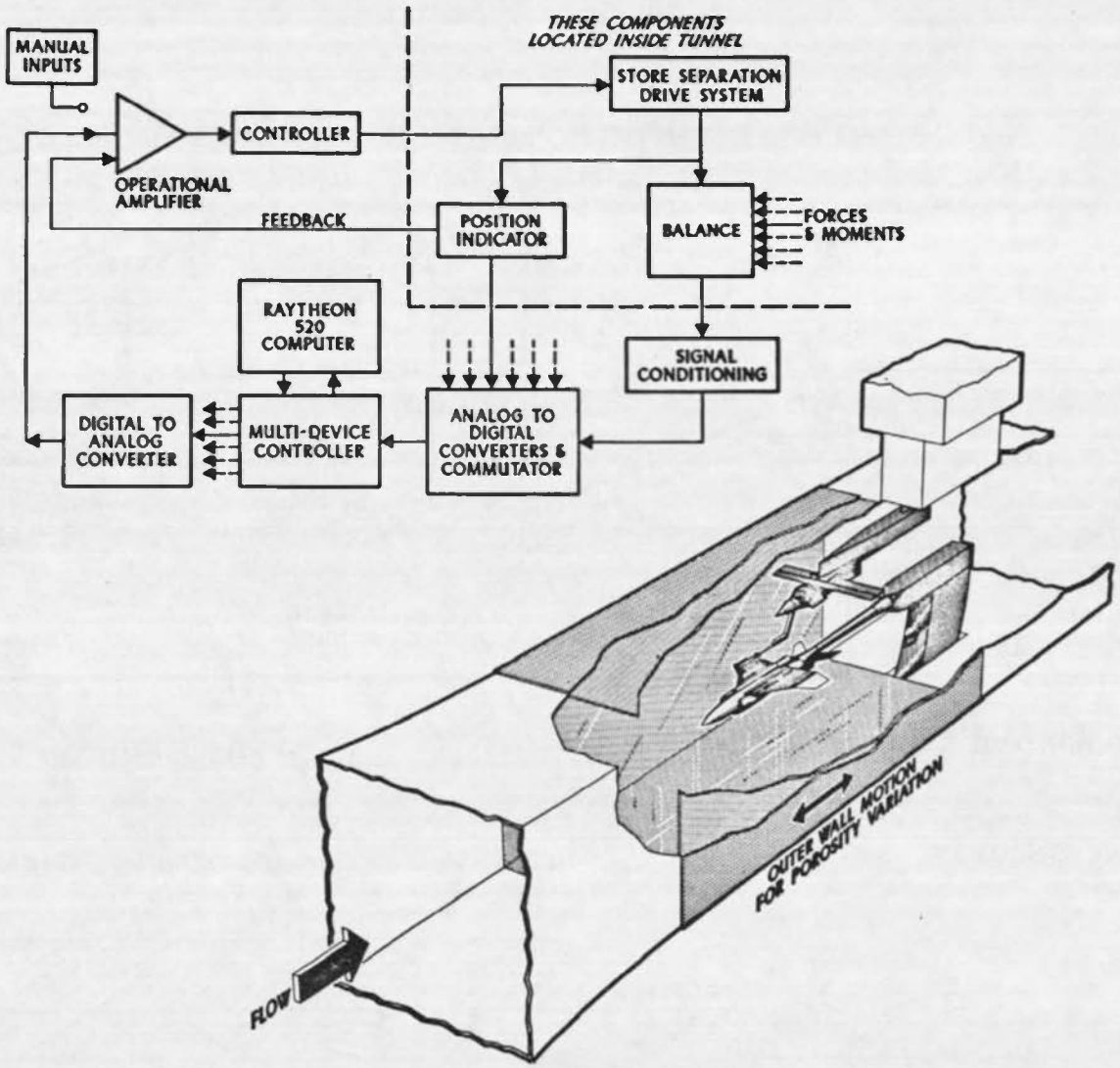

Fig. 1 Isometric Drawing of a Typical Store Separation Installation and a Block Diagram of the Computer Control Loop

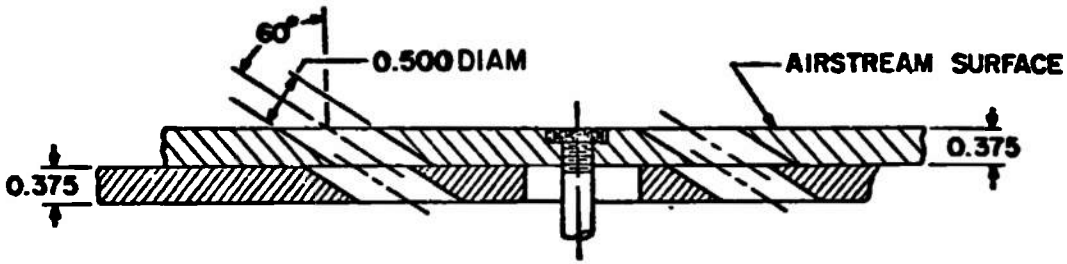

TYPICAL PERFORATED WALL CROSS SECTION

TUNNEL STATIONS AND DIMENSIONS ARE IN INCHES

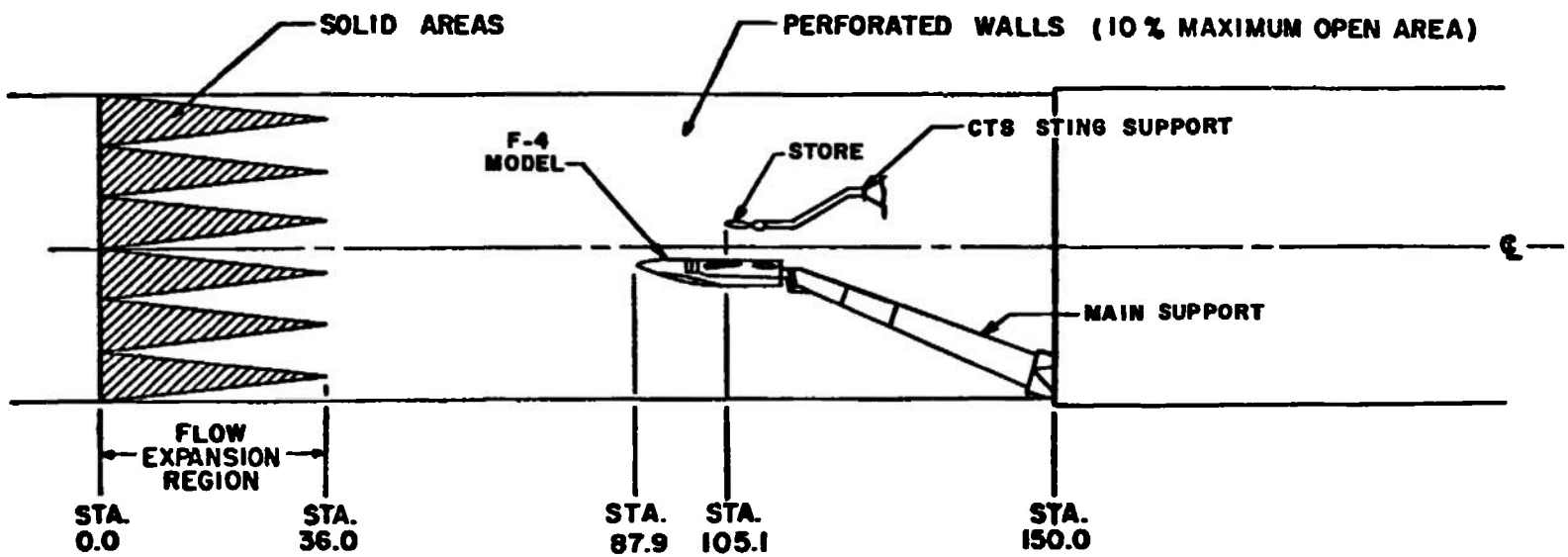

Fig. 2 Schematic of the Tunnel Test Section Showing Model Location

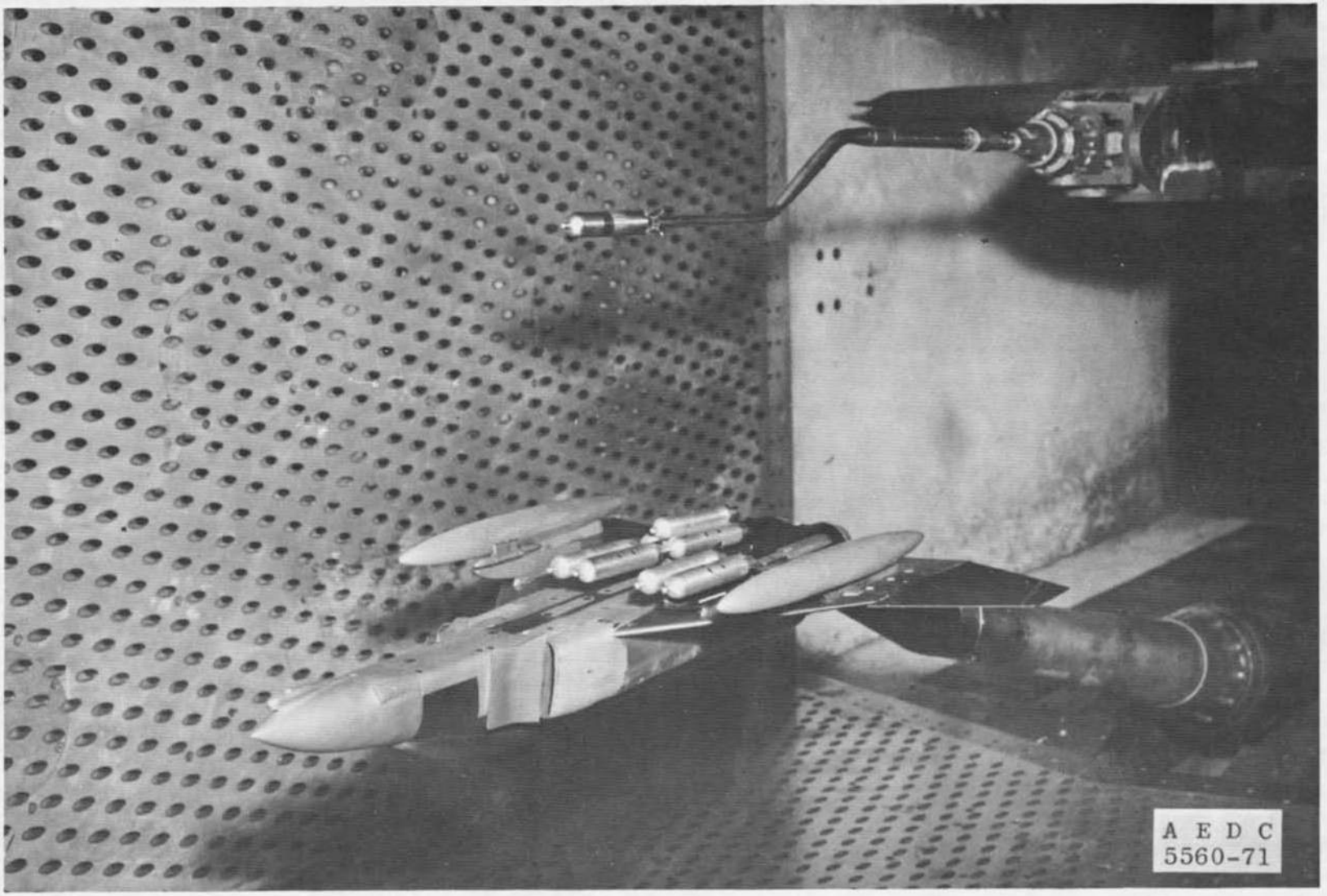

Fig. 3 Photograph of Tunnel Test Section Showing Model Installation

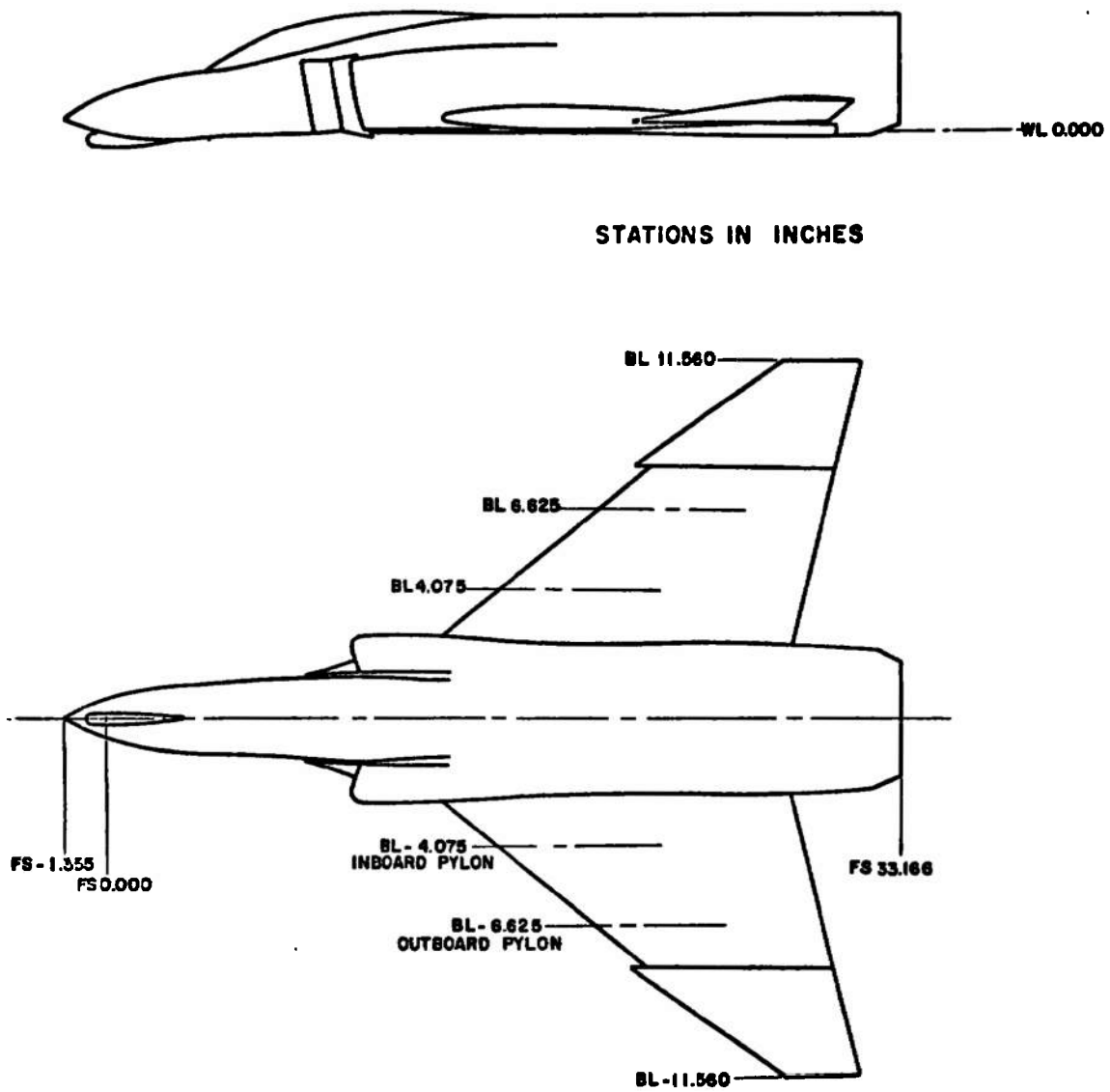

Fig. 4 Sketch of the F-4C Parent-Aircraft Model

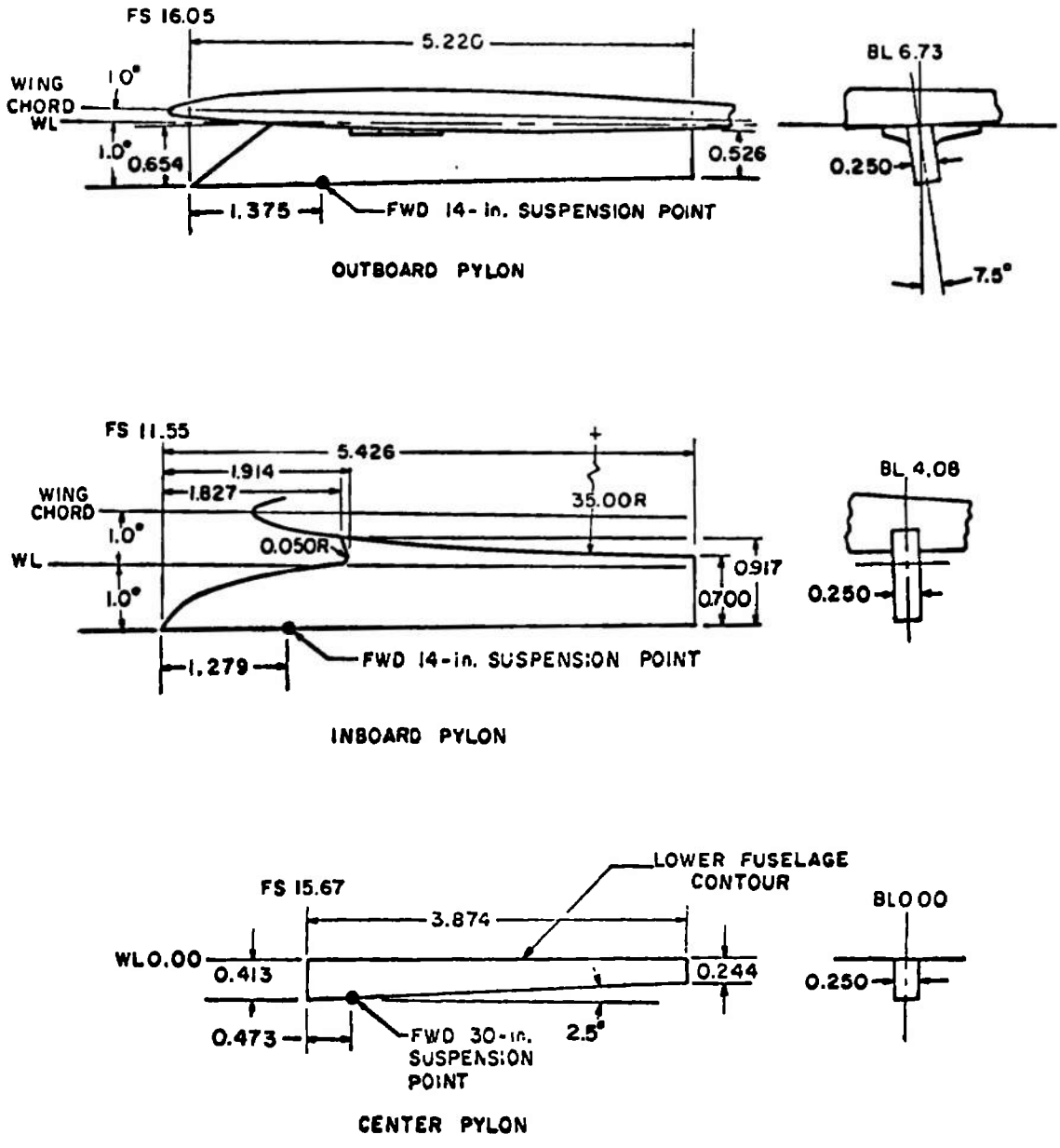

Fig. 5 Details and Dimensions of the F-4C Pylon Models

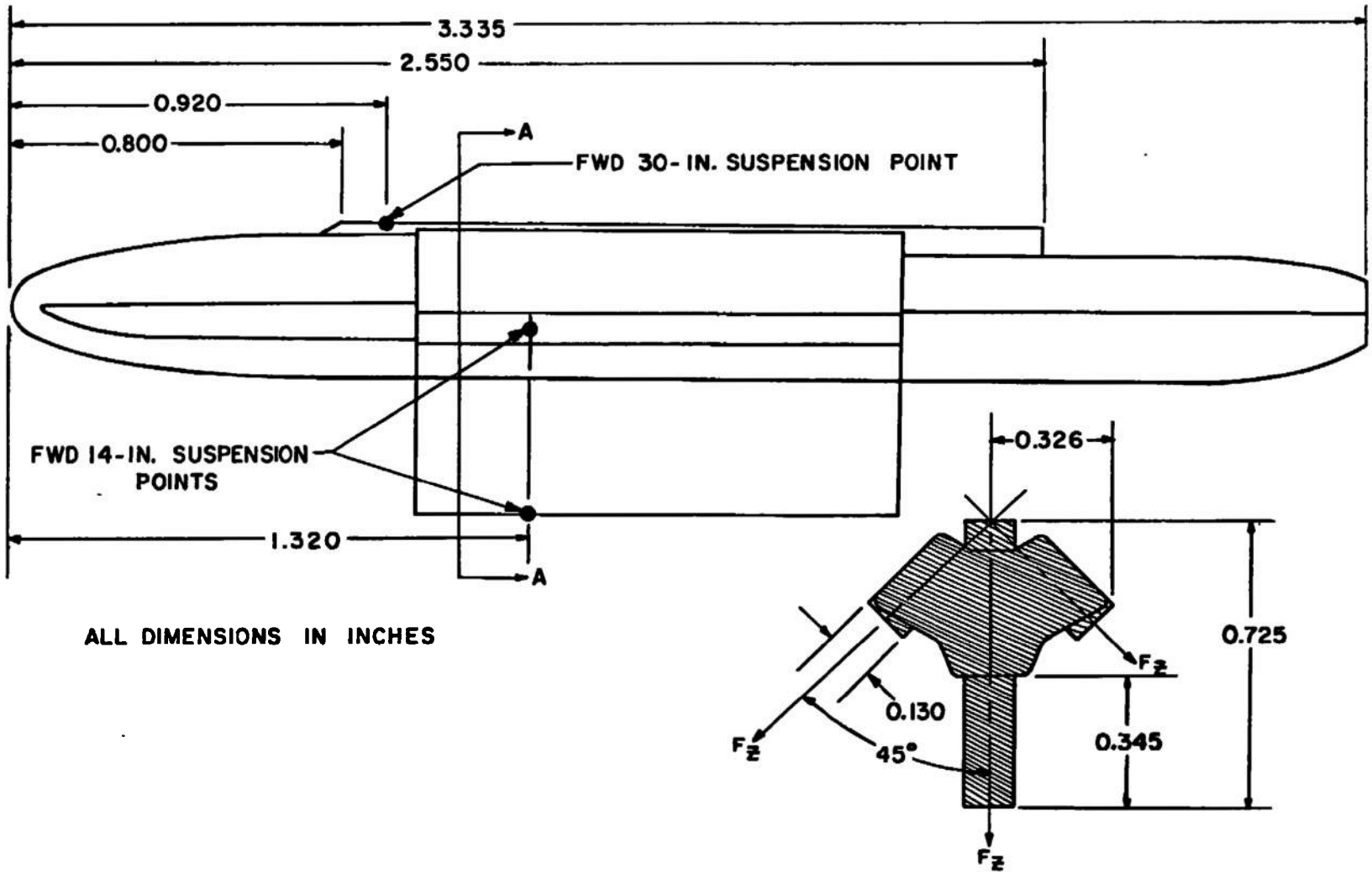

Fig. 6 Details and Dimensions of the TER Model

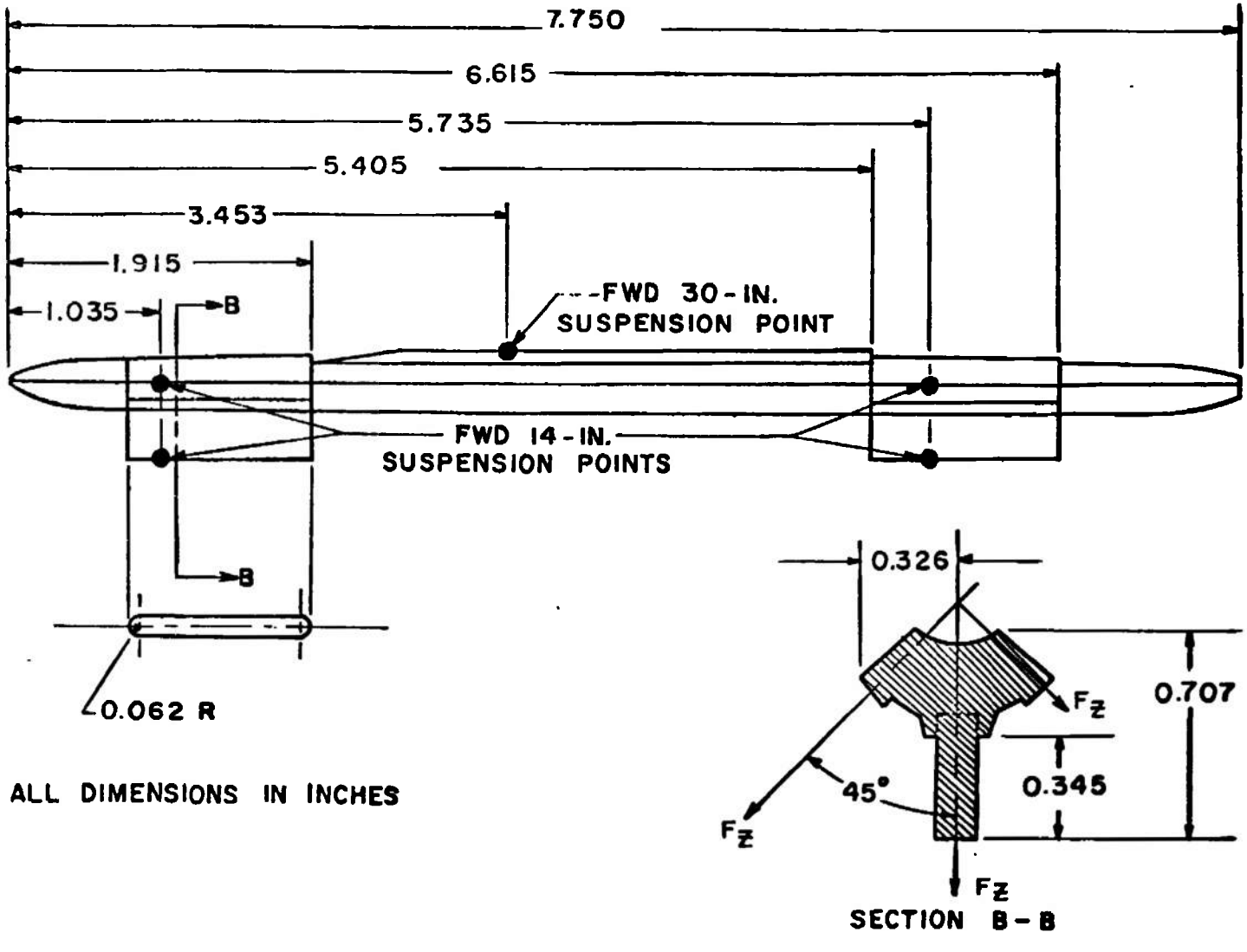

Fig. 7 Details and Dimensions of the MER Model

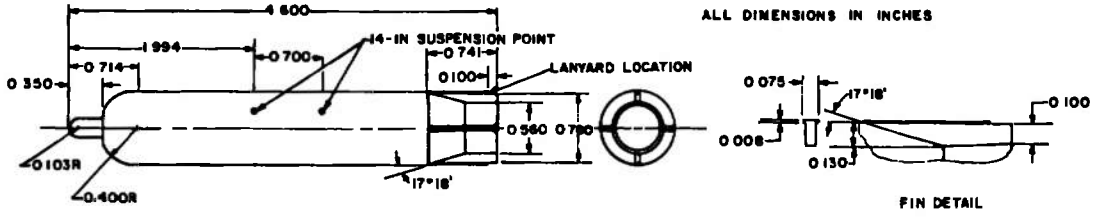

a. Unmodified Folded Fin Model

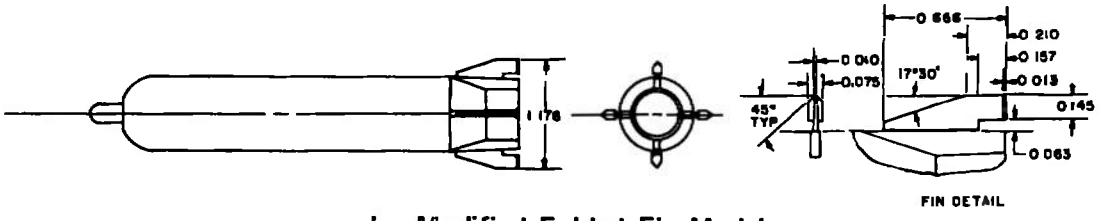

b. Modified Folded Fin Model

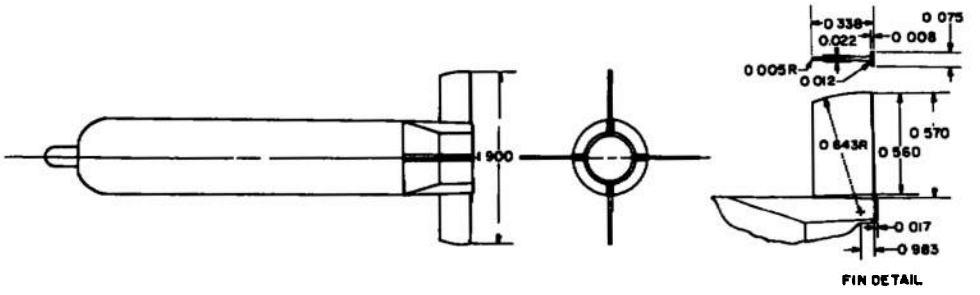

c. Unmodified Extended Fin Model

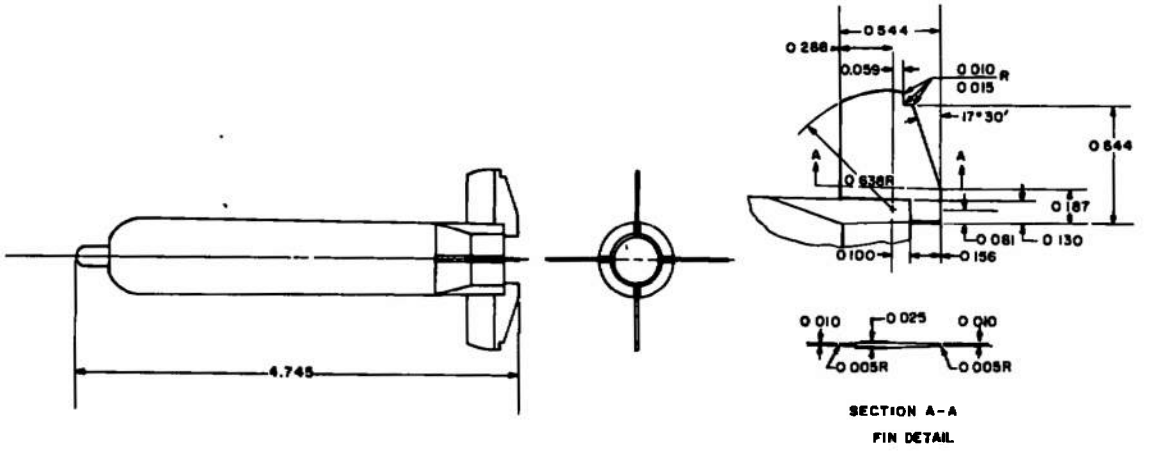

d. Modified Extended Fin Model

Fig. 8 Details and Dimensions of the SUU-51/B Fin Modification

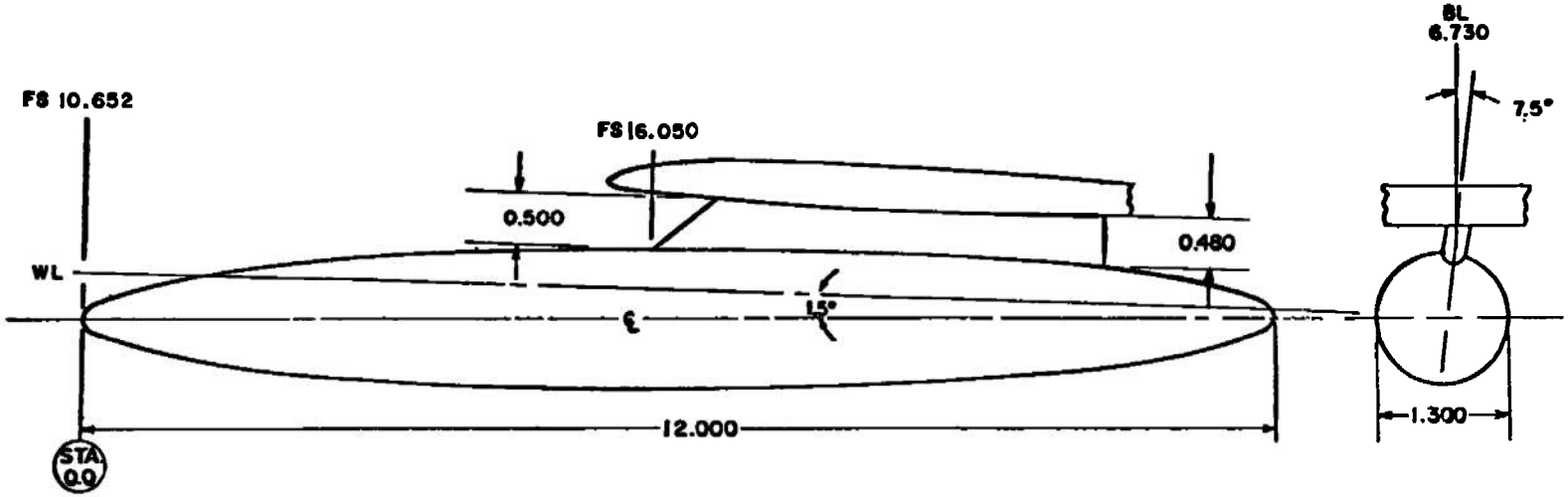

ALL DIMENSIONS AND MODEL STATIONS IN INCHES

BODY CONTOUR, TYPICAL BOTH ENDS

STATION	BODY DIAM	STATION	BODY DIAM
0.000	0.000	2.500	1.116
0.025	0.100	2.750	1.156
0.050	0.144	3.000	1.190
0.150	0.258	3.250	1.218
0.250	0.340	3.500	1.242
0.500	0.498	3.750	1.260
0.750	0.622	4.000	1.274
1.000	0.724	4.250	1.286
1.250	0.812	4.500	1.294
1.500	0.890	4.750	1.298
1.750	0.958	5.000	1.300
2.000	1.016	6.000	1.300
2.250	1.070		

Fig. 9 Details and Dimensions of the Dummy 370-gal Fuel Tank

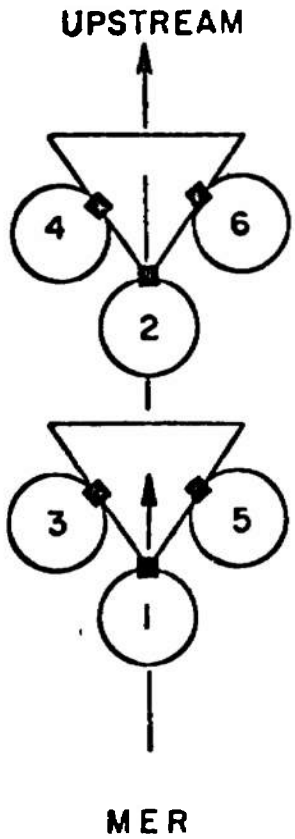

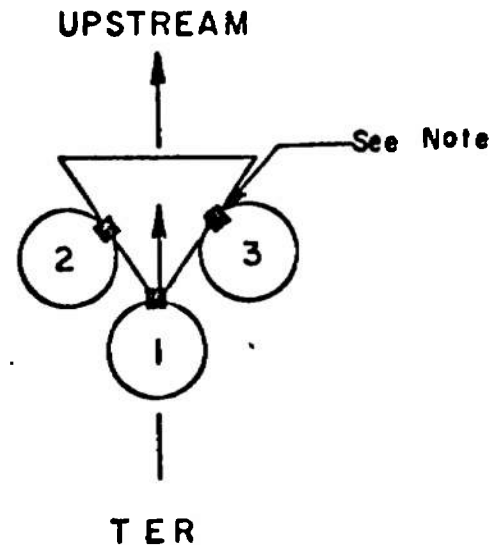

NOTE: The square indicates the orientation of the suspension lugs

TYPE RACK	STATION	ROLL ORIENTATION, deg
MER	1	0
	2	0
	3	45
	4	45
	5	-45
	6	-45
TER	1	0
	2	45
	3	-45

Fig. 10 Schematic of the TER and MER Store Stations and Orientation

CONFIGURATION 1

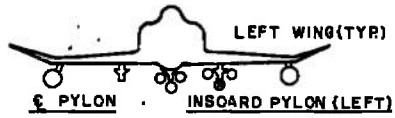

℄ PYLON	INSOARD PYLON (LEFT)
MER STA. 1 : DUMMY	TER STA. 1 : LAUNCH
MER STA. 2. EMPTY	TER STA 2. DUMMY
MER STA. 3 : DUMMY	TER STA.3 : DUMMY
MER STA.4 : DUMMY	
MER STA.5 : DUMMY	
MER STA. 6 : DUMMY	

CONFIGURATION 2

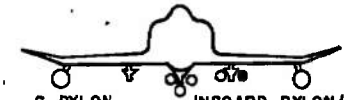

℄ PYLON	INSOARD PYLON (LEFT)
MER STA 1 . DUMMY	TER STA.1 : EMPTY
MER STA.2 . EMPTY	TER STA.2 : LAUNCH
MER STA.3 : DUMMY	TER STA. 3 : DUMMY
MER STA.4 . DUMMY	
MER STA.5. DUMMY	
MER STA.6 . DUMMY	

CONFIGURATION 3

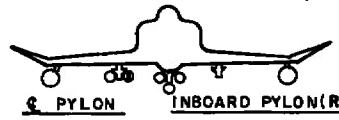

℄ PYLON	INBOARD PYLON (RIGHT)
MER STA. 1 : DUMMY	TER STA 1 : EMPTY
MER STA 2 . EMPTY	TER STA 2. LAUNCH
MER STA. 3 DUMMY	TER STA. 3 DUMMY
MER STA 4 . DUMMY	
MER STA. 5 . DUMMY	
MER STA. 6 : DUMMY	

CONFIGURATION 4

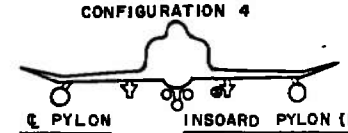

℄ PYLON	INSOARD PYLON (LEFT)
MER STA. 1 . DUMMY	TER STA. 1 : EMPTY
MER STA. 2 : EMPTY	TER STA. 2 : EMPTY
MER STA 3. DUMMY	TER STA 3 : LAUNCH
MER STA. 4 DUMMY	
MER STA. 5 : DUMMY	
MER STA. 6 : DUMMY	

CONFIGURATION 5

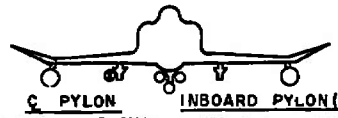

℄ PYLON	INBOARD PYLON (RIGHT)
MER STA. 1 : DUMMY	TER STA. 1 : EMPTY
MER STA. 2 : EMPTY	TER STA. 2 . EMPTY
MER STA. 3 : DUMMY	TER STA. 3 : LAUNCH
MER STA. 4 : DUMMY	
MER STA 5 : DUMMY	
MER STA. 6 : DUMMY	

CONFIGURATION 6

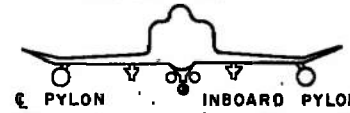

℄ PYLON	INBOARD PYLON (LEFT)
MER STA. 1 : LAUNCH	TER
MER STA. 2 : EMPTY	
MER STA. 3 : DUMMY	
MER STA 4 : DUMMY	
MER STA. 5 : DUMMY	
MER STA. 6 : DUMMY	

CONFIGURATION 7

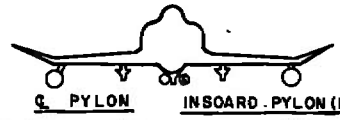

℄ PYLON	INSOARD PYLON (LEFT)
MER STA. 1 : EMPTY	TER
MER STA. 2 : EMPTY	
MER STA. 3 LAUNCH	
MER STA. 4 : DUMMY	
MER STA. 5 : DUMMY	
MER STA. 6 : DUMMY	

CONFIGURATION 8

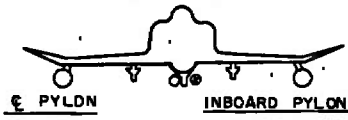

℄ PYLON	INBOARD PYLON (LEFT)
MER STA. 1 : EMPTY	TER
MER STA. 2 . EMPTY	
MER STA. 3 : EMPTY	
MER STA. 4 : LAUNCH	
MER STA. 5 : DUMMY	
MER STA 6 : DUMMY	

CONFIGURATION 10

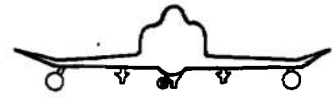

℄ PYLON	INBOARD PYLON (LEFT)
MER STA 1 : EMPTY	TER
MER STA. 2 : EMPTY	
MER STA. 3 : EMPTY	
MER STA. 4 : EMPTY	
MER STA. 5 : EMPTY	
MER STA. 6 . DUMMY	

CONFIGURATION 11

℄ PYLON	INBOARD PYLON (RIGHT)
MER STA. 1 : DUMMY	TER STA. 1 . LAUNCH
MER STA. 2 : EMPTY	TER STA 2 : DUMMY
MER STA 3 : DUMMY	TER STA 3 : EMPTY
MER STA. 4 DUMMY	
MER STA 5 DUMMY	
MER STA 6 . DUMMY	

NOTES

(1) EMPTY TER ON LEFT INBOARD PYLON AND 370 GALLON FUEL TANKS ON OUTBOARD PYLONS FOR ALL CONFIGURATIONS TESTED

(2) ALL LEFT-WING RELEASES WERE SIMULATED BY RELEASES FROM THE RIGHT WING

(3) ⊗ = LAUNCH-STORE

Fig. 11 F-4C Load Configurations

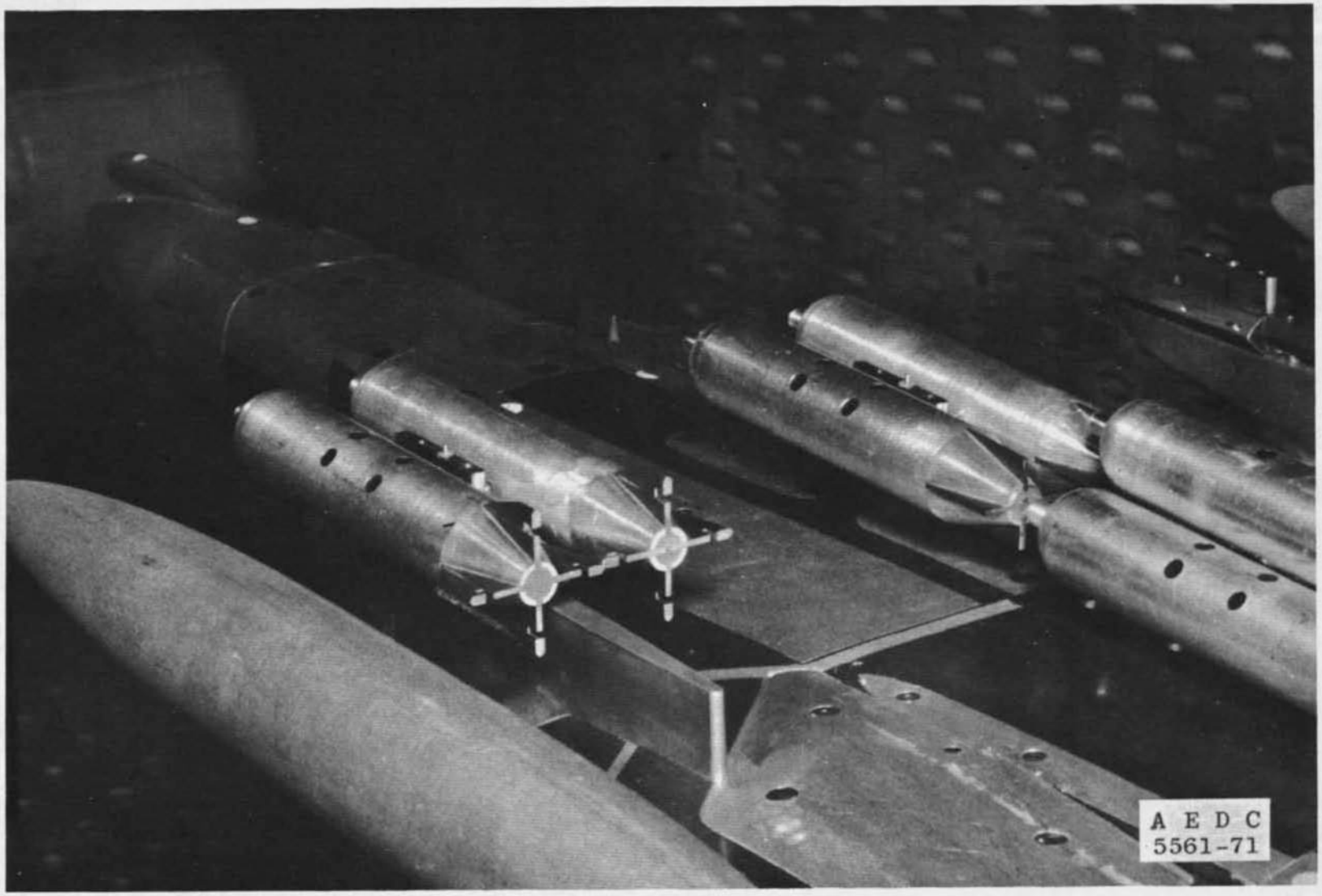

Fig. 12 Load Configuration 1

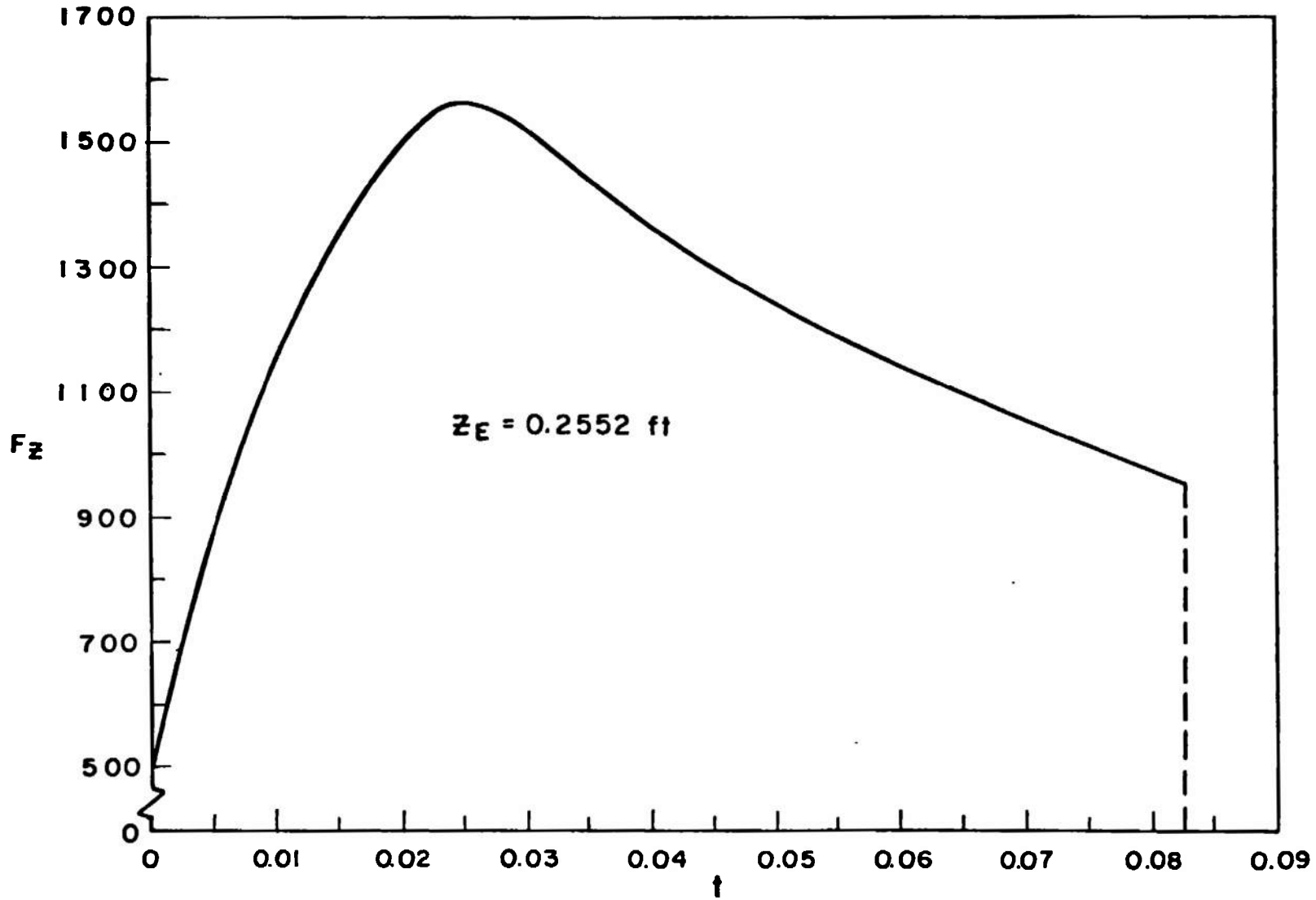

Fig. 13 TER and MER Ejector Force Function

SYM	CONF	M_∞	α_p	$\bar{\theta}$	$\bar{X}$
⊡	2	0.66	1.6	0	NOM
⊙	2	0.66	1.6	0	FWD

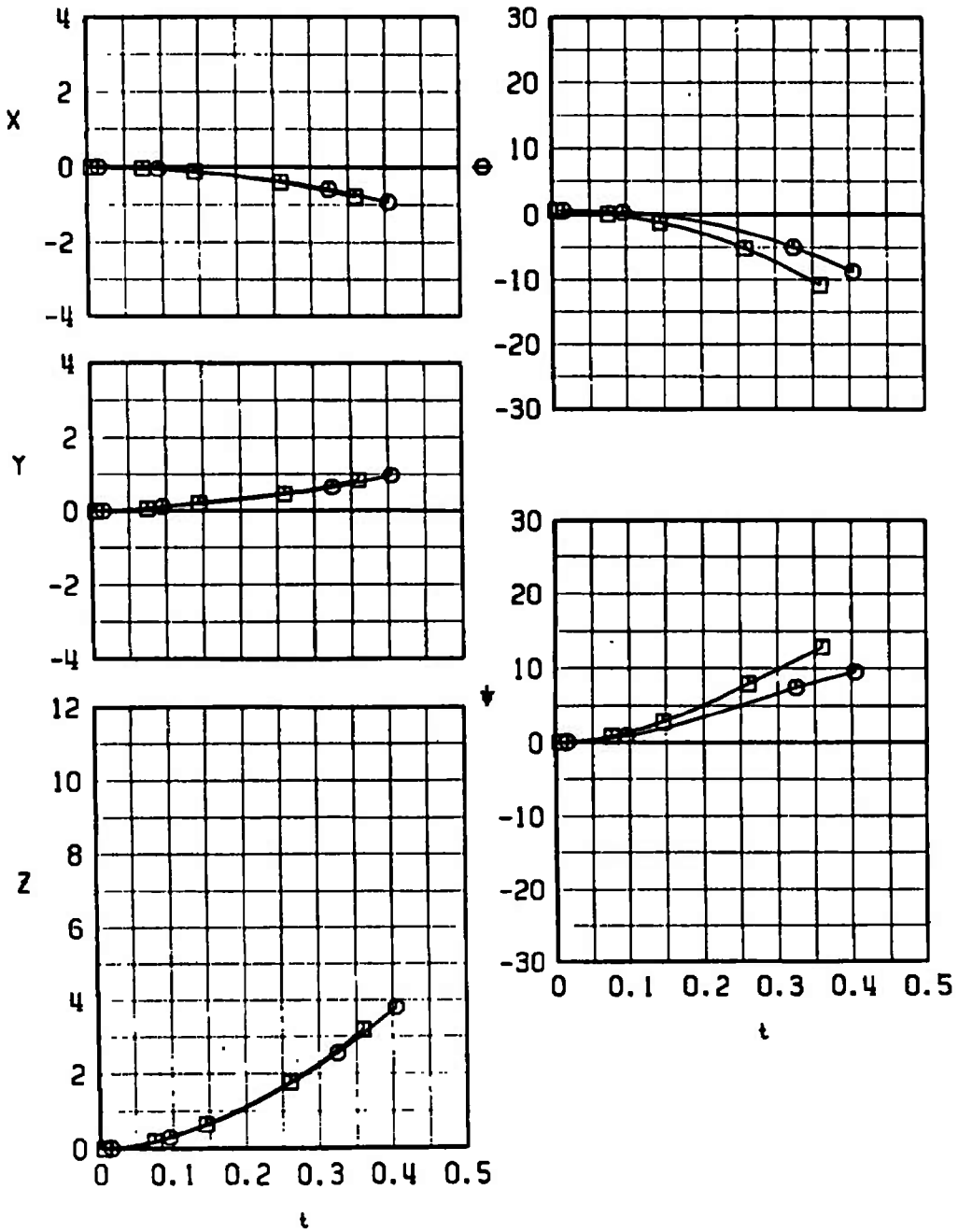

a. $M_\infty = 0.66$

Fig. 14 Effect of Store Center-of-Gravity Location on Store Separation Characteristics for Load Configuration 2

SYM	CONF	M_∞	α_p	$\bar{e}$	$\bar{X}$
⊡	2	0.74	0.9	0	NOM
⊙	2	0.74	0.9	0	FWD

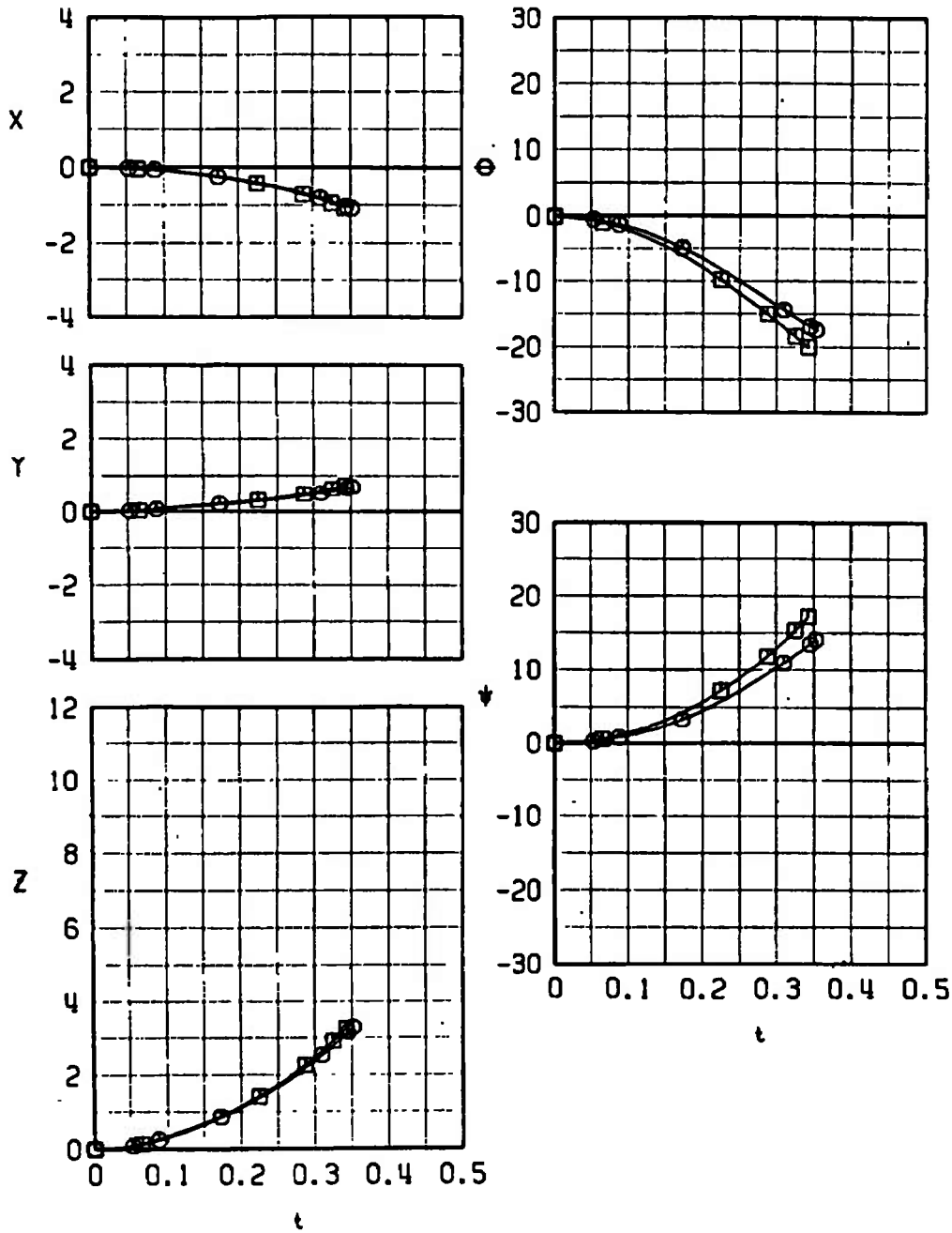

b. $M_\infty = 0.74$

Fig. 14 Continued

SYM	CONF	M_∞	α_p	$\bar{\phi}$	$\bar{X}$
⊡	2	0.82	0.4	0	NOM
⊙	2	0.82	0.4	0	FWD

FLAGGED SYMBOLS INDICATE EXTENDED FIN DATA

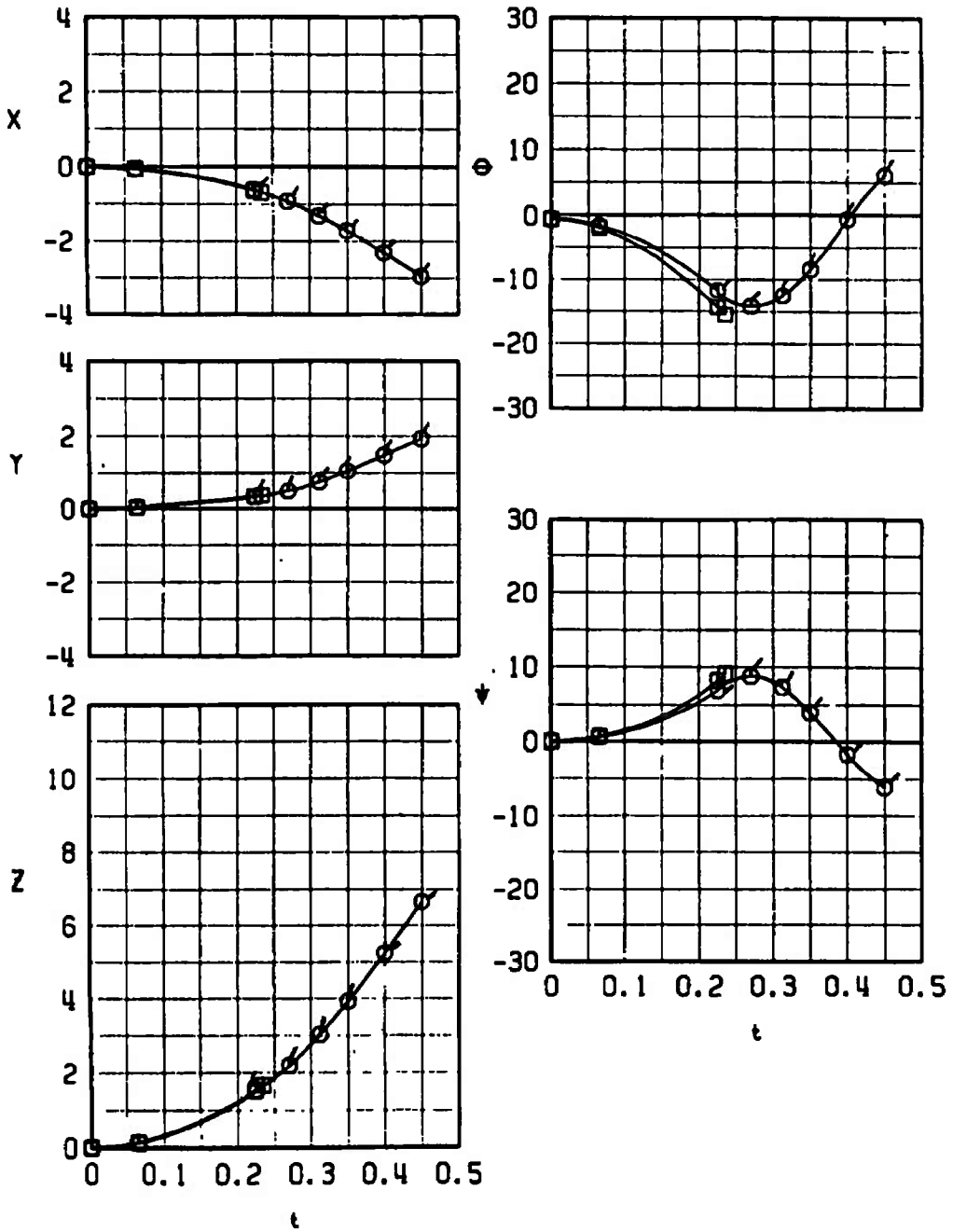

c. $M_\infty = 0.82$

Fig. 14 Concluded

SYM	CONF	M_∞	α_p	$\bar{\theta}$	$\bar{X}$
⊡	4	0.66	1.6	0	NOM
⊙	4	0.66	1.6	0	FWD

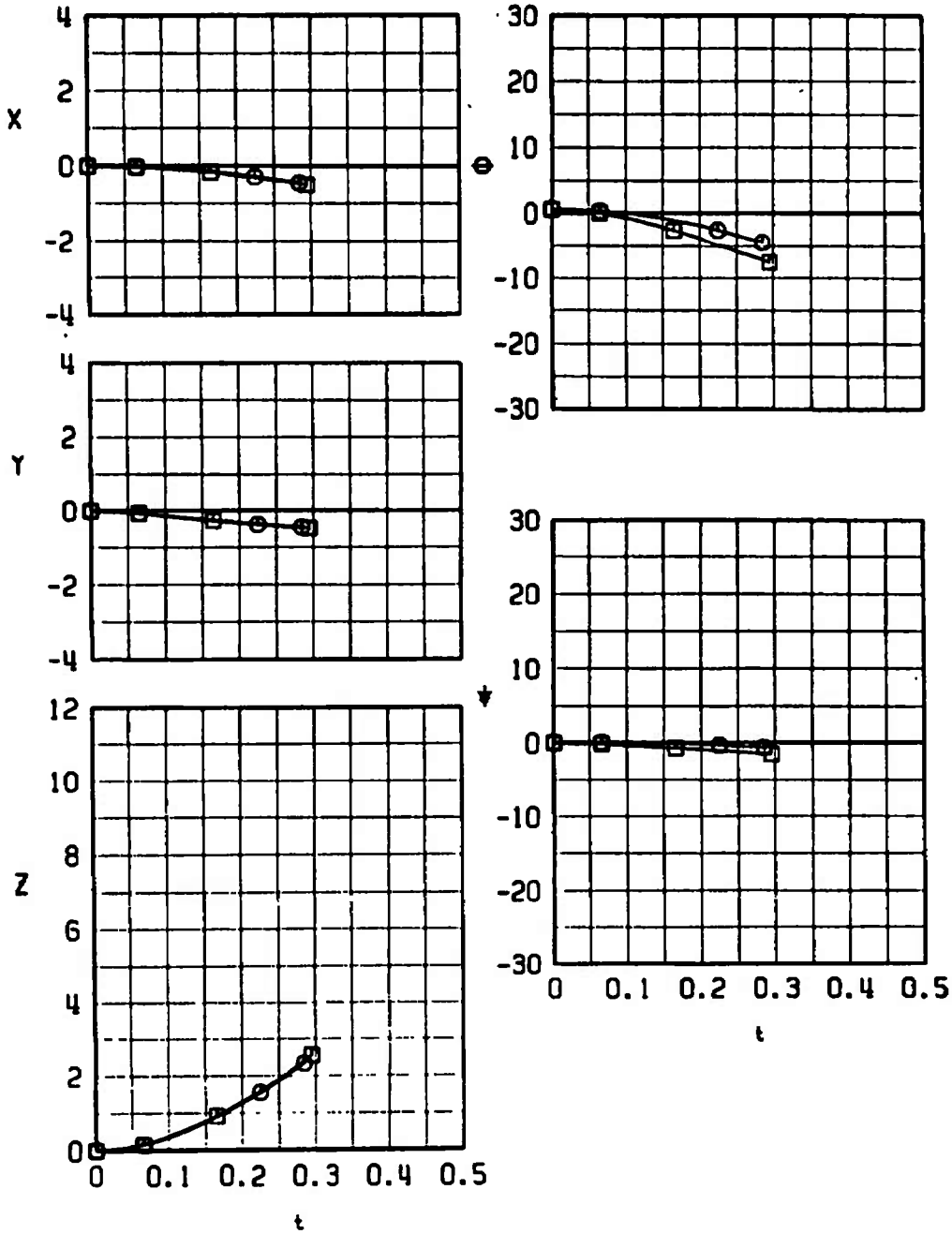

a. $M_\infty = 0.66$

Fig. 15 Effect of Store Center-of-Gravity Location on Store Separation Characteristics for Load Configuration 4

SYM	CONF	M_∞	α_p	$\bar{\Phi}$	$\bar{X}$
⊡	4	0.74	0.9	0	NOM
⊙	4	0.74	0.9	0	FWD

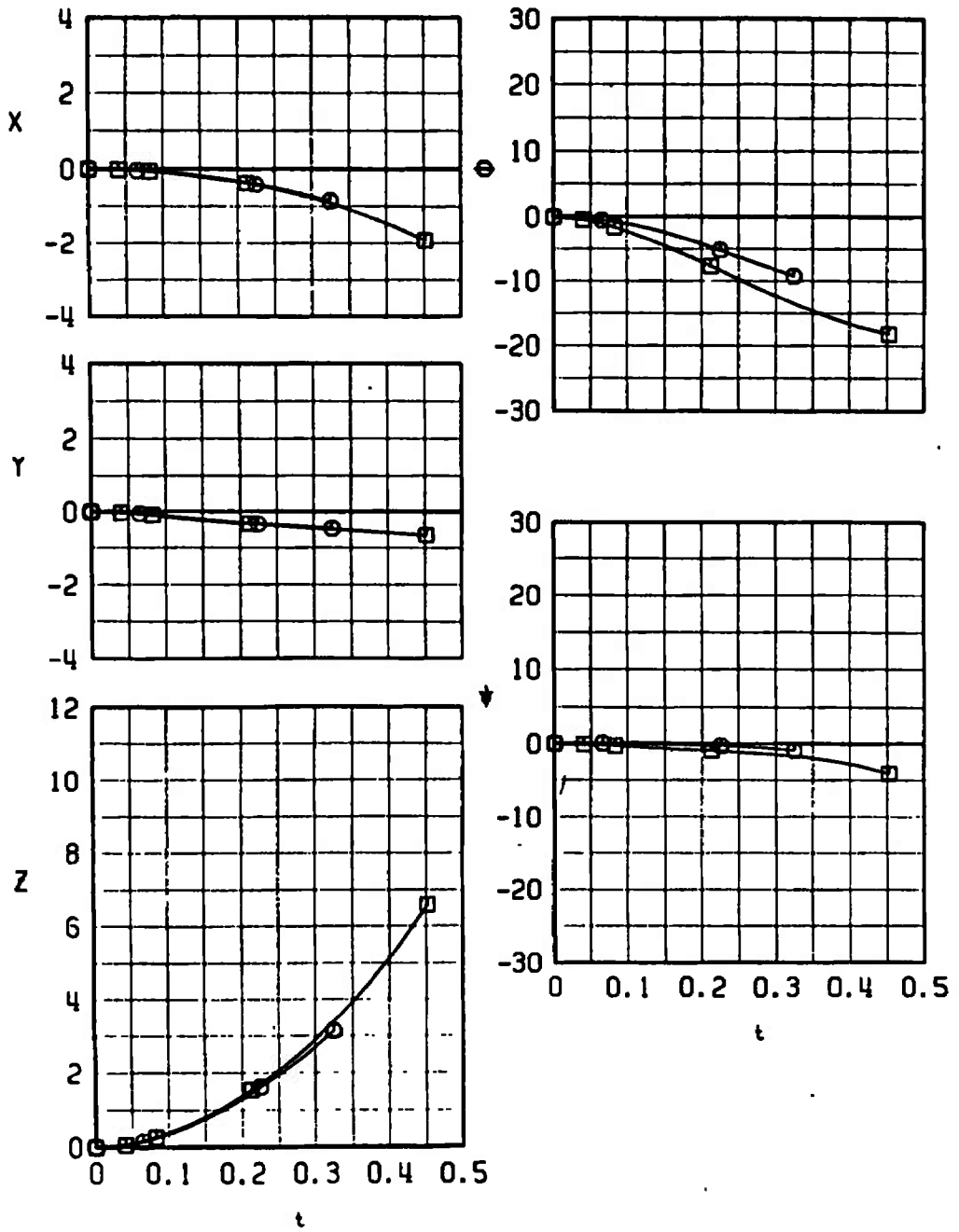

b. $M_\infty = 0.74$

Fig. 15 Continued

SYM	CONF	M_∞	α_p	$\bar{\delta}$	$\bar{X}$
⊡	4	0.82	0.4	0	NOM
⊙	4	0.82	0.4	0	FWD

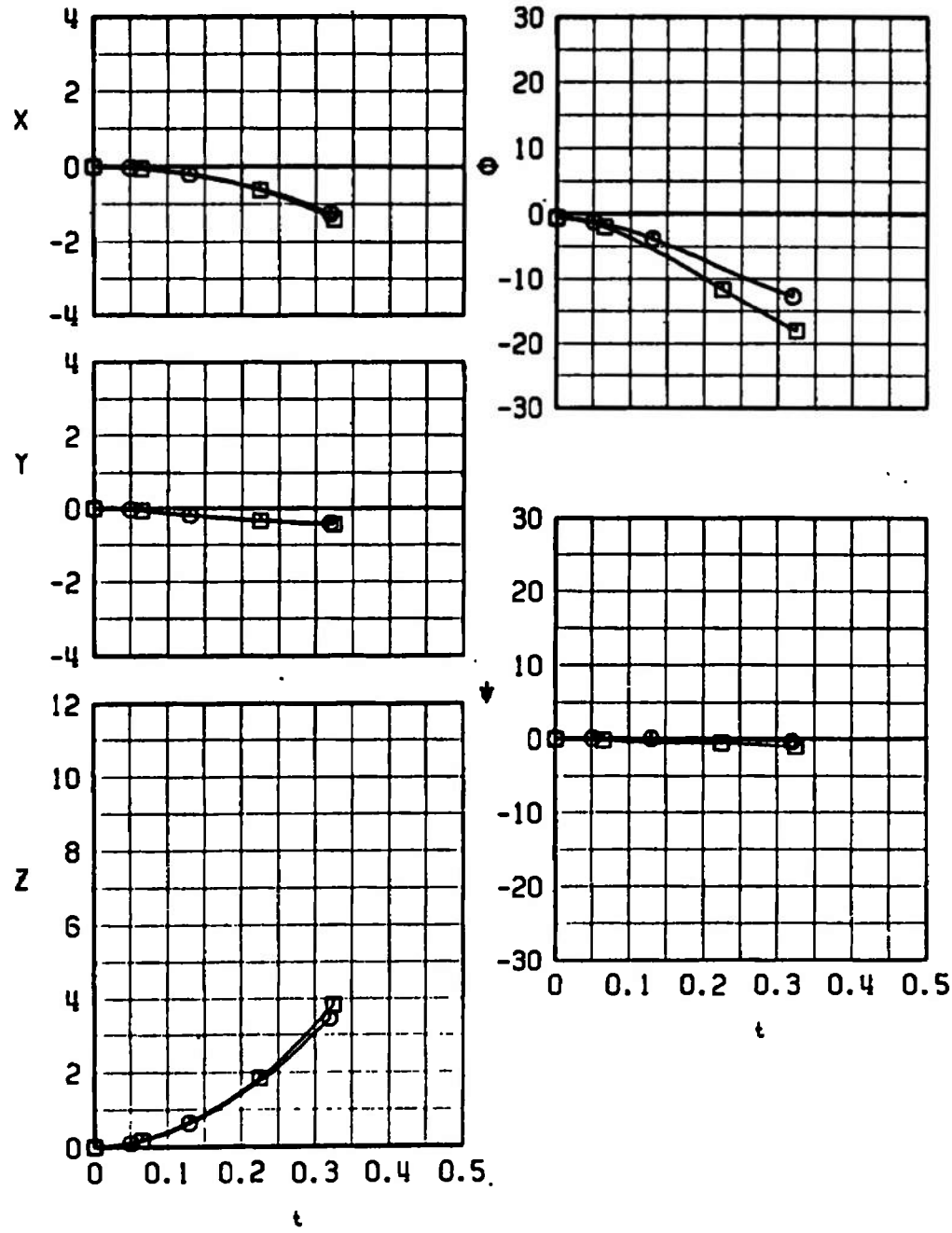

c. $M_\infty = 0.82$
Fig. 15 Continued

SYM	CONF	M_∞	α_p	$\bar{\Phi}$	$\bar{X}$
⊡	4	0.90	0.1	0	NOM
⊙	4	0.90	0.1	0	FWD

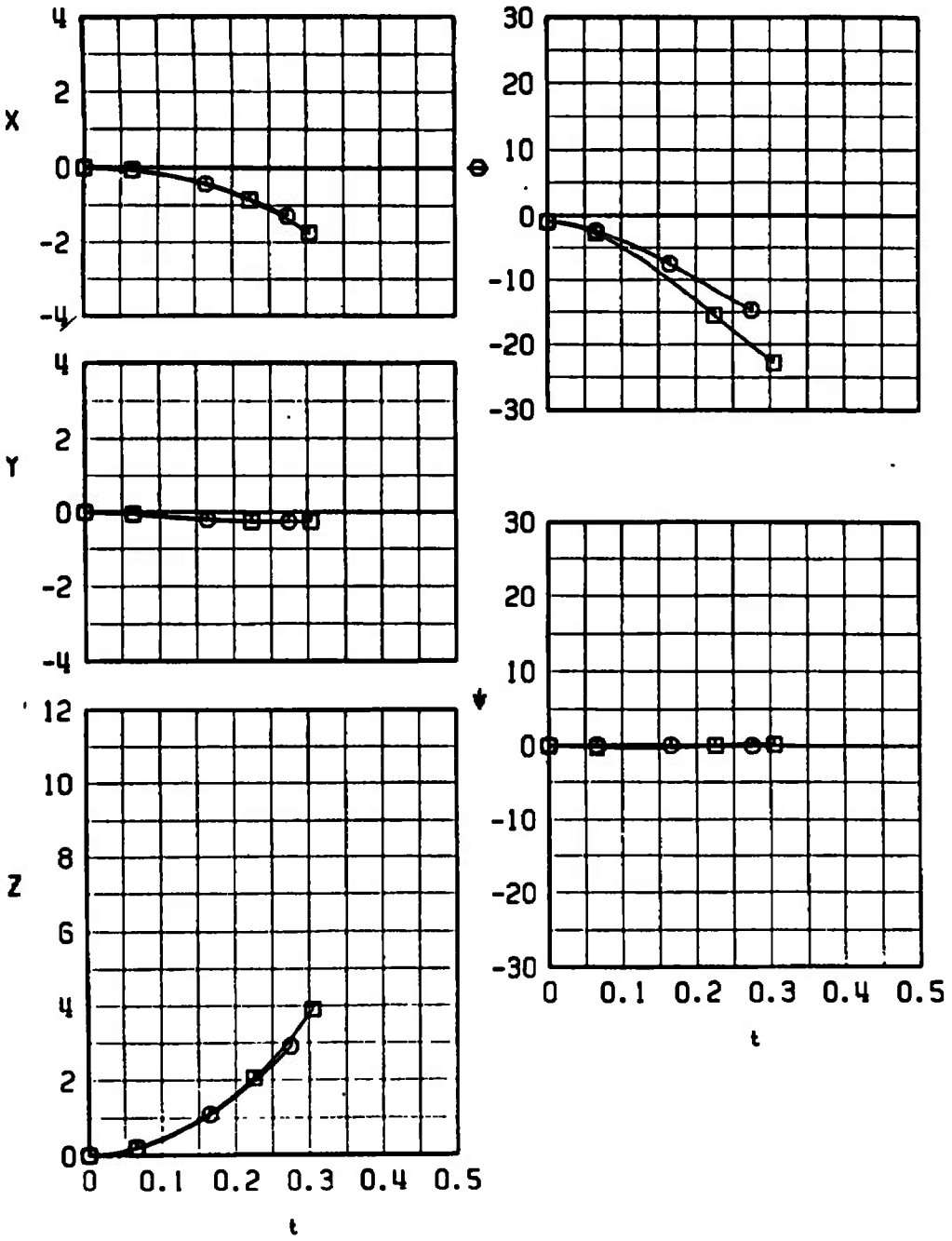

d. $M_\infty = 0.90$

Fig. 15 Concluded

SYM	CONF	M_∞	α_p	$\bar{\theta}$	$\bar{X}$
⊡	5	0.66	1.6	0	NOM
⊙	5	0.66	1.6	0	FWD

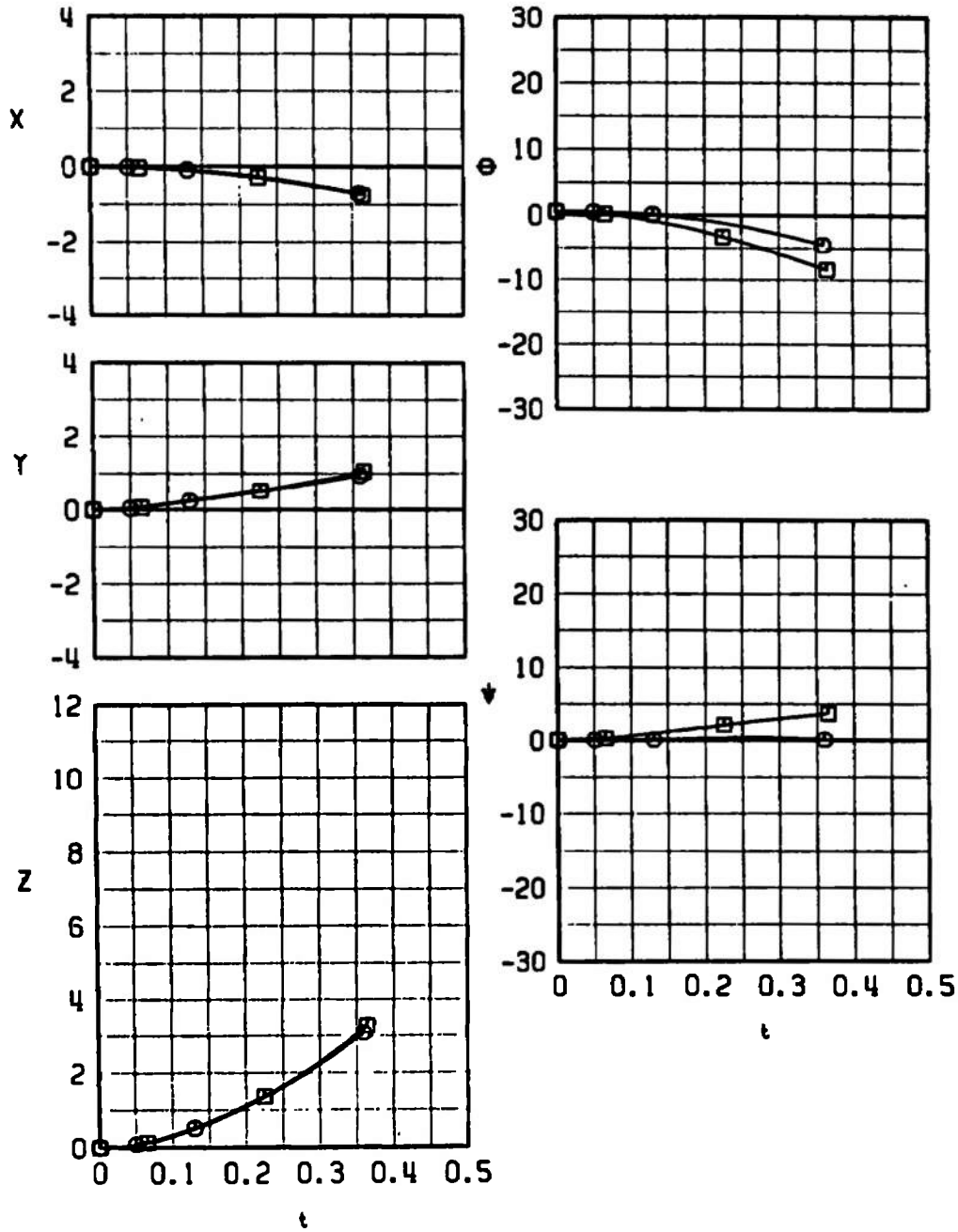

a. $M_\infty = 0.66$

Fig. 16 Effect of Store Center-of-Gravity Location on Store Separation Characteristics for Load Configuration 5

SYM	CONF	M_∞	α_p	$\bar{\phi}$	$\bar{X}$
⊡	5	0.74	0.9	0	NOM
⊙	5	0.74	0.9	0	FWD

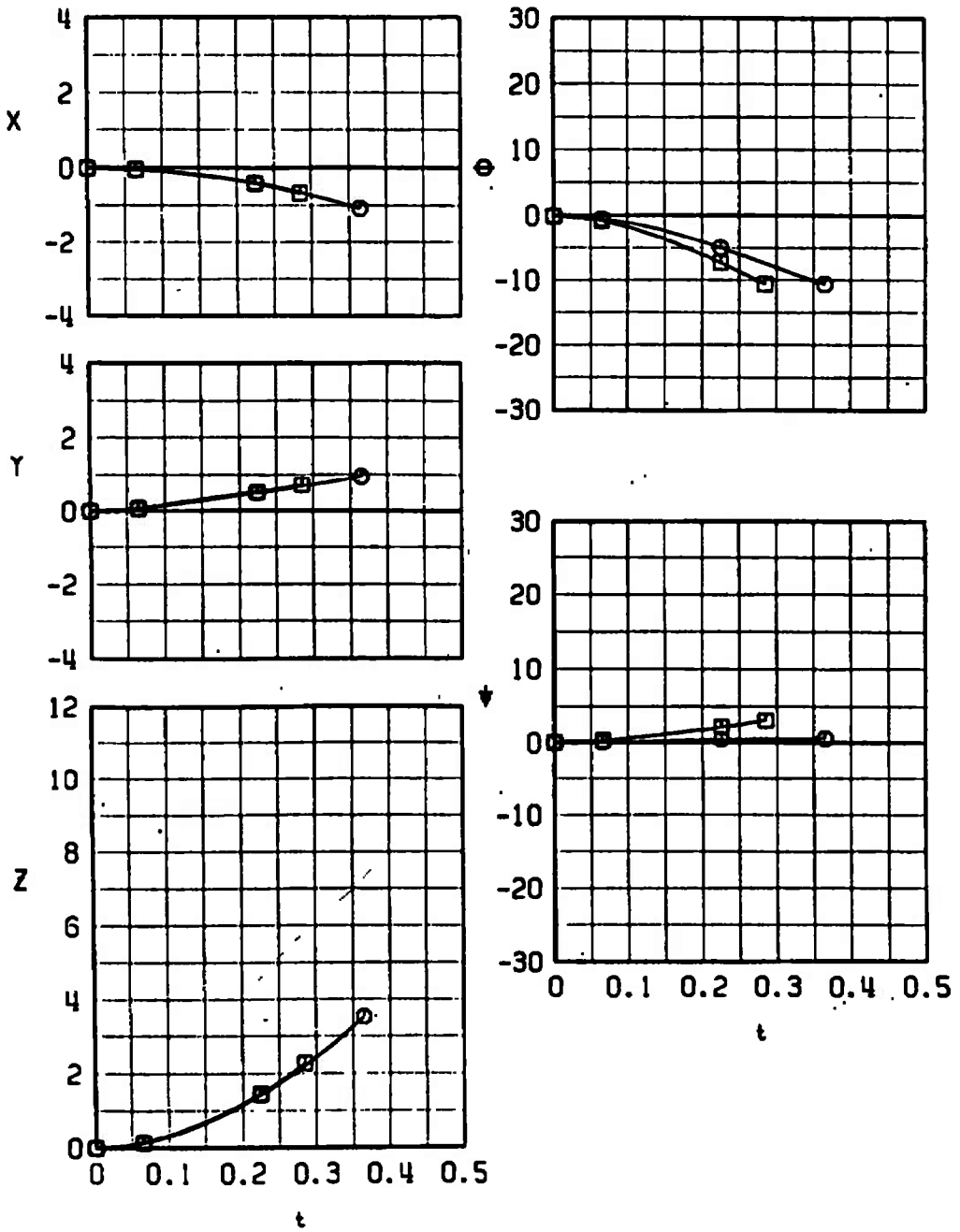

b. $M_\infty = 0.74$
Fig. 16 Continued

SYM	CONF	M_∞	α_p	$\bar{e}$	$\bar{X}$
⊡	5	0.82	0.4	0	NOM
⊙	5	0.82	0.4	0	FWD

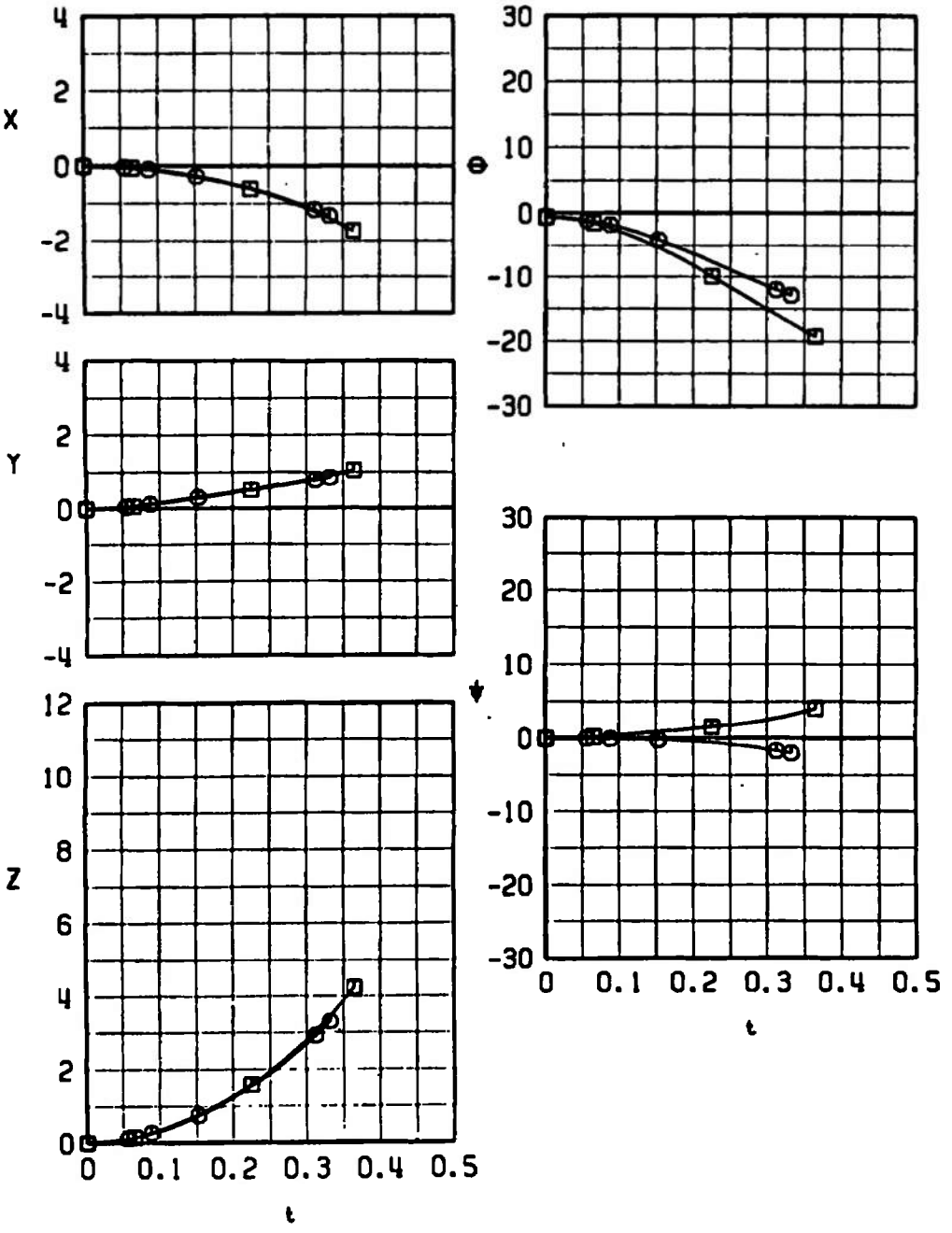

c. $M_\infty = 0.82$

Fig. 16 Continued

SYM	CONF	M_∞	α_p	$\bar{\phi}$	$\bar{X}$
□	5	0.90	0.1	0	NOM
○	5	0.90	0.1	0	FWD

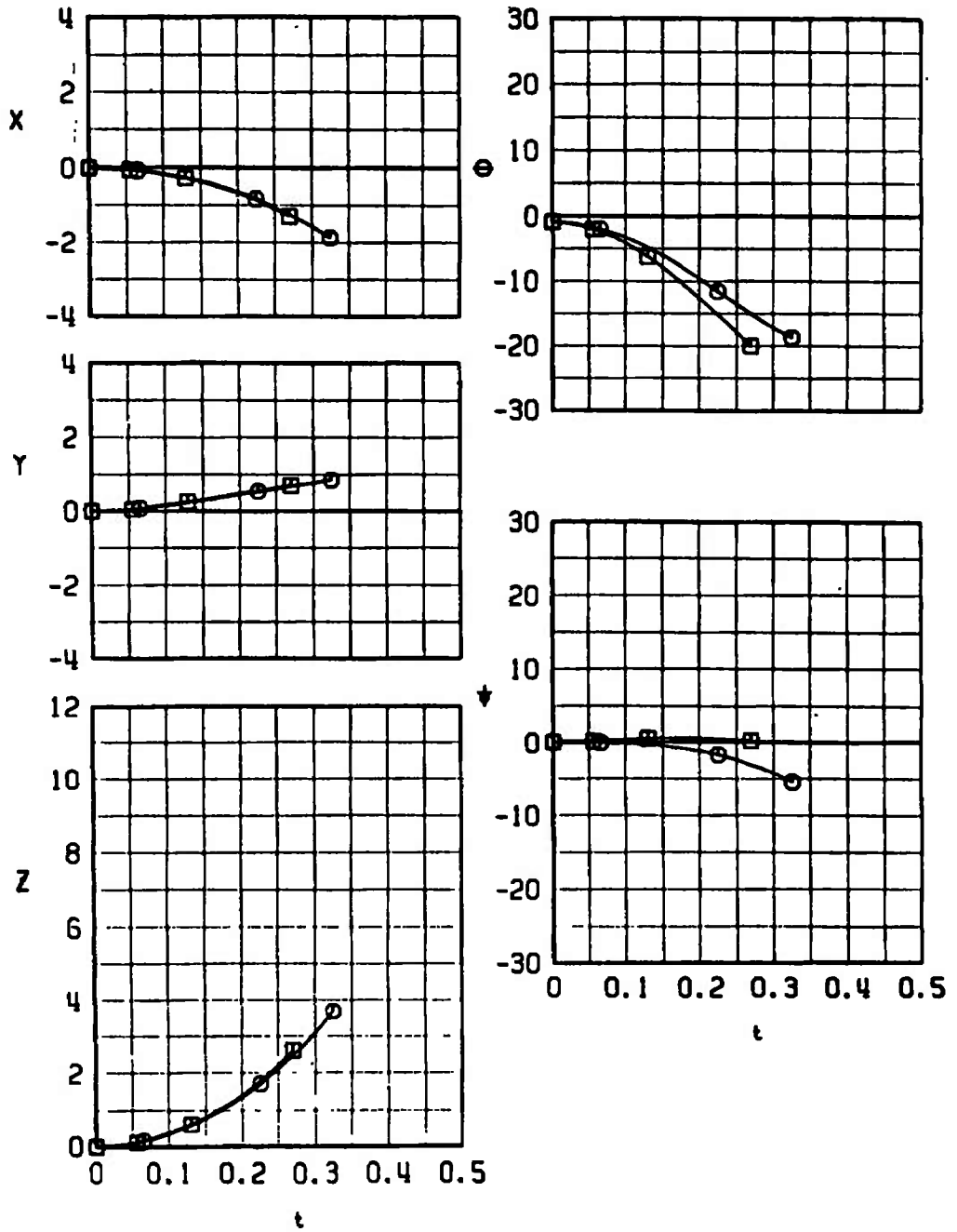

d. $M_\infty = 0.90$
Fig. 16 Concluded

SYM	CONF	M_∞	α_p	$\bar{\theta}$	$\bar{X}$
□	2	0.66	1.6	0	FWD
○	2	0.74	0.9	0	FWD
△	2	0.82	0.4	0	FWD

FLAGGED SYMBOLS INDICATE EXTENDED FIN DATA

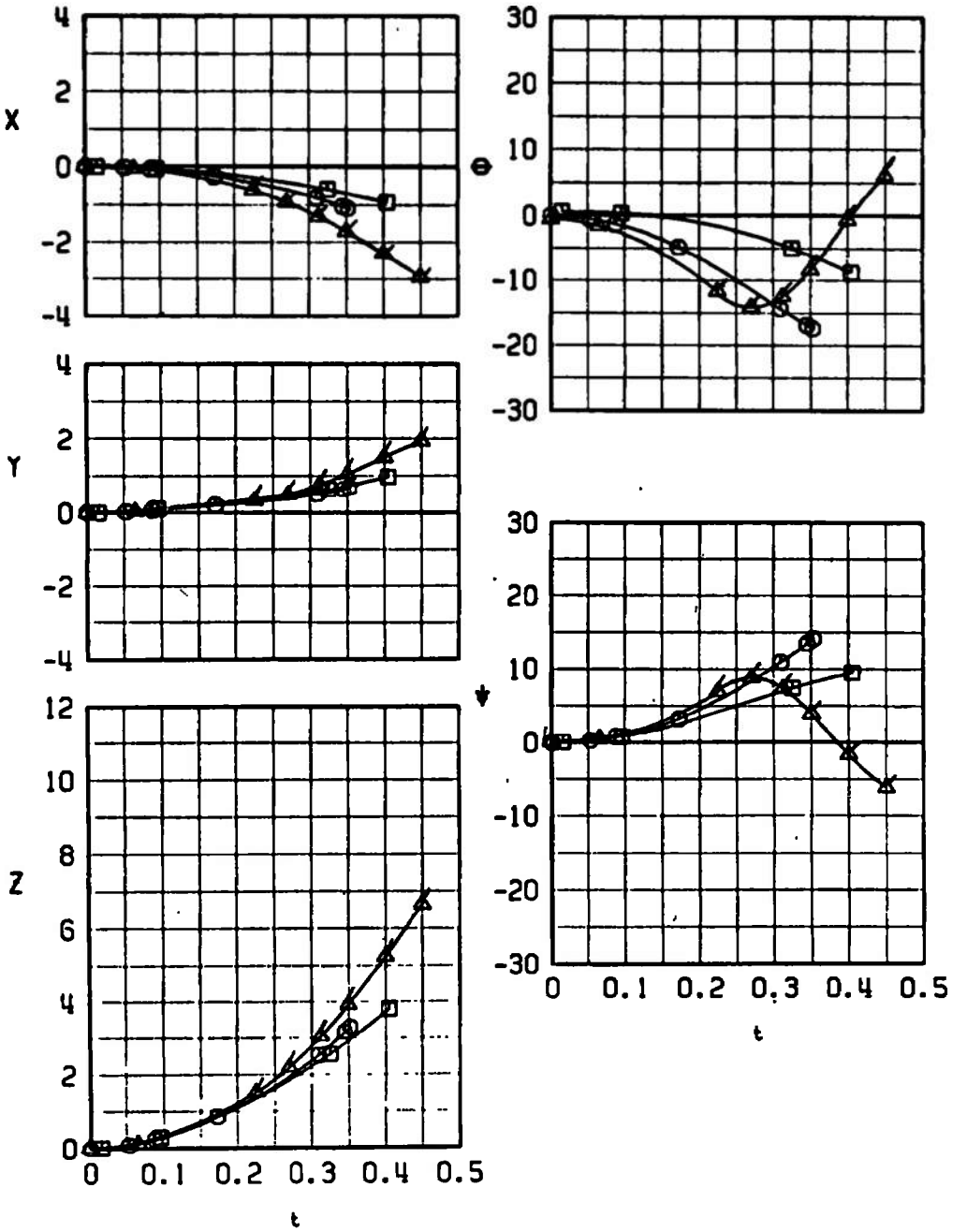

a. Configuration 2

Fig. 17 Effect of Mach Number on the Forward Shifted Center-of-Gravity Store Separation Characteristics

SYM	CONF	M_∞	α_p	$\bar{\theta}$	$\bar{X}$
□	3	0.66	1.6	0	FWD
△	3	0.82	0.4	0	FWD
◁	3	0.90	0.1	0	FWD

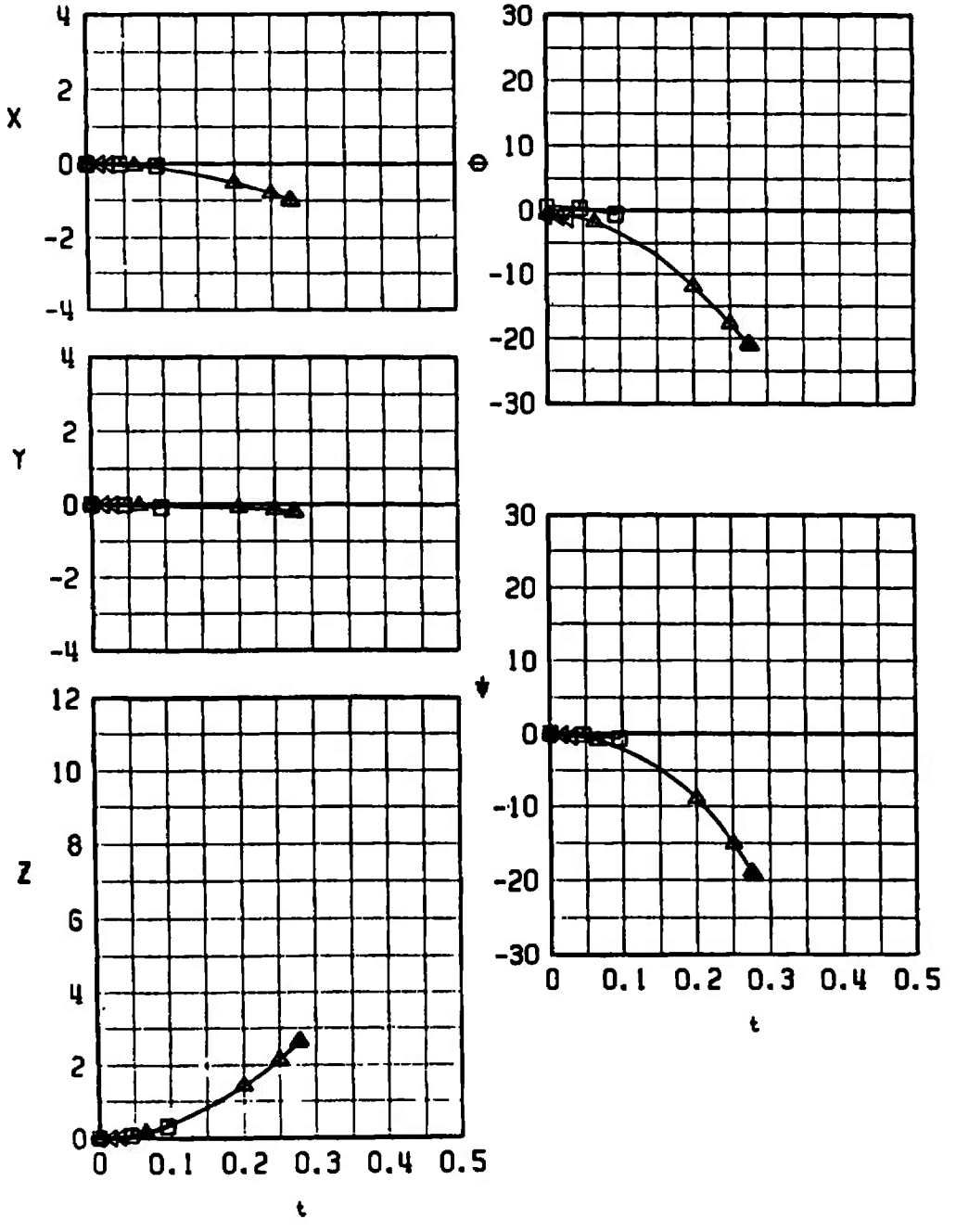

b. Configuration 3
Fig. 17 Continued

SYM	CONF	M_∞	α_p	$\bar{\theta}$	$\bar{X}$
□	4	0.66	1.6	0	FWD
○	4	0.74	0.9	0	FWD
△	4	0.82	0.4	0	FWD
◁	4	0.90	0.1	0	FWD

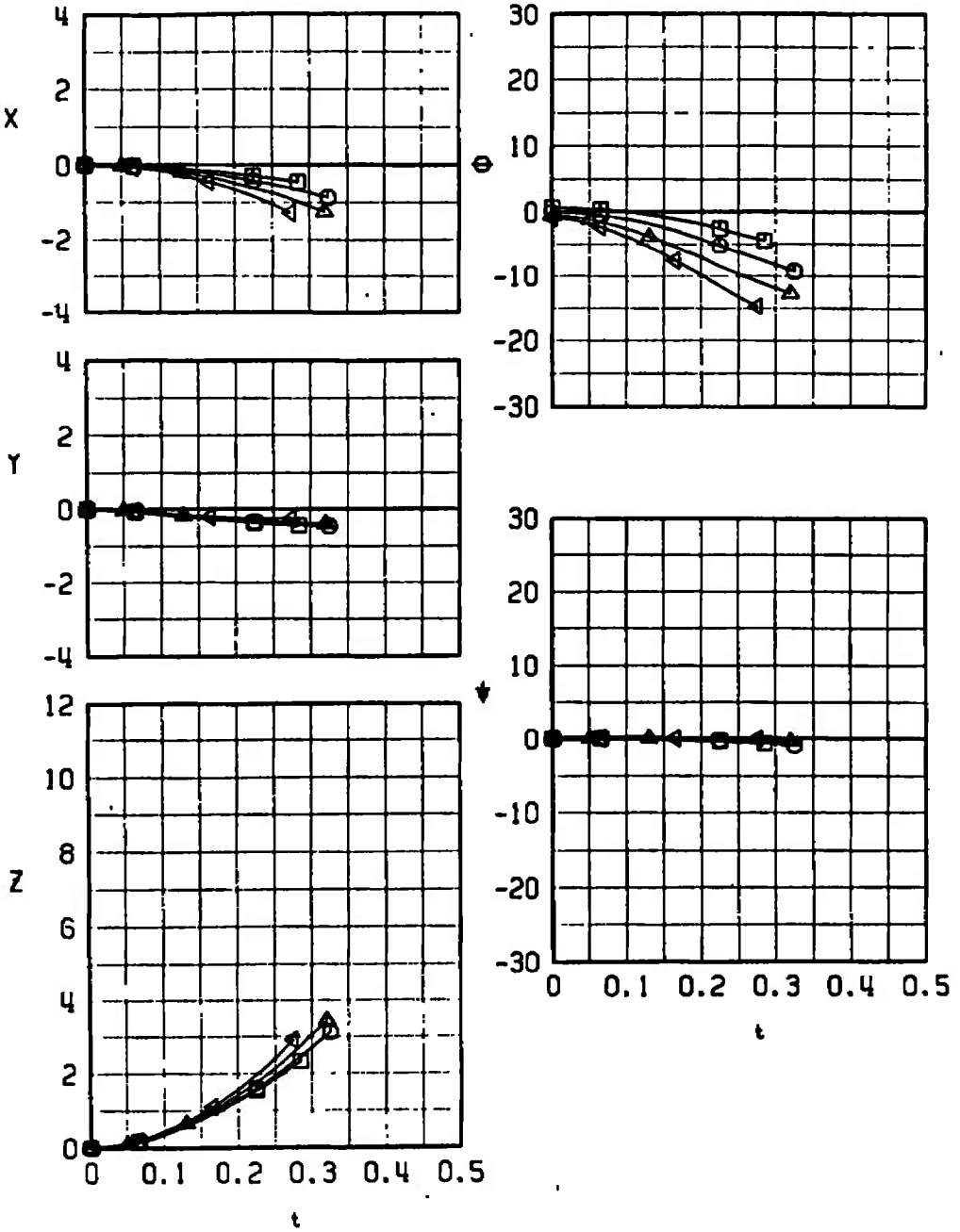

c. Configuration 4
Fig. 17 Continued

SYM	CONF	M_∞	α_p	$\bar{\theta}$	$\bar{X}$
□	5	0.66	1.6	0	FWD
○	5	0.74	0.9	0	FWD
△	5	0.82	0.4	0	FWD
◁	5	0.90	0.1	0	FWD

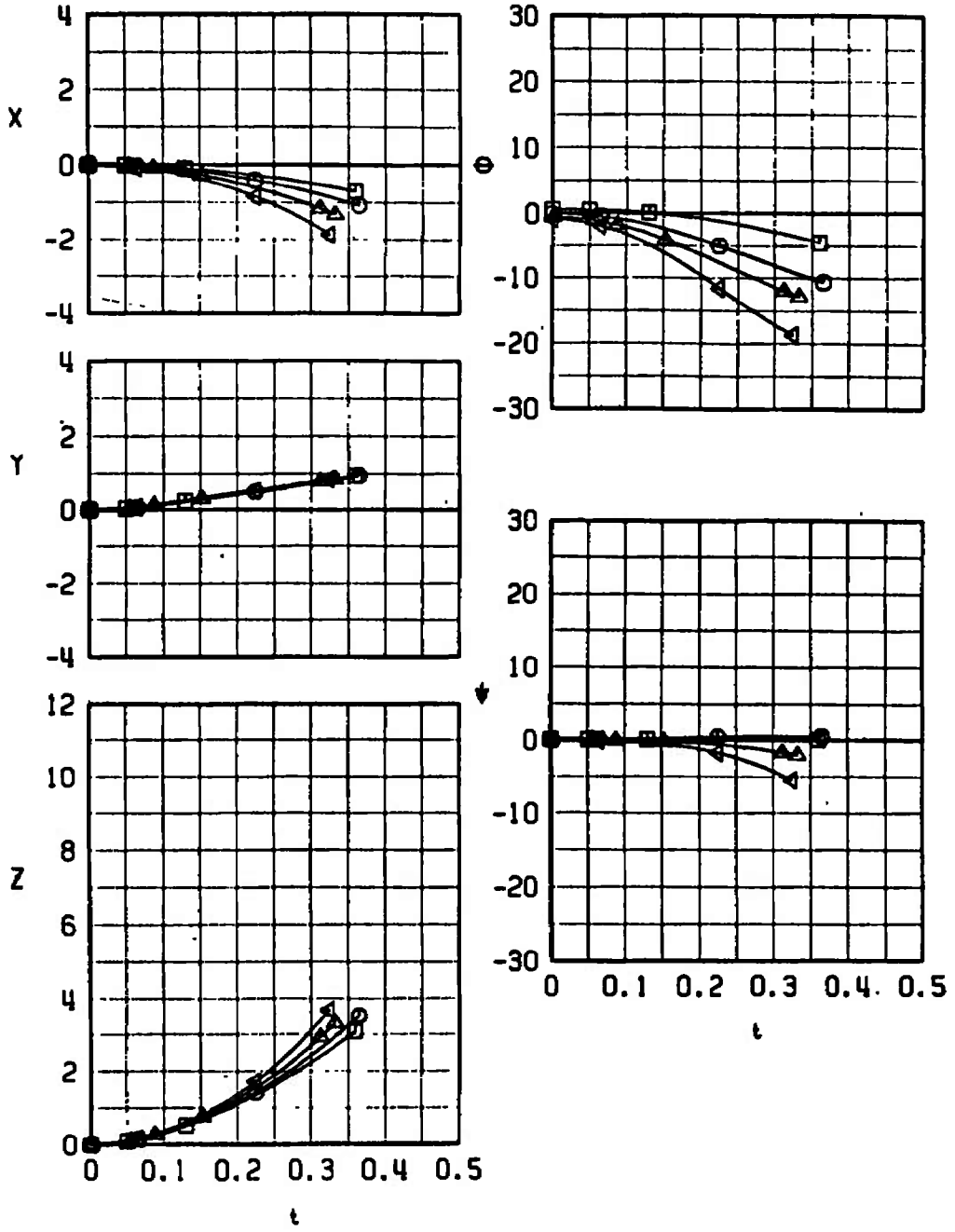

d. Configuration 5
Fig. 17 Continued

SYM	CONF	M_∞	α_p	$\bar{\phi}$	$\bar{X}$
☐	6	0.66	1.6	0	FWD
○	6	0.74	0.9	0	FWD
△	6	0.82	0.4	0	FWD
◁	6	0.90	0.1	0	FWD

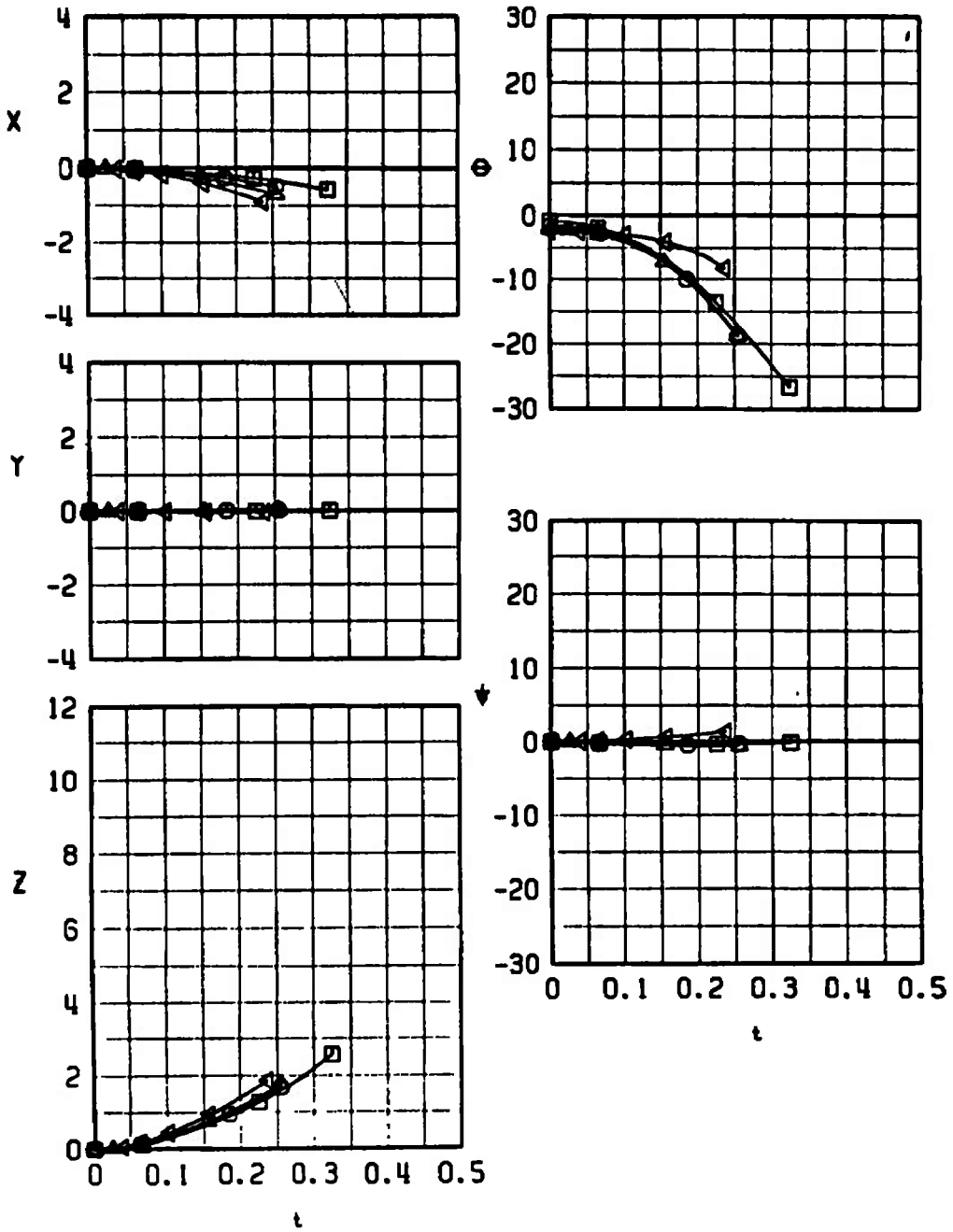

e. Configuration 6
Fig. 17 Continued

SYM	CONF	M_∞	α_p	$\bar{\theta}$	$\bar{X}$
□	7	0.66	1.6	0	FWD
△	7	0.82	0.4	0	FWD
◁	7	0.90	0.1	0	FWD

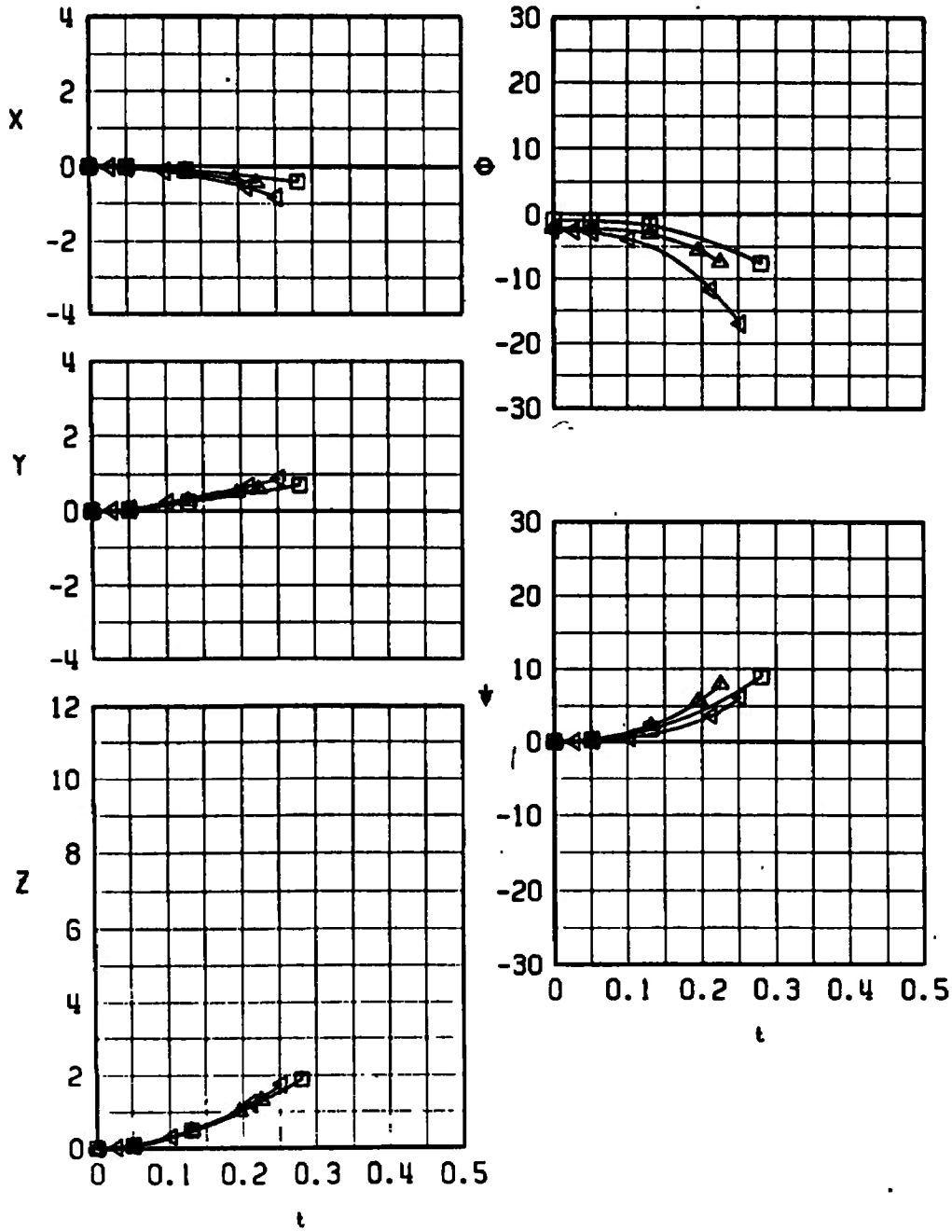

f. Configuration 7
Fig. 17 Continued

SYM	CONF	M_∞	α_p	$\bar{\phi}$	$\bar{X}$
□	8	0.66	1.6	0	FWD
◁	8	0.90	0.1	0	FWD

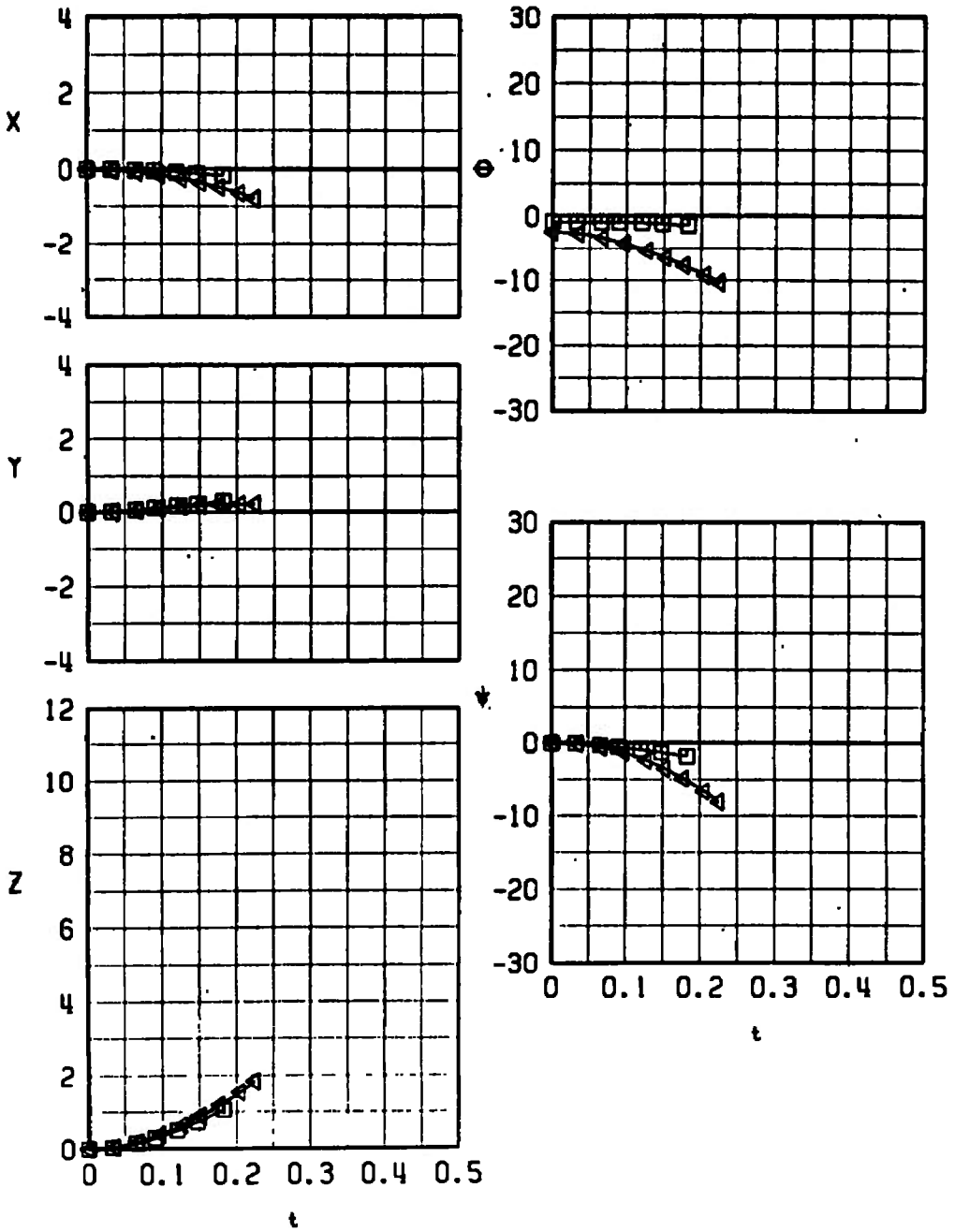

g. Configuration 8
Fig. 17 Continued

SYM	CONF	M_∞	α_p	$\bar{\theta}$	$\bar{X}$
□	10	0.66	1.6	0	FWD
◁	10	0.90	0.1	0	FWD

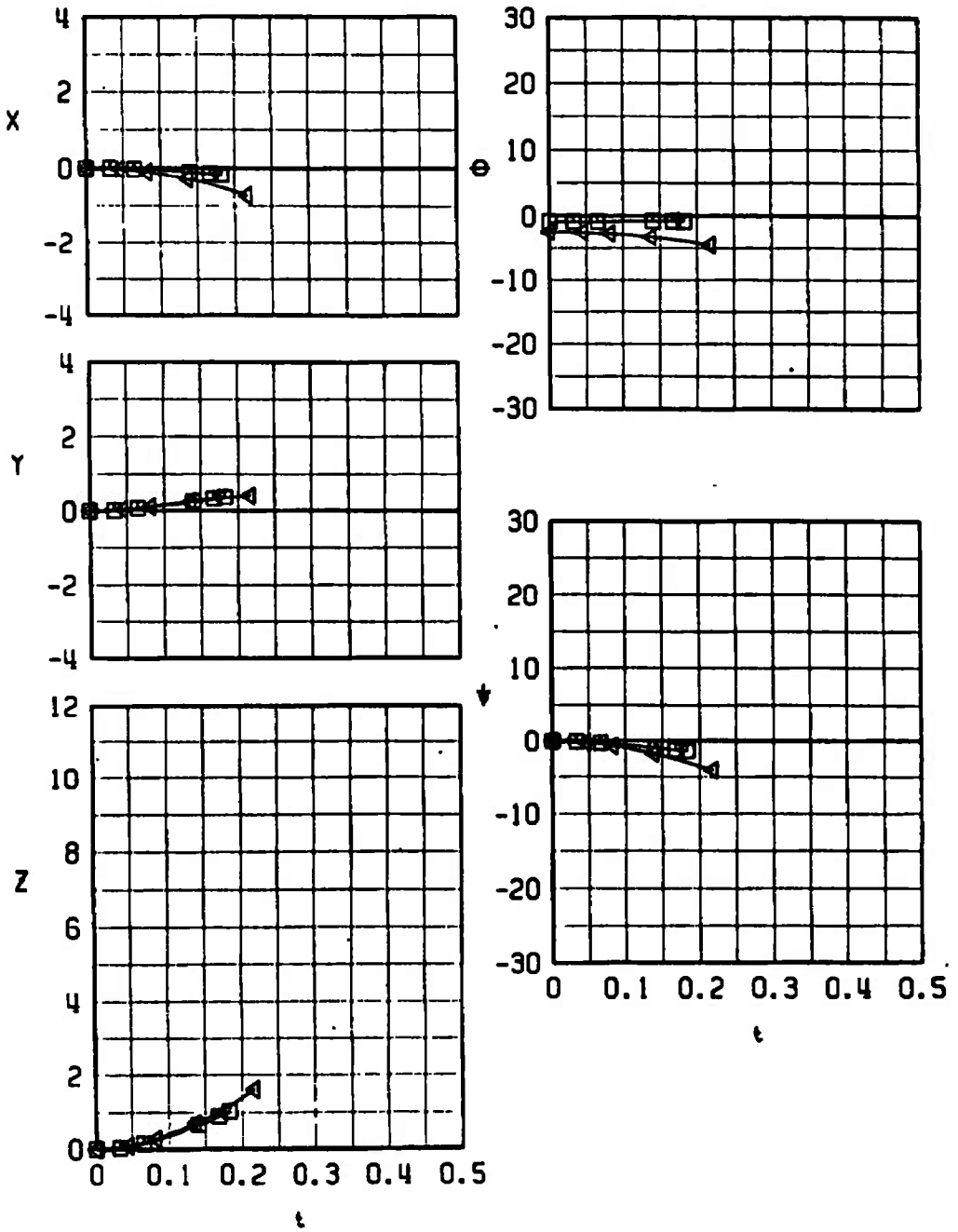

h. Configuration 10
Fig. 17 Continued

SYM	CONF	M_∞	α_p	$\bar{\phi}$	$\bar{X}$
⊙	11	0.74	0.9	0	FWD
△	11	0.82	0.4	0	FWD
◁	11	0.90	0.1	0	FWD

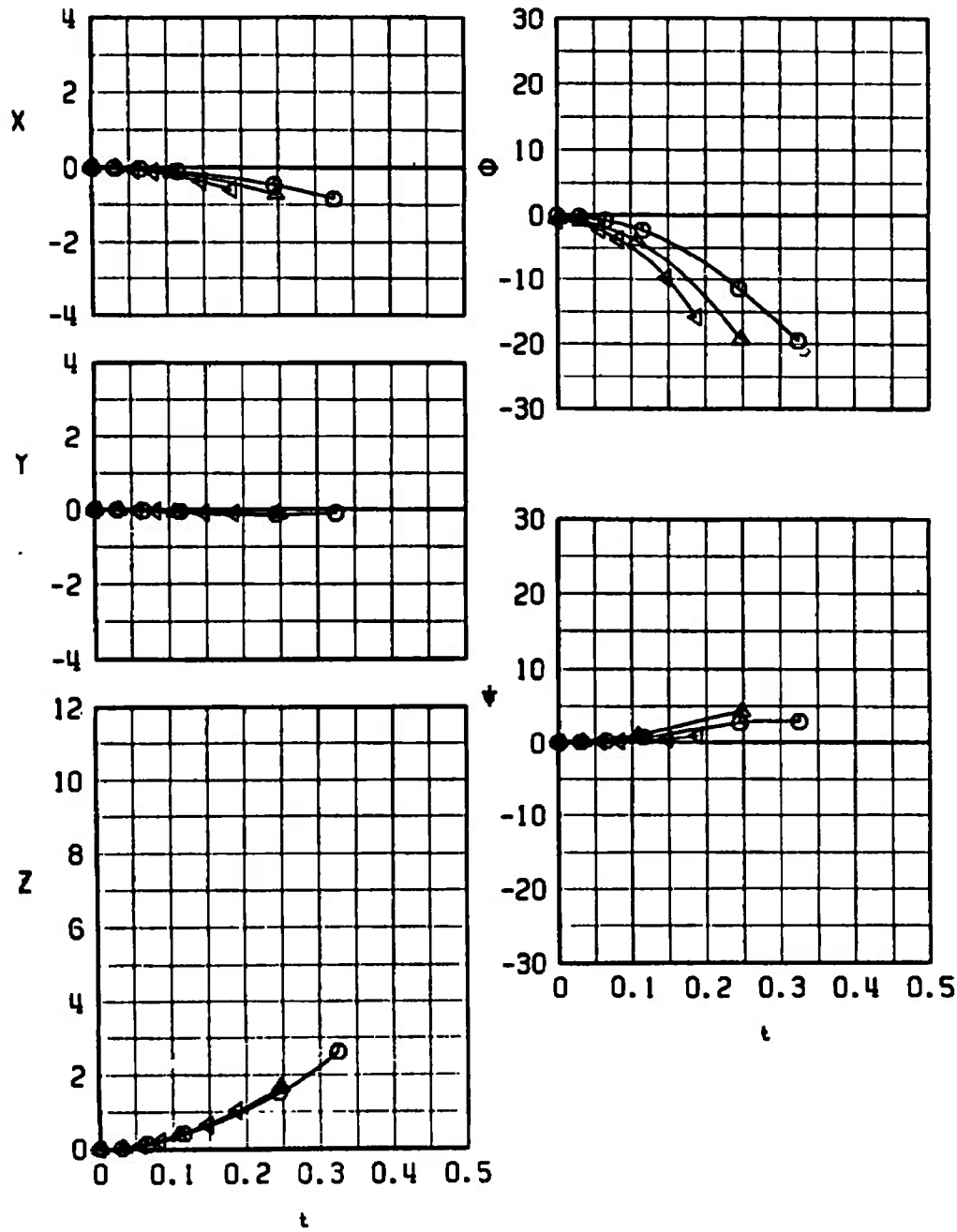

i. Configuration 11
Fig. 17 Concluded

SYM	CONF	M_∞	α_p	$\bar{\theta}$	$\bar{X}$
□	2	0.66	1.6	0	NOM
○	2	0.74	0.9	0	NOM
△	2	0.82	0.4	0	NOM

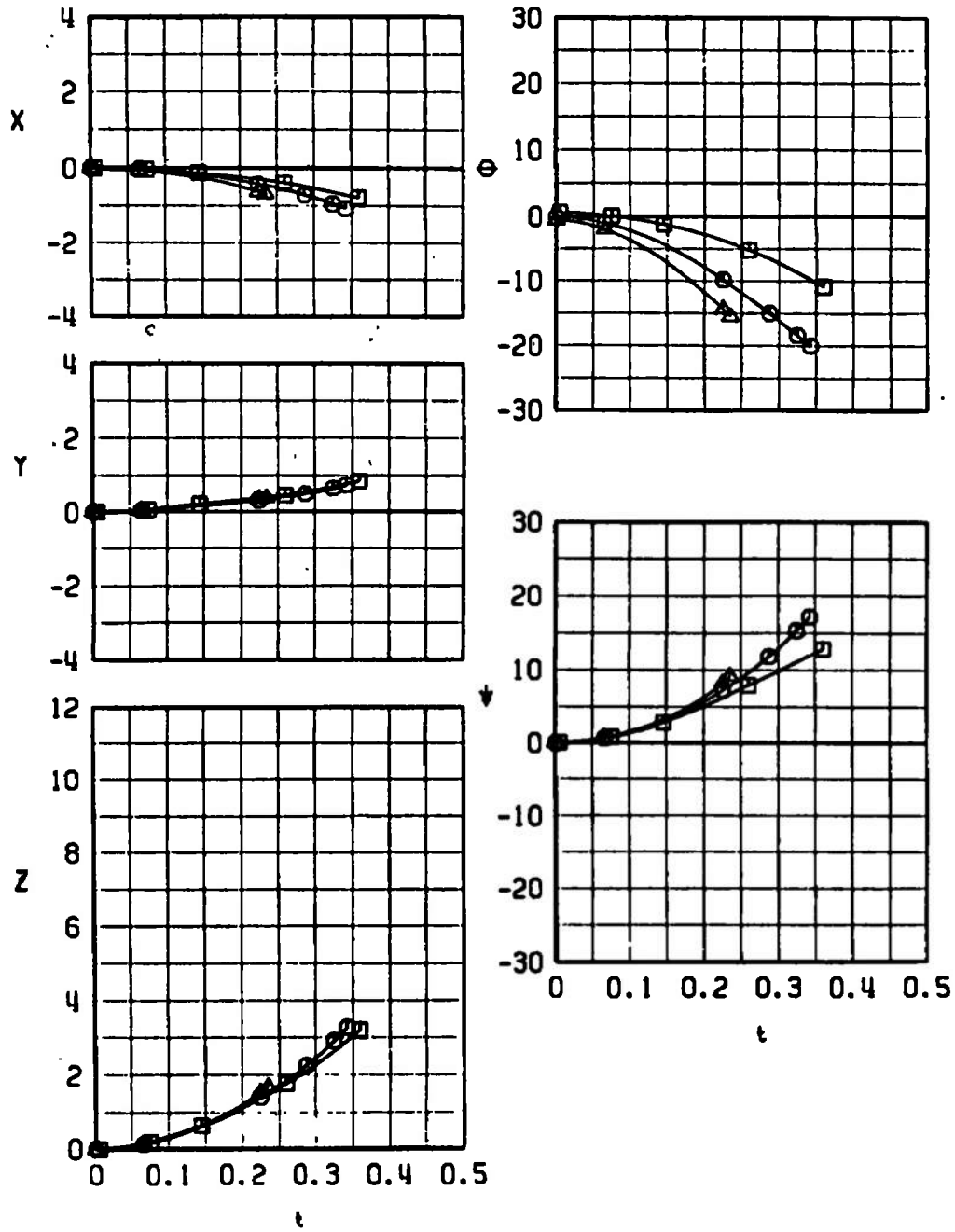

a. Configuration 2

Fig. 18 Effect of Mach Number on the Nominal Center-of-Gravity Store Separation Characteristics

SYM	CONF	M_∞	α_p	$\bar{\phi}$	$\bar{\chi}$
□	4	0.66	1.6	0	NOM
○	4	0.74	0.9	0	NOM
△	4	0.82	0.4	0	NOM
◁	4	0.90	0.1	0	NOM

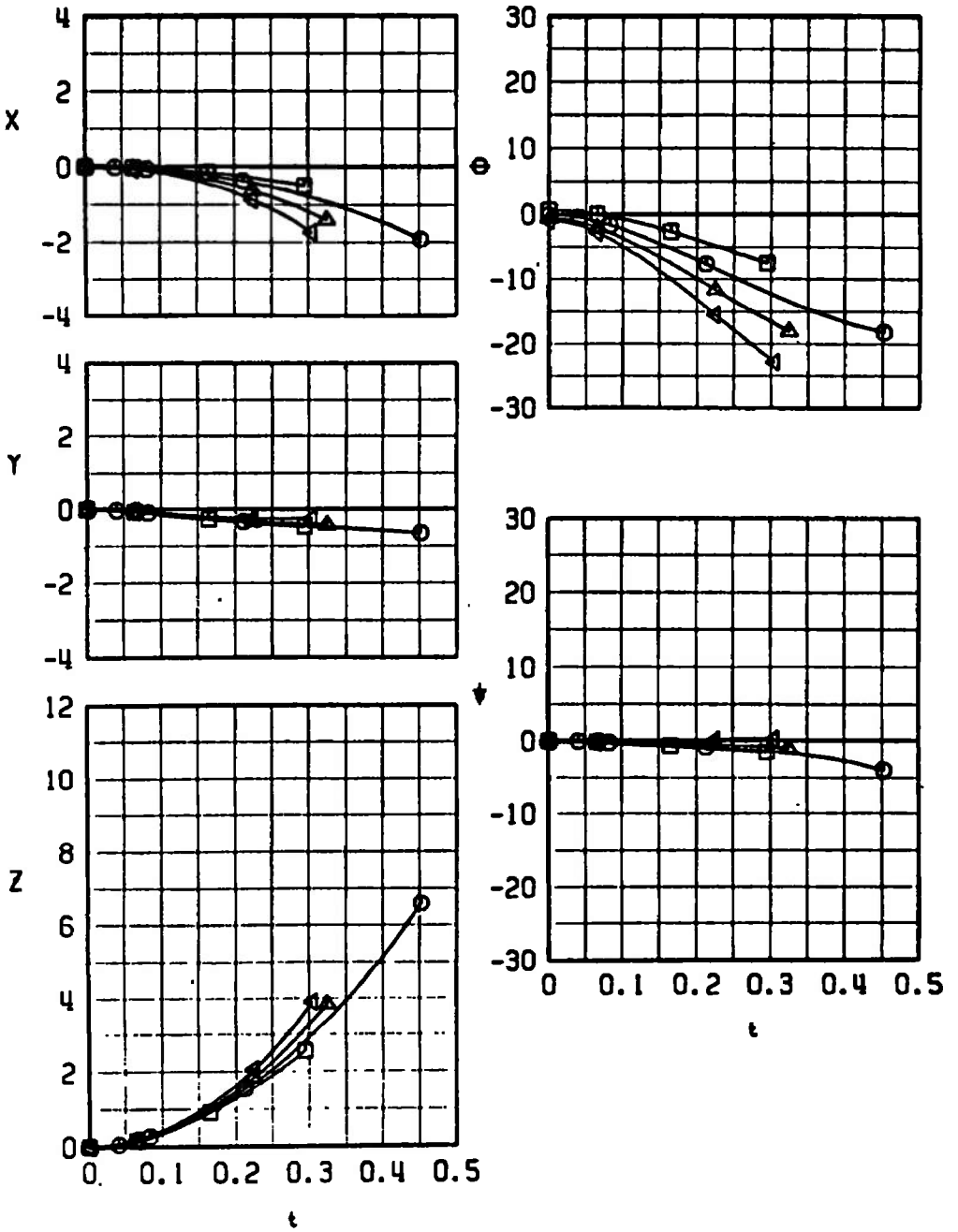

b. Configuration 4
Fig. 18 Continued

SYM	CONF	M_∞	α_p	$\bar{\phi}$	$\bar{X}$
□	5	0.66	1.6	0	NOM
○	5	0.74	0.9	0	NOM
△	5	0.82	0.4	0	NOM
◁	5	0.90	0.1	0	NOM

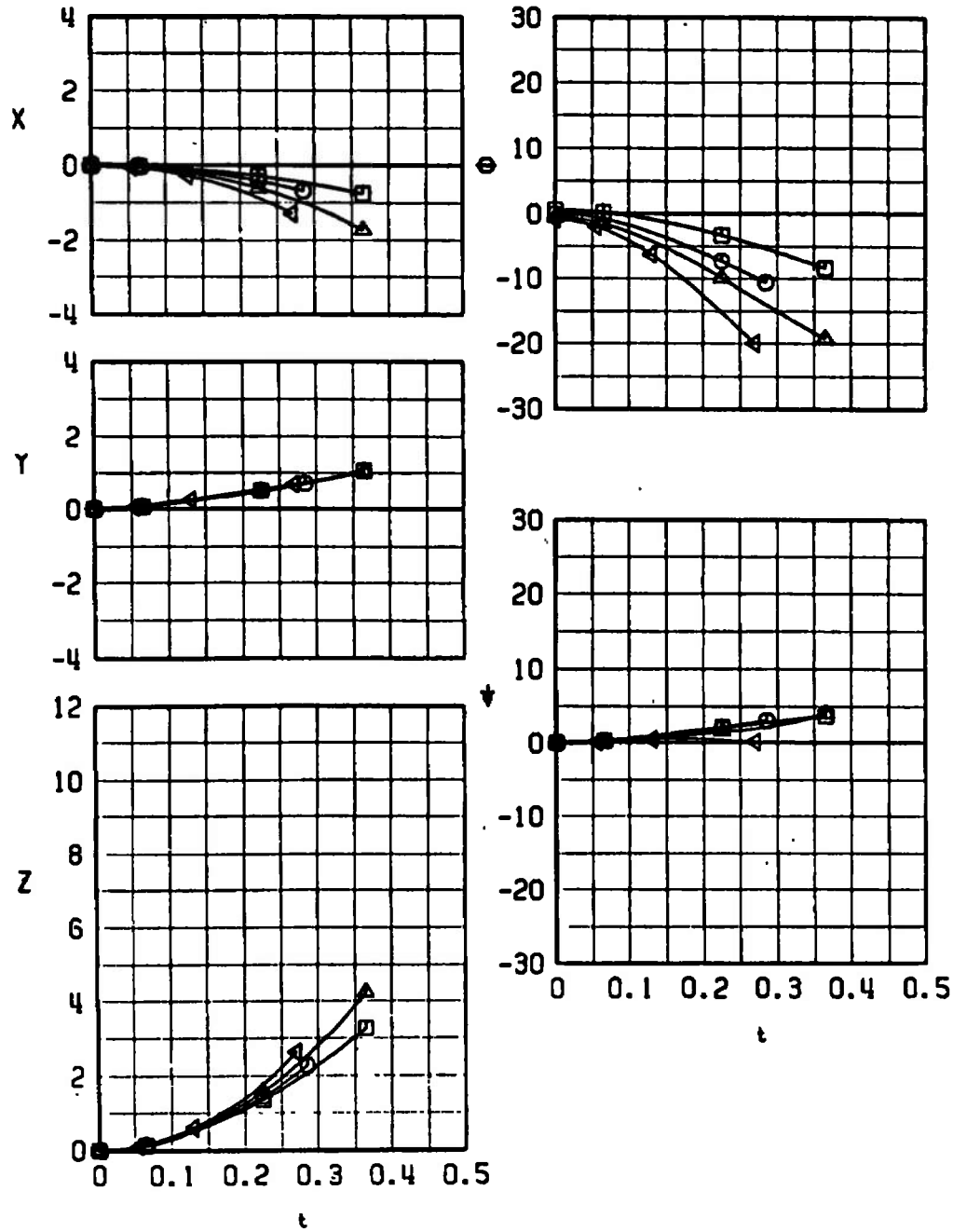

c. Configuration 5
Fig. 18 Concluded

SYM	CONF	M_∞	α_p	$\bar{\theta}$	$\bar{X}$
□	2	0.66	1.6	0	FWD
○	2	0.66	-0.1	-45	FWD

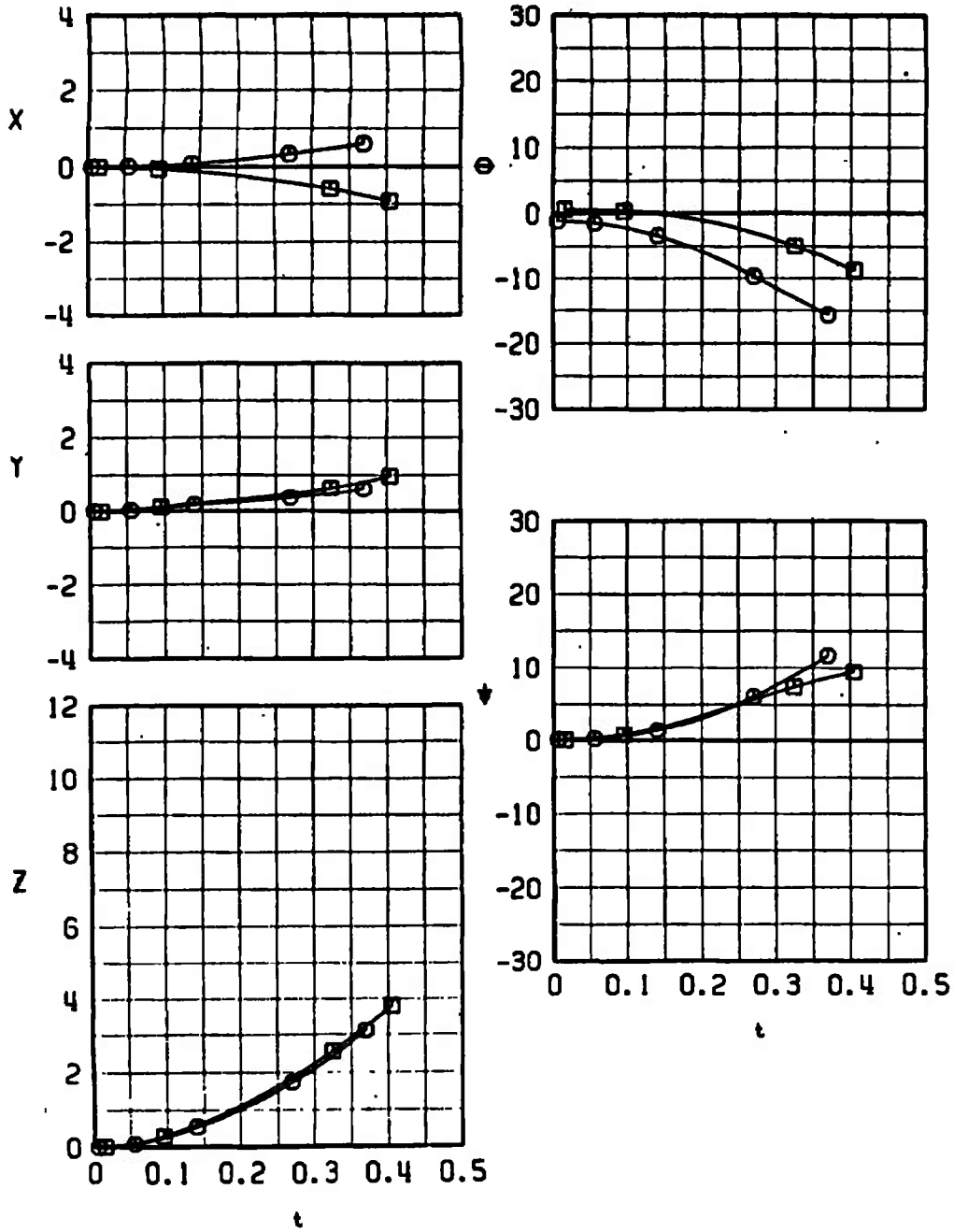

a. $M_\infty = 0.66$

Fig. 19 Effect of Aircraft Dive Angle on the Forward Shifted Center-of-Gravity Store Separation Characteristics for Load Configuration 2

SYM	CONF	M_∞	α_p	$\bar{\phi}$	$\bar{X}$
⊡	2	0.74	0.9	0	FWD
⊙	2	0.74	-0.4	-45	FWD

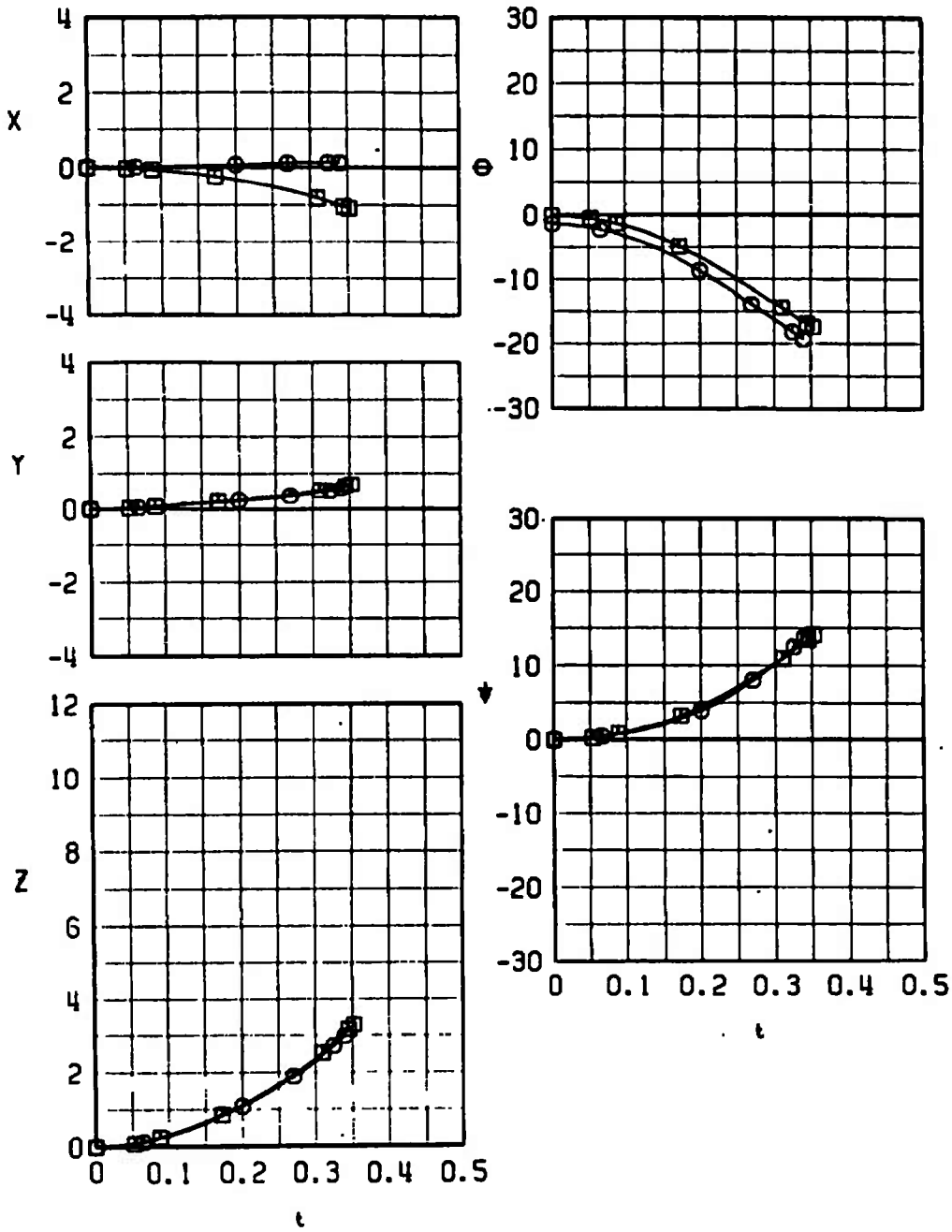

b. $M_\infty = 0.74$
Fig. 19 Continued

SYM	CONF	M_∞	α_p	$\bar{\theta}$	$\bar{X}$
□	2	0.82	0.4	0	FWD
○	2	0.82	-0.6	-45	FWD

FLAGGED SYMBOLS INDICATE EXTENDED FIN DATA

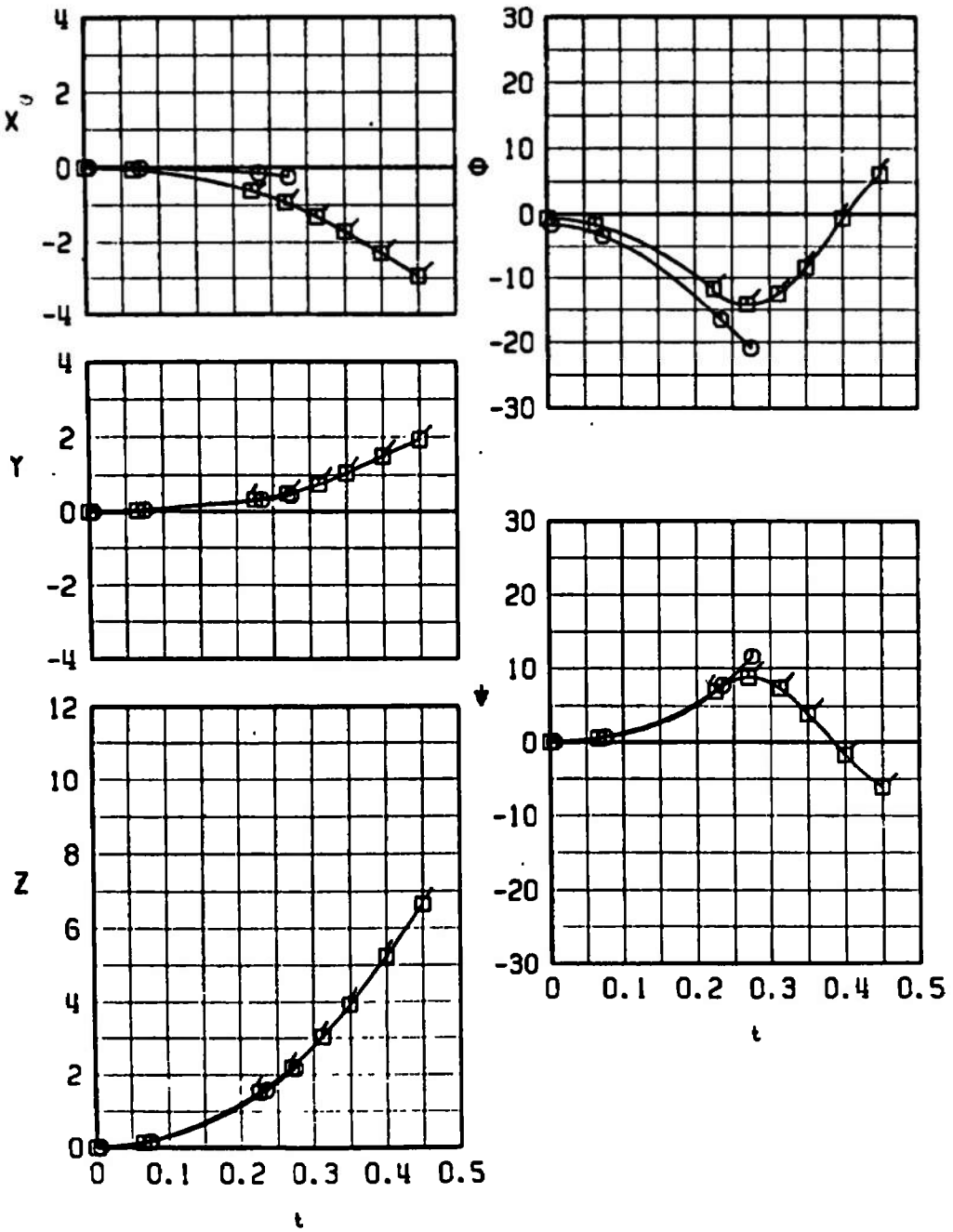

c. $M_\infty = 0.82$

Fig. 19 Concluded

SYM	CONF	M_∞	α_p	$\bar{\theta}$	$\bar{X}$
□	3	0.66	1.6	0	FWD
○	3	0.66	-0.1	-45	FWD

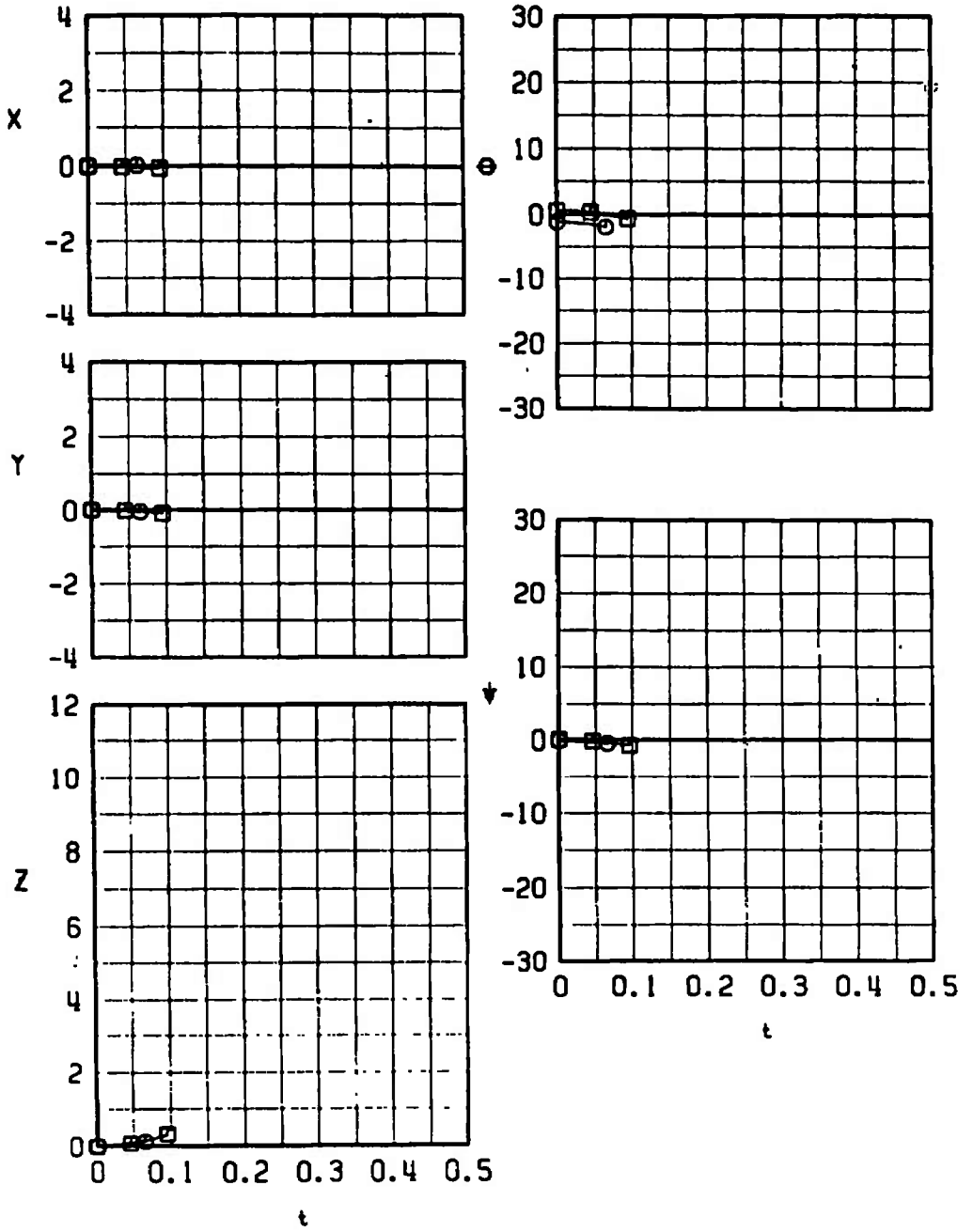

a. $M_\infty = 0.66$

Fig. 20 Effect of Aircraft Dive Angle on the Forward Shifted Center-of-Gravity Store Separation Characteristics for Load Configuration 3

SYM	CONF	M_∞	α_p	$\bar{\theta}$	$\bar{X}$
□	3	0.82	0.4	0	FWD
○	3	0.82	-0.6	-45	FWD

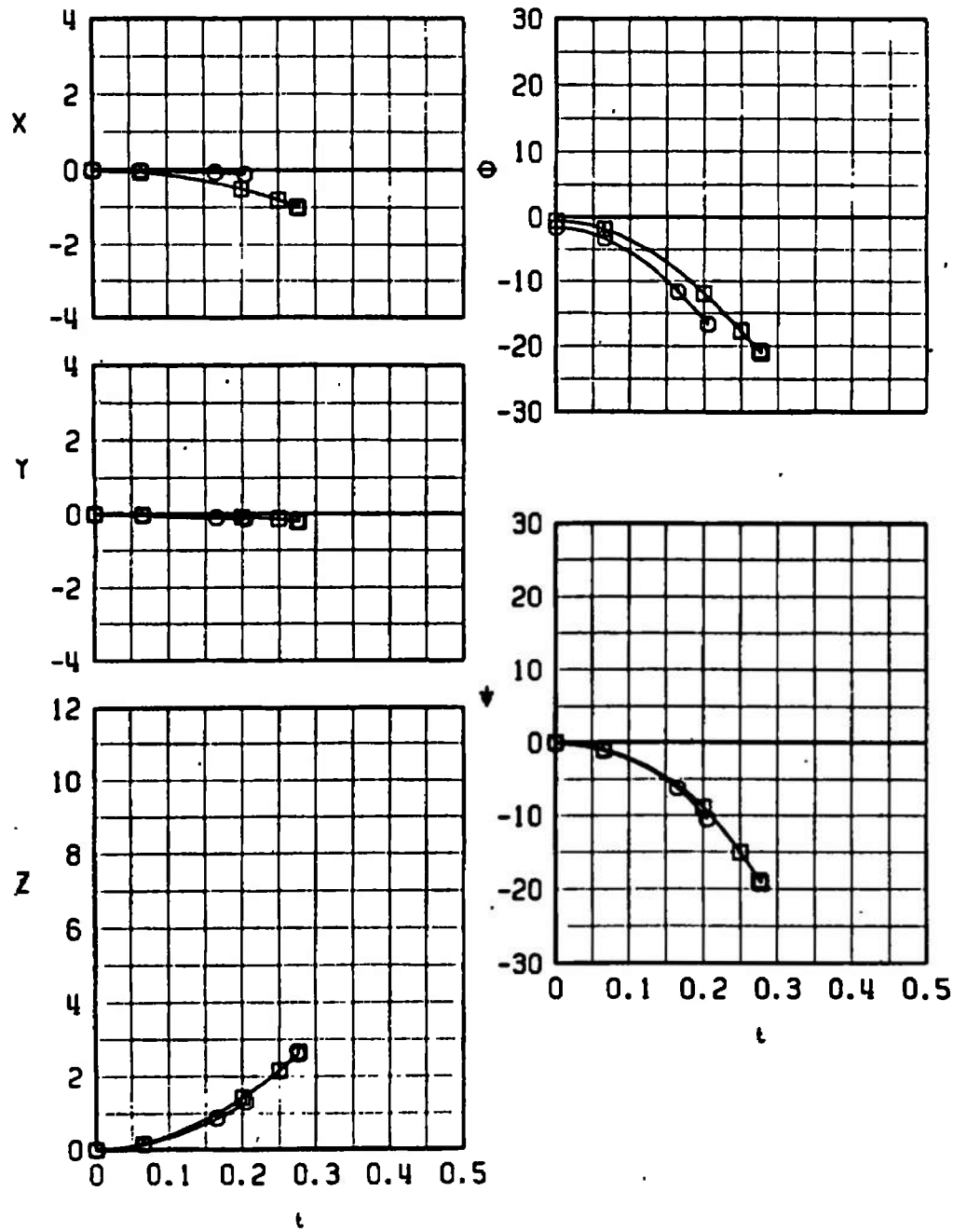

b. $M_\infty = 0.82$

Fig. 20 Concluded

SYM	CONF	M_∞	α_p	$\bar{\theta}$	$\bar{X}$
⊡	4	0.66	1.6	0	FWD
⊙	4	0.66	-0.1	-45	FWD

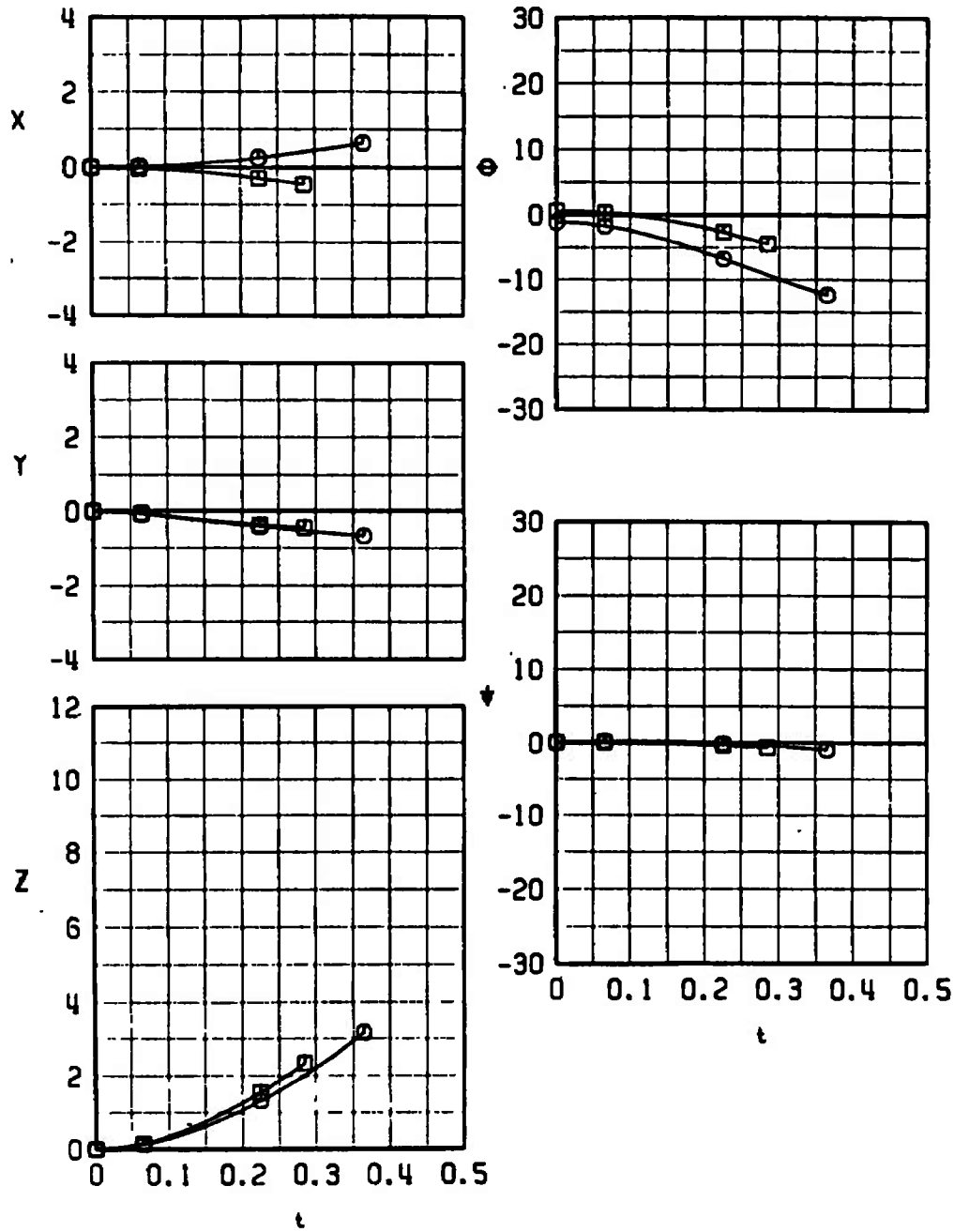

a. $M_\infty = 0.66$

Fig. 21 Effect of Aircraft Dive Angle on the Forward Shifted Center-of-Gravity Store Separation Characteristics for Load Configuration 4

SYM	CONF	M_∞	α_p	$\bar{\theta}$	$\bar{X}$
⊡	4	0.74	0.9	0	FWD
⊙	4	0.74	-0.4	-45	FWD

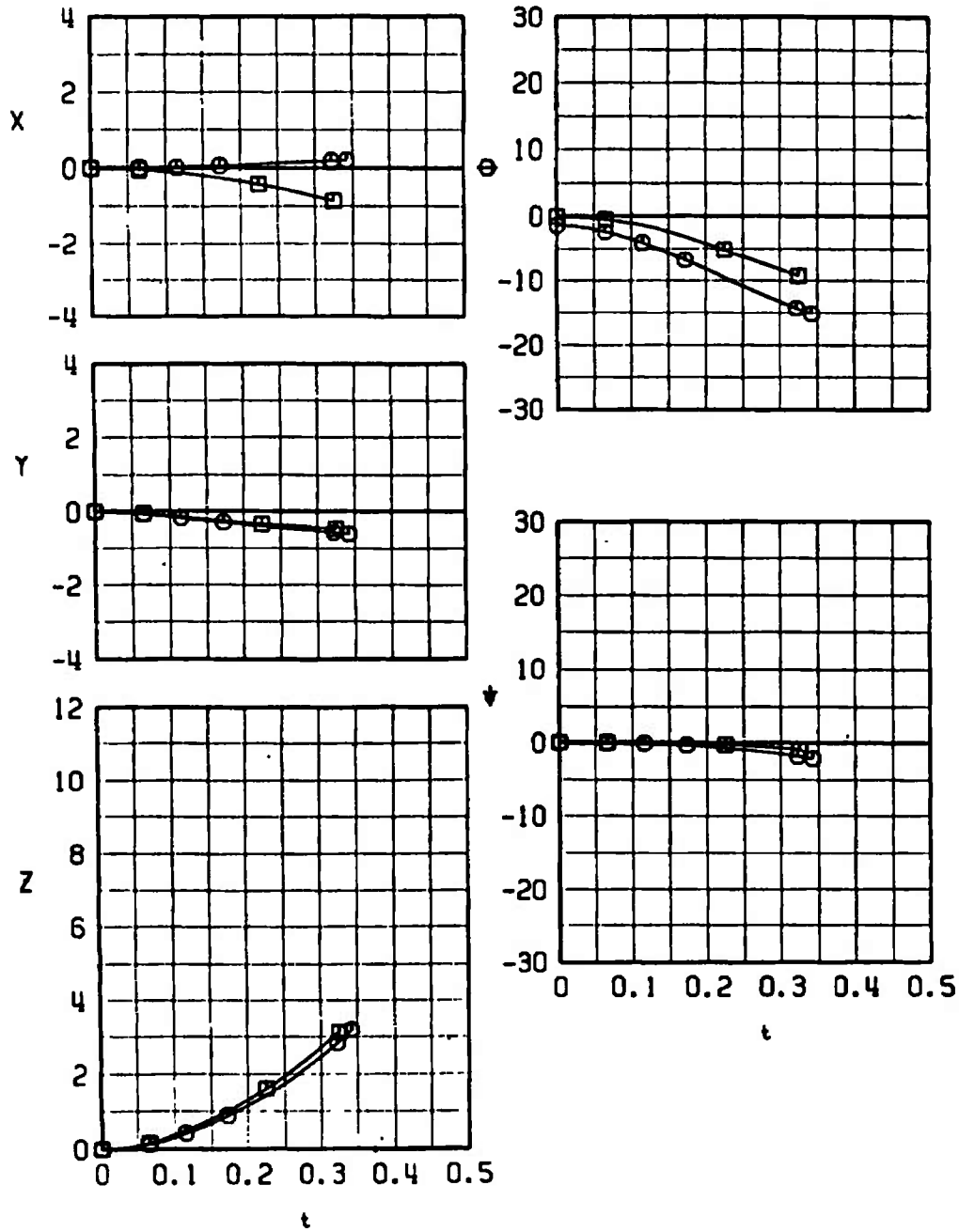

b. $M_\infty = 0.74$

Fig. 21 Concluded

SYM	CONF	M_∞	α_p	$\bar{\phi}$	$\bar{X}$
□	5	0.66	1.6	0	FWD
○	5	0.66	-0.1	-45	FWD

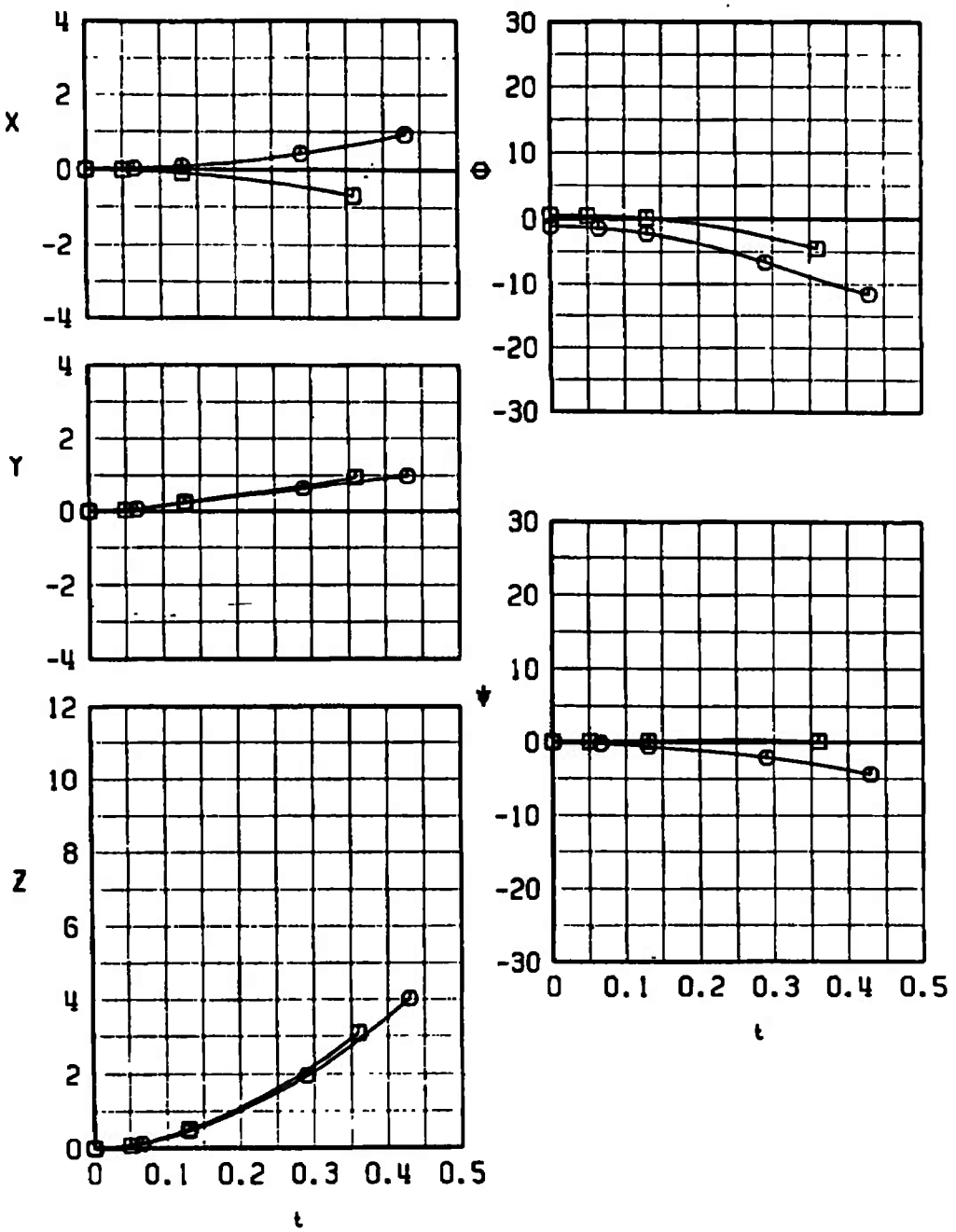

a. $M_\infty = 0.66$

Fig. 22 Effect of Aircraft Dive Angle on the Forward Shifted Center-of-Gravity Store Separation Characteristics for Load Configuration 5

SYM	CONF	M_∞	α_p	$\bar{\phi}$	$\bar{X}$
⊡	5	0.74	0.9	0	FWD
⊙	5	0.74	-0.4	-45	FWD

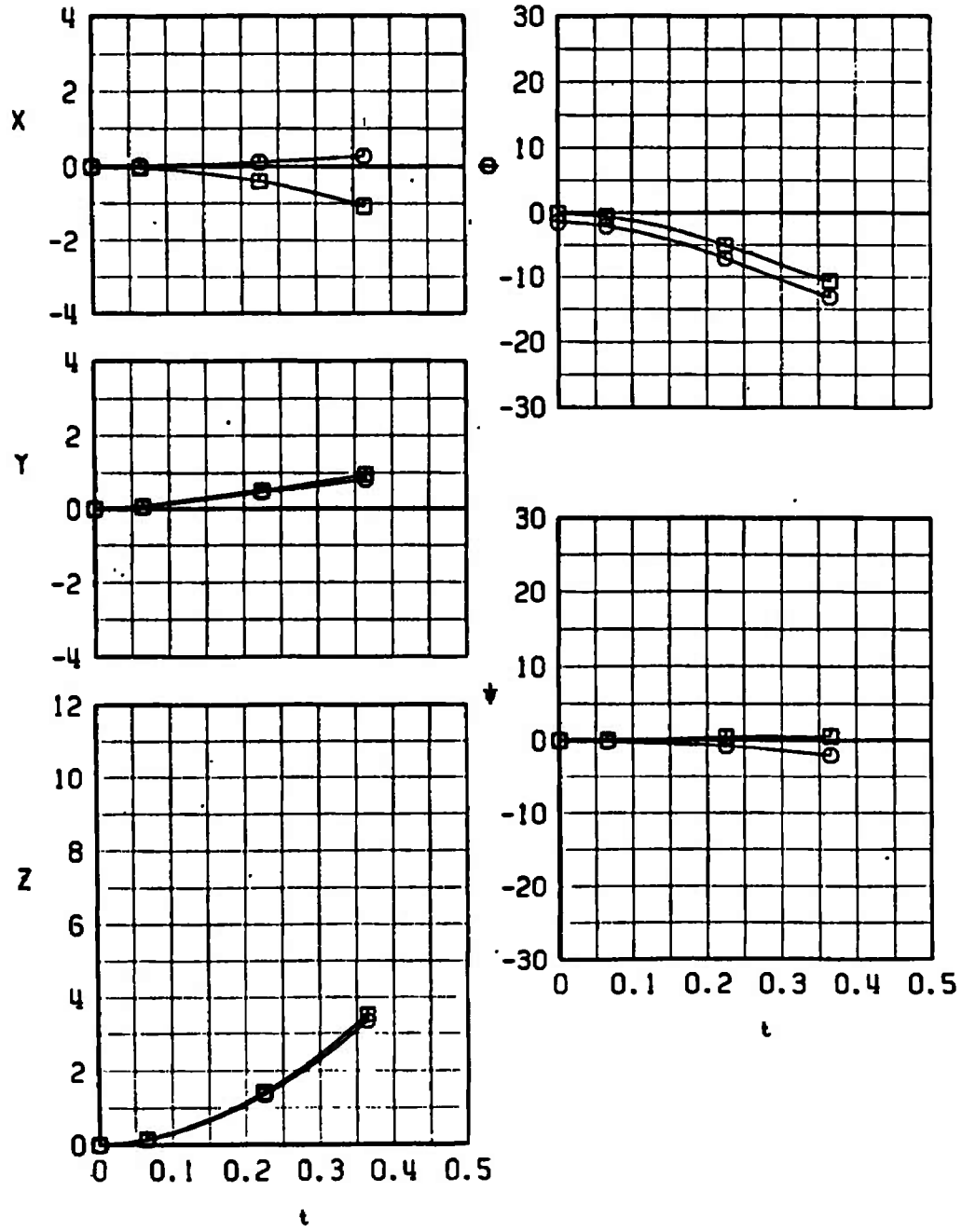

b. $M_\infty = 0.74$

Fig. 22 Concluded

SYM	CONF	M_∞	α_p	$\bar{\theta}$	$\bar{X}$
□	6	0.66	1.6	0	FWD
○	6	0.66	-0.1	-45	FWD

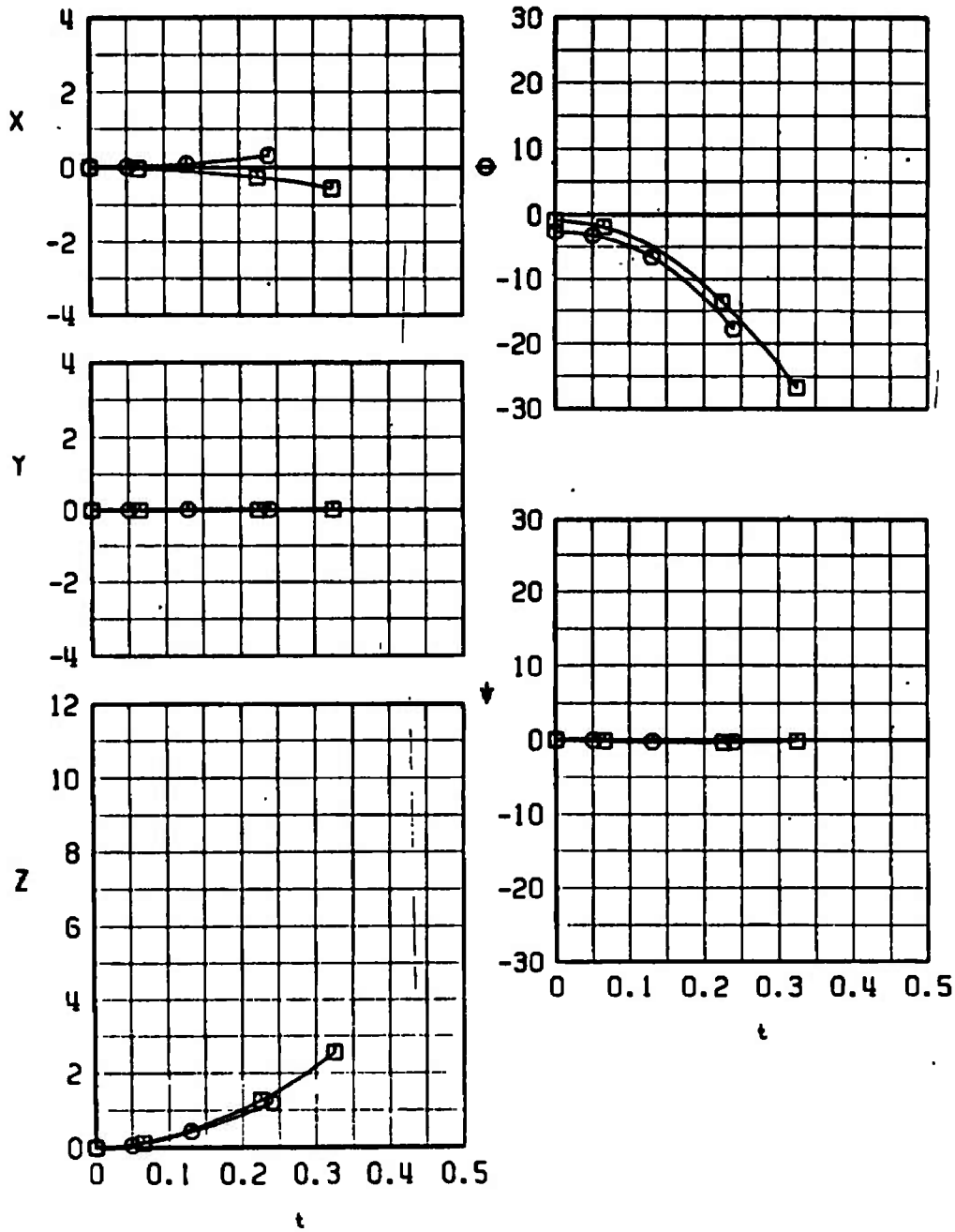

a. $M_\infty = 0.66$

Fig. 23 Effect of Aircraft Dive Angle on the Forward Shifted Center-of-Gravity Store Separation Characteristics for Load Configuration 6

SYM	CONF	M_∞	α_p	$\bar{\phi}$	$\bar{X}$
□	6	0.90	0.1	0	FWD
○	6	0.90	-0.7	-45	FWD

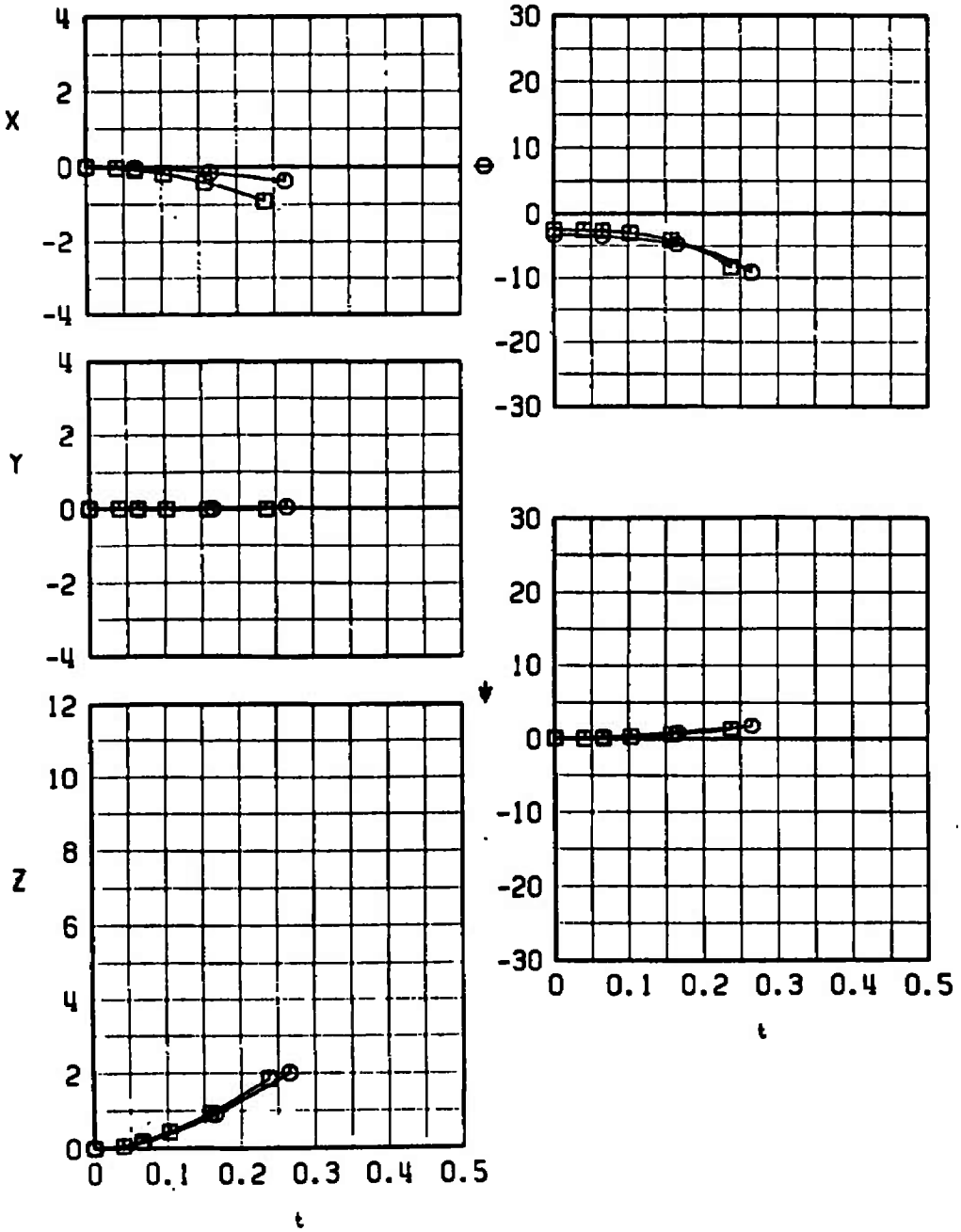

b. $M_\infty = 0.90$

Fig. 23 Concluded

SYM	CONF	M_∞	α_p	$\bar{\theta}$	$\bar{X}$
□	7	0.66	1.6	0	FWD
○	7	0.66	-0.1	-45	FWD

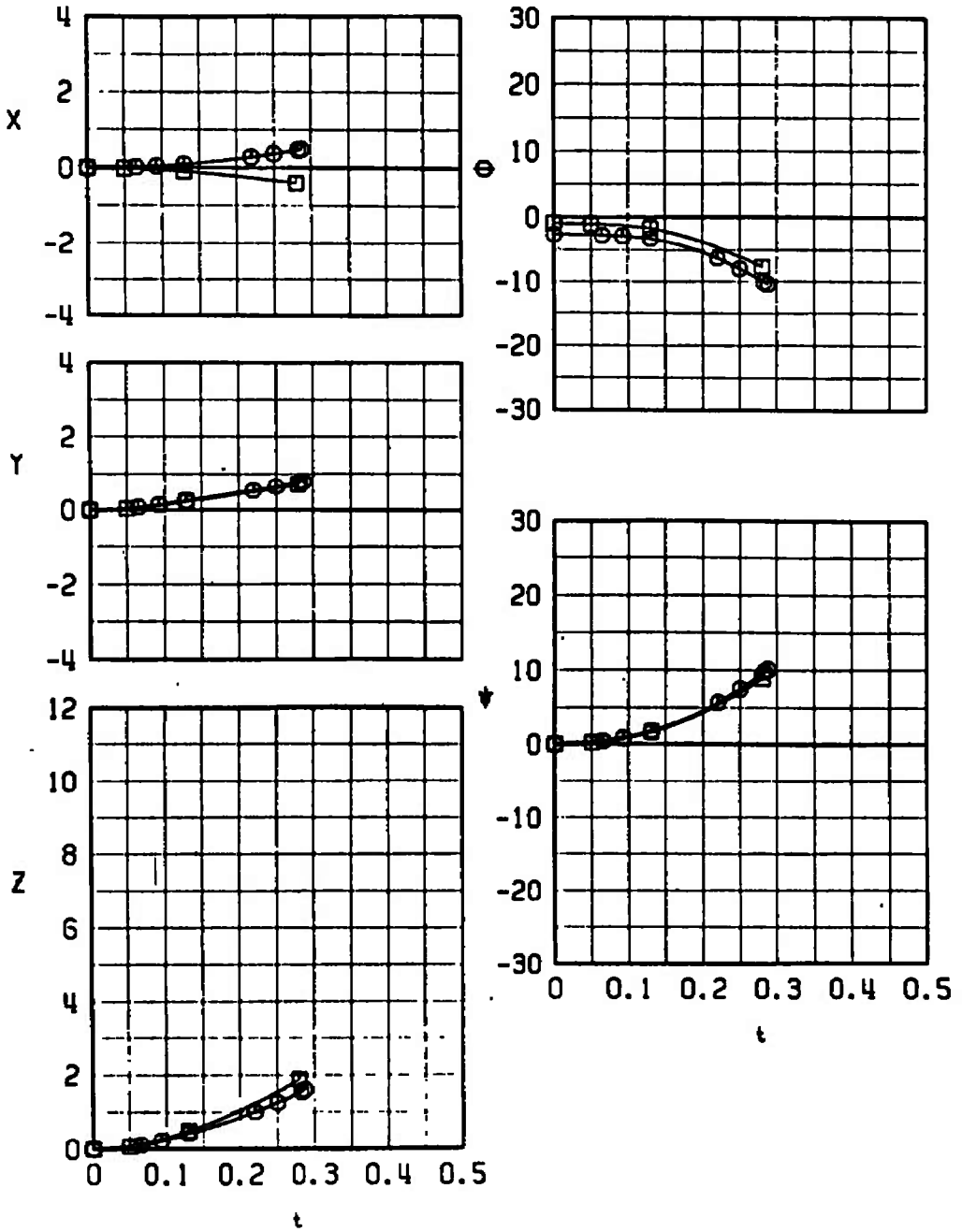

a. $M_\infty = 0.66$

Fig. 24 Effect of Aircraft Dive Angle on the Forward Shifted Center-of-Gravity Store Separation Characteristics for Load Configuration 7

SYM	CONF	M_∞	α_p	$\bar{\phi}$	$\bar{\chi}$
□	7	0.90	0.1	0	FWD
○	7	0.90	-0.7	-45	FWD

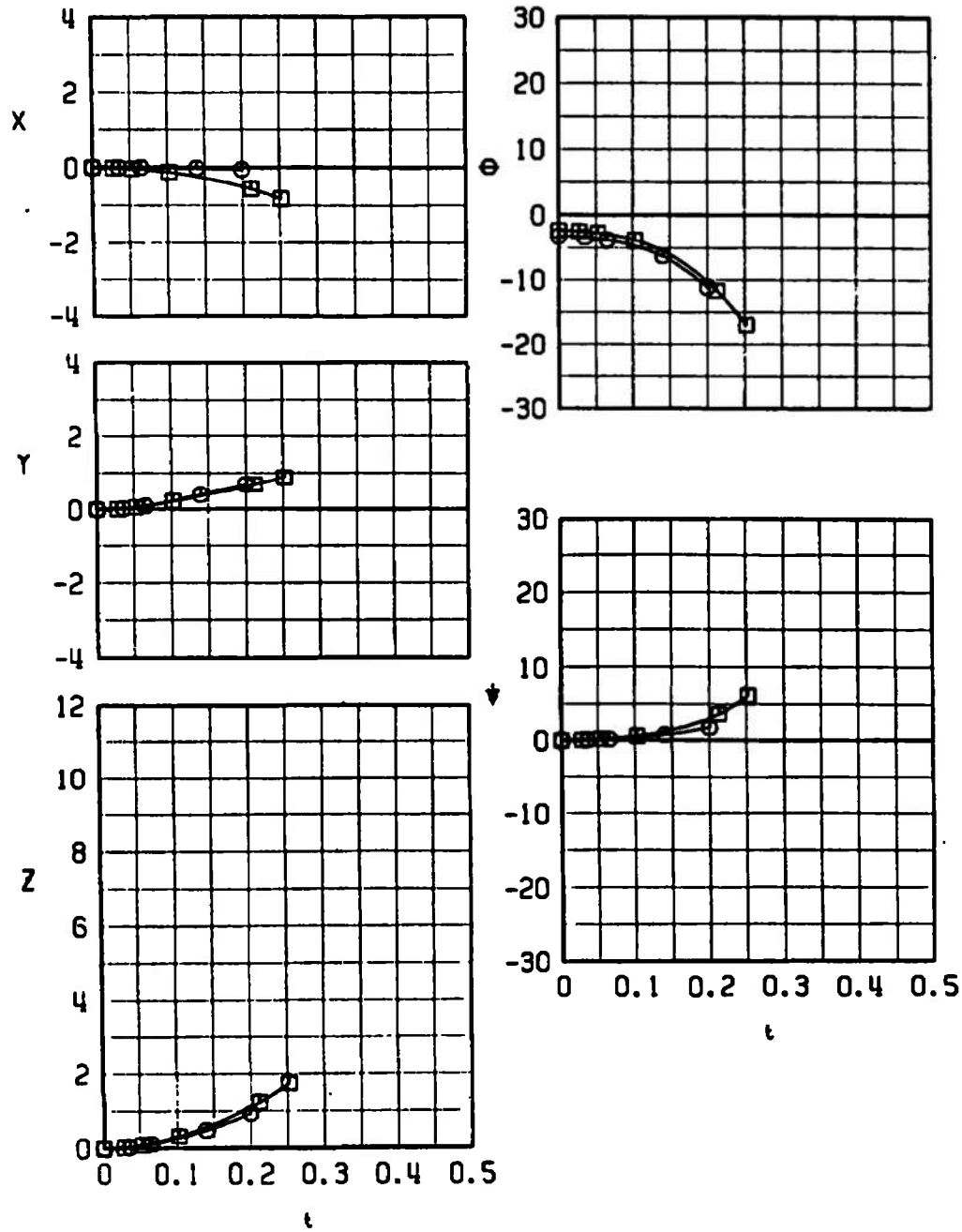

b. $M_\infty = 0.90$

Fig. 24 Concluded

SYM	CONF	M_∞	α_p	$\bar{\theta}$	$\bar{X}$
⊡	8	0.66	1.6	0	FWD
⊙	8	0.66	-0.1	-45	FWD

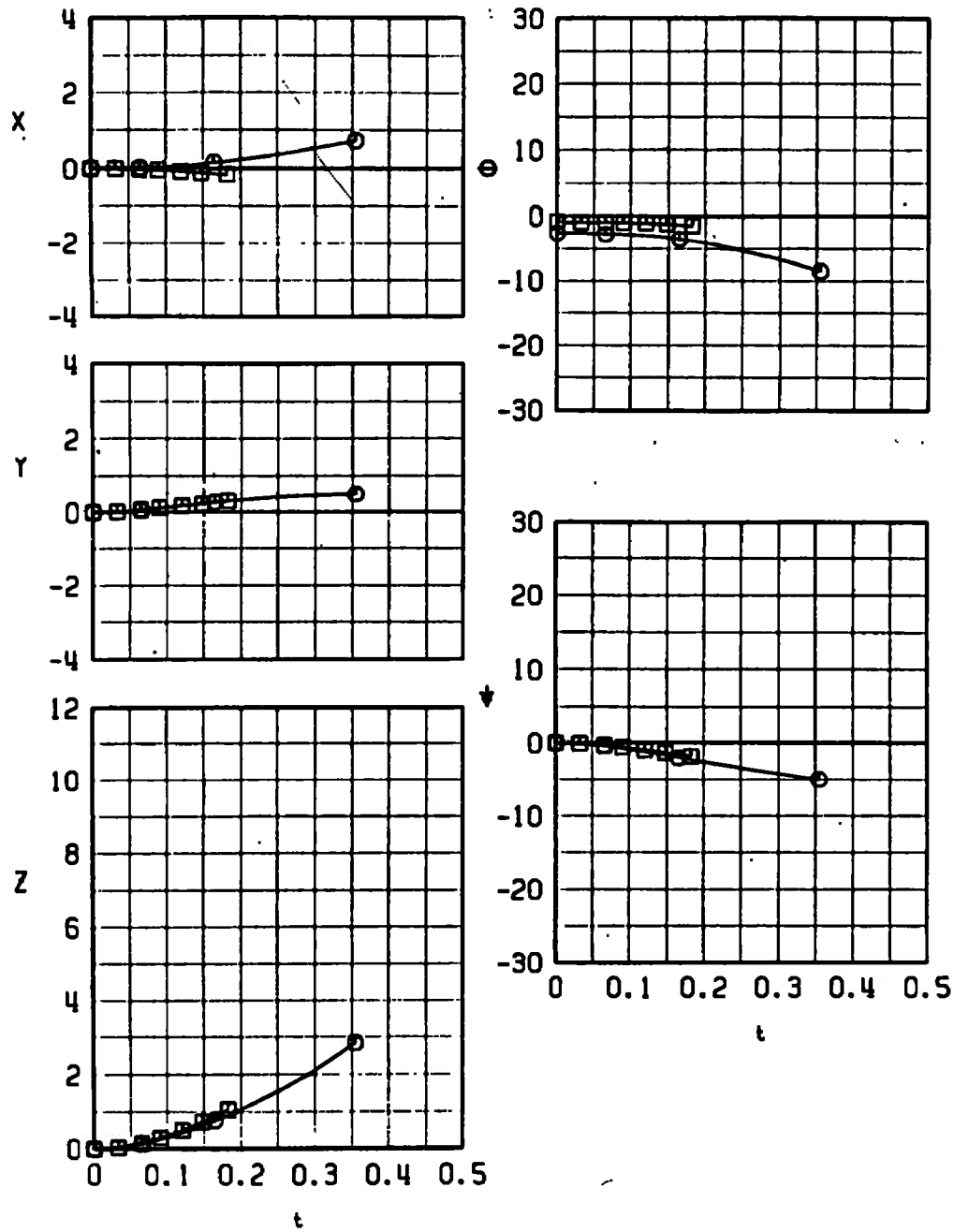

a. $M_\infty = 0.66$

Fig. 25 Effect of Aircraft Dive Angle on the Forward Shifted Center-of-Gravity Store Separation Characteristics for Load Configuration 8

SYM	CONF	M_∞	α_p	$\bar{\phi}$	$\bar{X}$
□	8	0.90	0.1	0	FWD
○	8	0.90	-0.7	-45	FWD

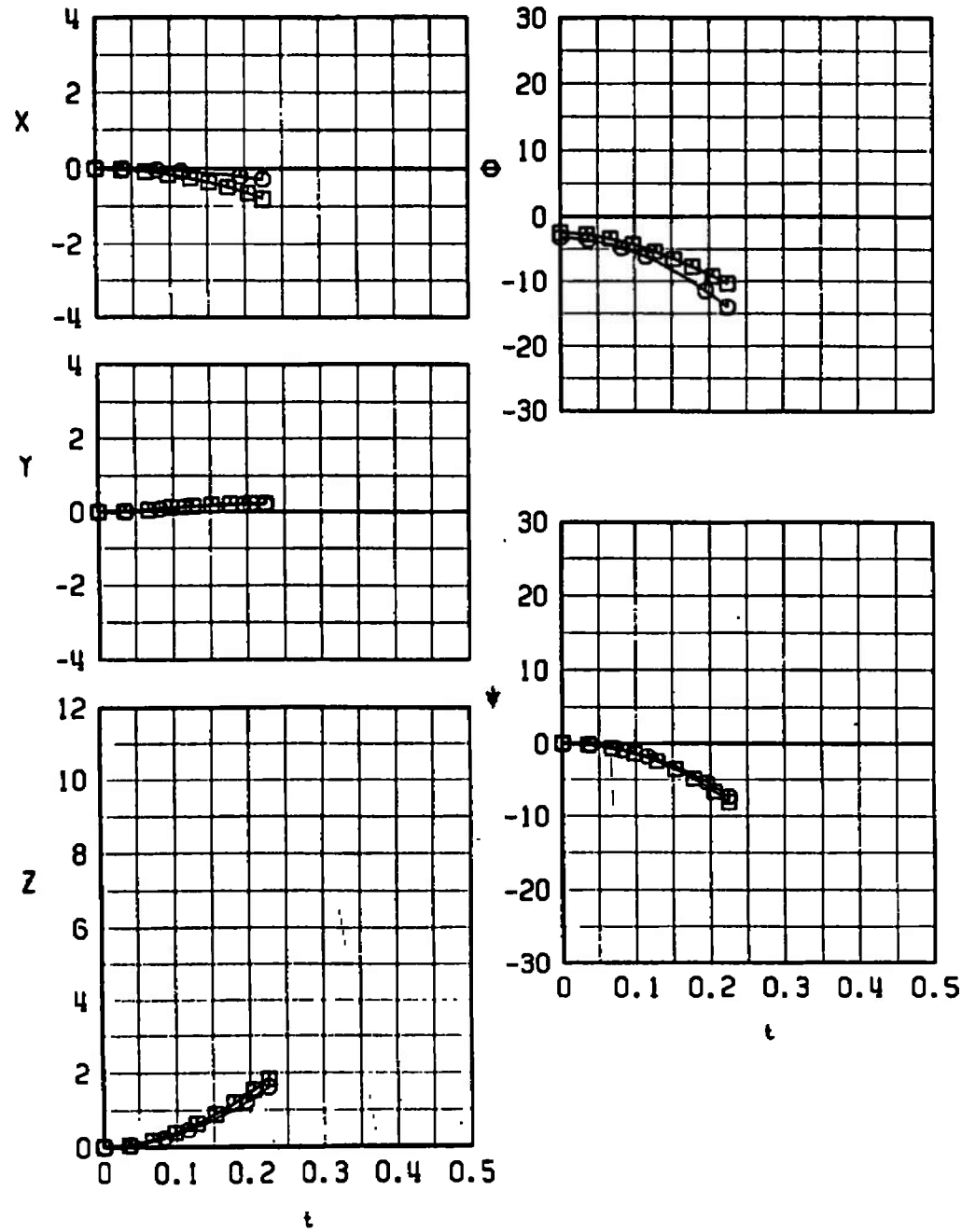

b. $M_\infty = 0.90$
Fig. 25 Concluded

SYM	CONF	M_∞	α_p	$\bar{\theta}$	$\bar{X}$
⊡	11	0.74	0.9	0	FWD
⊙	11	0.74	-0.4	-45	FWD

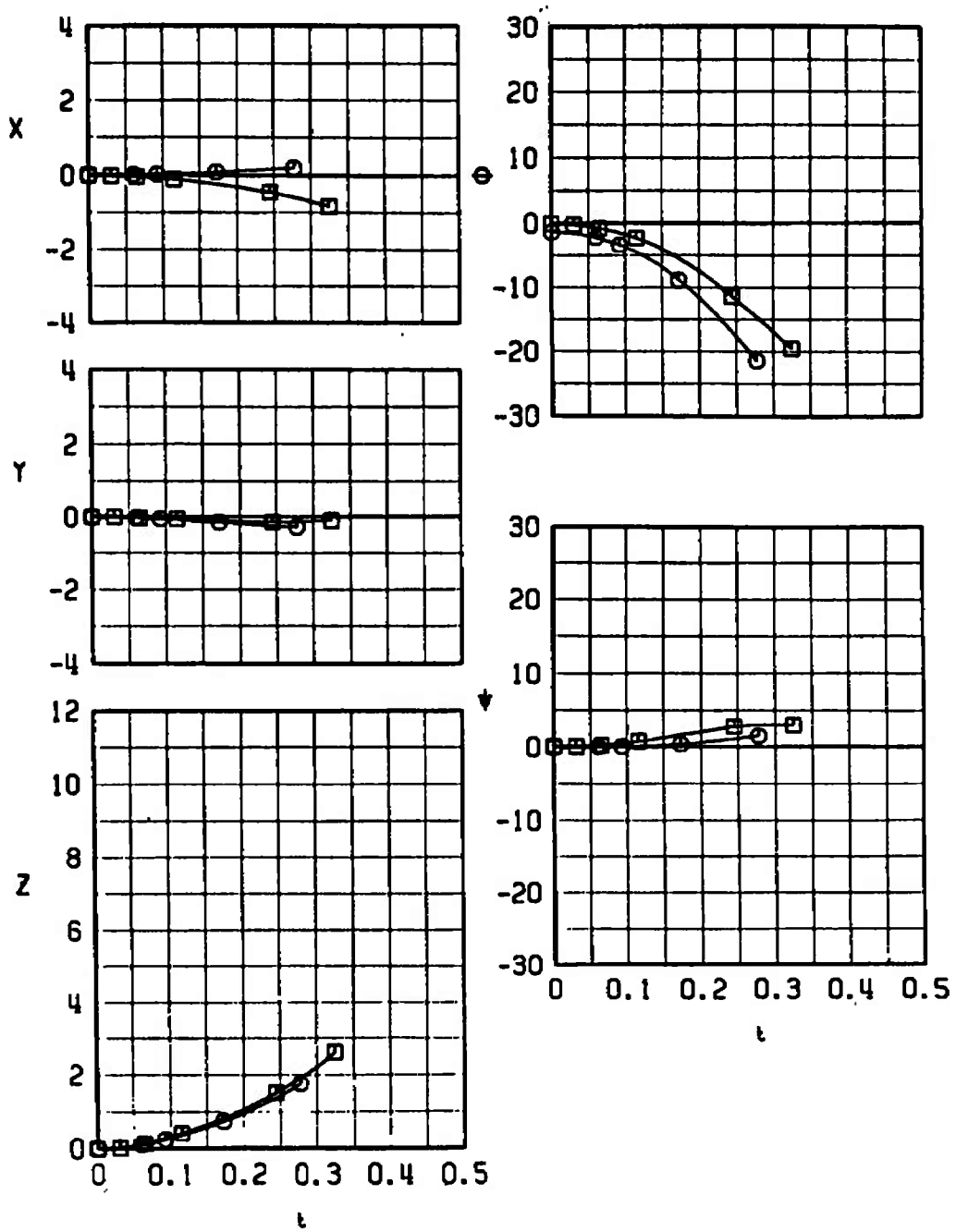

Fig. 26 Effect of Aircraft Dive Angle on the Forward Shifted Center-of-Gravity Store Separation Characteristics for Load Configuration 11

TABLE I
FULL-SCALE STORE PARAMETERS USED IN THE TRAJECTORY CALCULATIONS

Parameter	Folded Fin Configuration		Deployed Fin Configuration	
Mass, $\bar{m}$, slugs	25.85		25.85	
Center-of-gravity location, X_{cg}, $\bar{X}$, ft	4.09, Nom	3.923, FWD	4.09, Nom	3.923, FWD
Ejector piston location, X_{I_i}, $\bar{X}$, ft	0.0152 Nom	-0.151 FWD	N/A	
Ejector Stroke length, Z_E, ft	0.2552		N/A	
Distance of the store cg above the store axial centerline, ft	-0.015		0.015	
Store reference area, S, ft^2	1.395		1.395	
Store reference diameter, b, ft	1.333		1.333	
Pitch moment of inertia, I_{yy}, slugs-ft^2	71.9		71.9	
Yaw moment of inertia, I_{zz}, slugs-ft^2	71.6		71.6	
Product of inertia, I_{xz}, slugs-ft^2	0		0	
Pitch-damping derivative, C_{m_q}, per radian	-35		-110	
Yaw-damping derivative, C_{n_r}, per radian	-35		-110	

TABLE II
MAXIMUM FULL-SCALE POSITION UNCERTAINTIES RESULTING FROM BALANCE PRECISION LIMITATIONS

M_∞	t, sec	ΔX, ft	ΔY, ft	ΔZ, ft	$\Delta\theta$, deg	$\Delta\psi$, deg
0.66	0.3	0.02	0.02	0.01	0.2	0.3
0.66	0.5	0.05	0.05	0.03	0.5	0.8
0.90	0.3	0.04	0.04	0.02	0.4	0.6
0.90	0.5	0.10	0.10	0.05	1.0	1.6

UNCLASSIFIED

Security Classification

DOCUMENT CONTROL DATA - R & D

(Security classification of title, body of abstract and indexing annotation must be entered when the overall report is classified)

1 ORIGINATING ACTIVITY (Corporate author)	2a. REPORT SECURITY CLASSIFICATION
Arnold Engineering Development Center Arnold Air Force Station, Tennessee 37389	UNCLASSIFIED
	2b. GROUP N/A

3 REPORT TITLE

CAPTIVE-TRAJECTORY STORE-SEPARATION CHARACTERISTICS OF THE SUU-51/B WITH MODIFIED TAIL FINS FROM THE F-4C AIRCRAFT

4 DESCRIPTIVE NOTES (Type of report and inclusive dates)

Final Report, July 9 to 19, 1971

5. AUTHOR(S) (First name, middle initial, last name)

J. M. Whoric, ARO, Inc.

This document has been approved for public release its distribution is unlimited. Per TAB 74-7 Lt 16 Aug. 74

6. REPORT DATE	7a. TOTAL NO OF PAGES	7b. NO. OF REFS
October 1971	71	2

8a. CONTRACT OR GRANT NO	9a. ORIGINATOR'S REPORT NUMBER(S)
b. PROJECT NO. 1120	AEDC-TR-71-222 AFATL-TR-71-130
c. Task 07	9b. OTHER REPORT NO(S) (Any other numbers that may be assigned this report)
d. Program Element 64724F	ARO-PWT-TR-71-167

10. DISTRIBUTION STATEMENT Distribution limited to U.S. Government agencies only; this report contains information on test and evaluation of military hardware; October 1971; other requests for this document must be referred to Air Force Armament Laboratory (DLGD), Eglin AFB, FL 32542.

11 SUPPLEMENTARY NOTES	12. SPONSORING MILITARY ACTIVITY
Available in DDC.	Air Force Armament Laboratory (DLGD), Eglin AFB, FL 32542

13. ABSTRACT

A wind tunnel test was conducted using 0.05-scale models to study the separation characteristics of the SUU-51/B external store with modified tail fins from the F-4C aircraft. Captive-trajectory store-separation data were obtained for two store cg locations and for 10 store wing loading configurations. The separation trajectories were initiated from the right-wing inboard pylon station utilizing the Triple Ejection Rack and from the centerline pylon utilizing the Multiple Ejection Rack. The flight conditions simulated were Mach numbers from 0.66 to 0.90 at an altitude of 5000 ft. Parent aircraft dive angles of 0 and 45 deg were simulated.

Distribution limited to U. S. Government agencies only; this report contains information on test and evaluation of military hardware; October 1971; other requests for this document must be referred to Air Force Armament Laboratory (DLGD), Eglin AFB, FL 32542.

DD FORM 1 NOV 65 1473

UNCLASSIFIED

Security Classification

14. KEY WORDS	LINK A		LINK B		LINK C	
	ROLE	WT	ROLE	WT	ROLE	WT
F-4C						
jet aircraft						
external stores						
separation						
ejection						

AFSC
Arnold AFS Tenn